Double Trouble

Foraminiferal Calcification in a Changing Ocean

Members of the dissertation committee:

Prof. dr. J.B.M. Middelburg

Prof. dr. L.J. Lourens

Prof. dr. A. Sluijs

Prof. dr. H.J. Spero

Dr. C. Rollion-Bard

This research was funded by the Darwin Center for Biogeosciences:

'Double Trouble: Consequences of Ocean Acidification - Past, Present and Future - Evolutionary changes in calcification mechanisms'

ISBN:

Printed by GVO drukkers & vormgevers, Ede, The Netherlands.

All rights reserved. No part of this publication may be reproduced in any form, by print or photo print, microfilm or any other means, without written permission by the author.

Double Trouble

Foraminiferal Calcification in a Changing Ocean

Dubbel Drama

Kalkvorming van foraminifera in een veranderende oceaan

(met een samenvatting in het Nederlands)

PROEFSCHRIFT

ter verkrijging van de graad van doctor aan de Universiteit Utrecht op gezag van de rector magnificus, prof. dr. G.J. van der Zwaan, ingevolge het besluit van het college voor promoties in het openbaar te verdedigen op vrijdag 20 januari 2017 des middags te 12.45 uur

door

Inge Evelien Yolanda van Dijk

geboren op 18 december 1987

te Utrecht

Promotor: Prof. dr. G-J. Reichart

Copromotor: Dr. L.J. de Nooijer

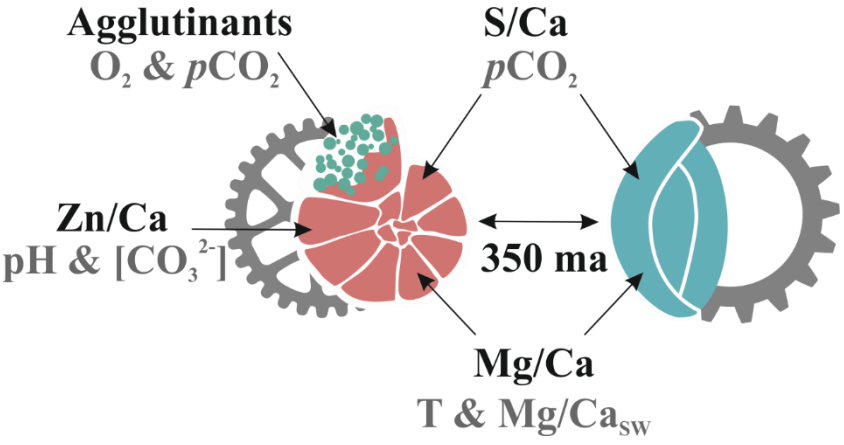
Agglutinants
O_2 & pCO_2
S/Ca
pCO_2
Zn/Ca
pH & $[CO_3^{2-}]$
350 ma
Mg/Ca
T & Mg/Ca_{sw}

Co-author affiliations

Joan M. Bernhard
Department of Geology and Geophysics, Woods Hole Oceanographic Institution, USA

Wim Boer
Department of Ocean Systems, NIOZ-Royal Netherlands Institute for Sea Research, the Netherlands, and Utrecht University

Malcolm B. Hart
School of Geography, Earth & Environmental Sciences, Plymouth University, United Kingdom

Gernot Nehrke
Department of Biogeosciences, Alfred Wegener Institute Helmholtz Centre for Polar and Marine Research, Germany

Lennart de Nooijer
Department of Ocean Systems, NIOZ-Royal Netherlands Institute for Sea Research, the Netherlands, and Utrecht University

Gert-Jan Reichart
Department of Ocean Systems, NIOZ-Royal Netherlands Institute for Sea Research, the Netherlands, and Utrecht University
Faculty of Geosciences, Earth Sciences Department, Utrecht University, the Netherlands

Takashi Toyofuku
Institute of Biogeosciences, Japan Agency for Marine-Earth Science and Technology (JAMSTEC), Japan

Johannes C. Wit
Department of Geology and Geophysics, Woods Hole Oceanographic Institution, USA

Mariëtte Wolthers
Faculty of Geosciences, Earth Sciences Department, Utrecht University, the Netherlands
University College London, Department of Chemistry, United Kingdom

Contents

Chapter 1

Introduction

Climate and the carbon system

Since the industrial revolution in the mid-eighteenth century, ongoing anthropogenic release of carbon resulted in a rapid increase of atmospheric carbon dioxide (IPCC, 2014). This increase is causing global warming, although both rate and magnitude of forecasted temperature increase are relatively uncertain. Global climate change is buffered by slow processes such as melting of the large ice sheets and uptake of excess heat by the oceans. The ocean also plays an important role in modulating atmospheric CO_2 levels by taking up a large portion of the emitted CO_2 (Houghton et al., 2001). It is estimated that they have absorbed approximately 25% of the anthropogenic carbon emissions over the last decades (Doney et al., 2009). When CO_2 enters the ocean, a suite of chemical reactions occur, leading to decreased carbonate saturation state and increased proton concentrations, a process called 'ocean acidification' due to the decrease in oceanic pH (Gattuso and Hansson, 2011). Carbonate precipitating organisms, important players in the ocean's carbon cycle and hence providing a major feedback on climate change, like e.g. corals, pteropods and coccolithophores, are thought to be negatively impacted by these changes (e.g., Kleypas et al., 1999; Riebesell et al., 2000; Orr et al., 2005). However, some calcifying organisms are reported to be unaffected, or even benefit from ocean acidification (Ries et al., 2009), which may be explained by the amount of control an organism has over the pH of their calcifying fluid (Ries, 2011).

Ocean acidification has been measured directly by monitoring surface water pH since the late 1980s (Feely et al., 2009). To predict the response of calcifying organisms to these changes and thereby estimate the potential feedback on atmospheric CO_2 concentrations, ocean acidification events in the geological past may be studied to provide insights. Increasing our understanding about feedbacks, the causes and, ultimately, consequences of past carbon perturbations (e.g. Hönisch et al., 2012), will help to improve insights into current and future changes in the oceans carbon cycle. Reconstructing past ocean carbon chemistry requires so-called proxies, which are measurable variables related to environmental parameters. Foraminifera, which can be found in (ancient) marine sediments, play an important role in the ocean carbon cycle and their micro fossils are excellent proxy signal carriers.

Foraminifera

Foraminifera are unicellular protists, primarily known for the representatives that form shells (also called tests) from calcium carbonate. Although foraminifera not producing $CaCO_3$ shells are far more diverse and widespread, their use in paleoceanography is limited and hence are not the focus of this thesis. Foraminifera have a very long geological record and survived many mass extinction events and perturbations of the oceans and climate. Calcareous foraminifera play a major role in the oceans carbon cycle, planktonic species determine up to 56% of the open marine $CaCO_3$ flux (Schiebel, 2002) and all benthic and planktonic foraminiferal together contribute almost 25% of the total carbonate production in the ocean (Langer, 2008), underscoring the importance of these organisms to the global $CaCO_3$ budget, and thereby the carbon cycle. Therefore, predicting and quantifying the response of foraminifera to ocean acidification has been the subject of numerous studies (Bijma et al., 2002; De Moel et al., 2009; Dueñas-Bohórquez et al., 2009; Moy et al., 2009; Allison et al., 2010; Beer et al., 2010; Dissard et al., 2010; e.g. Allison et al., 2011; Fujita et al., 2011; Keul et al., 2013a). Unfortunately, results are still ambiguous (summarized in Doo et al., 2014 and Keul et al., 2013a) making it difficult to predict overall changes in foraminiferal carbonate production in the future.

Foraminifera are popular tools to reconstruct a wide range of environmental parameters, since their carbonate shells provide an extensive fossil record. First, fossil foraminiferal assemblages can be used to reconstruct the paleo environment. For instance, the (relative) species abundance is known to reflect environmental conditions (Rutherford et al., 1999; Van der Zwaan et al., 1999), and the planktonic to benthic ratio of an assemblage can give constraints on the paleo water depth (Van der Zwaan et al., 1990). Secondly, the chemical composition of their shells is also known to reflect physical and chemical conditions of seawater. For instance, the Mg/Ca of foraminiferal shells is mainly governed by seawater temperature (Nürnberg et al., 1996), making it a reasonably well constrained paleothermometer (Elderfield and Ganssen, 2000; Lear et al., 2000). The relations between element incorporation or isotope fractionation in foraminiferal carbonate and environmental parameters can be studied using environmental samples, e.g. core tops or sediment traps, or by conducting controlled growth experiments in the laboratory. However, calibrating the impact of individual parameters of the inorganic carbon system on foraminiferal trace element incorporation is challenging due to the co-variation of carbon system parameters in nature (Zeebe and Wolf-Gladrow, 2001), which hence limits field calibrations. This co-variation does not allow isolating the impact of a single

parameter on foraminiferal calcite chemistry. Therefore, culture experiments, with carefully controlled environmental conditions, were designed to isolate impacts of carbon system parameters on foraminiferal calcite chemistry (Spero et al., 1997; Keul et al., 2013b).

Foraminiferal based carbon system proxies

Whereas a multitude of proxies exist for past sea water temperature, the paleoceanographers' toolbox for reconstructing past ocean carbon parameters is relatively limited. The boron isotopic composition of foraminiferal shells is among the more established proxies for reconstructing seawater pH (Sanyal et al., 1996; Hönisch and Hemming, 2005). This proxy is based on the isotopic fractionation between borate and boric acid, of which the ratio changes with seawater pH (Hershey et al., 1986). Since only borate is incorporated in foraminiferal calcite (Hemming and Hanson, 1992a), their $\delta^{11}B$ corresponds directly to seawater pH (Sanyal et al., 1996). A number of other elements incorporated during calcification by foraminifera are also shown to vary with inorganic carbon chemistry, including U (Russell et al., 2004; Keul et al., 2013b), B (Yu and Elderfield, 2007) and Zn (Marchitto et al., 2000; Chapter 6). However, partitioning of these elements is often not controlled by a single (inorganic carbon) parameter (e.g., Allen and Hönisch, 2012) and is known to vary between species. Such complications increase the 'noise' and therefore reduce the accuracy of past atmospheric CO_2 reconstructions. Hence, it is necessary to improve these proxies, by e.g. quantifying the impact of other environmental parameters or additional calibrations for other foraminiferal species. Also calcification adds to the uncertainty of carbonate proxies, which ideally would require a mechanistic understanding of the shell formation itself.

Double Trouble

Richard Feely (Barcelona, 2007) was the first to call the impact of anthropogenic addition of CO_2 "Double Trouble" as it causes both ocean warming and acidification. Since it has become increasingly clear that calcifying organisms are sensitive to the ongoing addition of CO_2 to the marine realm, albeit in different ways. Studying past ocean acidification events might help to unravel impact on different marine calcifyers, such as foraminifera. This, however, requires a process-based understanding of foraminiferal calcification as they are both recorders of past ocean change (proxies)

and affected by it themselves. Even though the mechanisms underlying calcification in calcareous foraminifera have recently been summarized (De Nooijer et al., 2014b), impact of biomineralization on element incorporation and isotope fractionation remain largely unknown. Currently two major issues concerning proxies based on foraminiferal carbonate are not fully understood. First, proxy-relations between environmental conditions and element incorporation in foraminiferal shell carbonate, are intrinsically coupled by foraminiferal calcification itself. Knowledge about the processes involved in calcification are crucial to increase our understanding of proxy relations, and hence allows predicting which (other) environmental parameters might impact a specific proxy. Second, the effect of long-term oscillations in seawater chemistry on foraminiferal calcification are not well constrained. Beside changes in seawater temperature and carbonate parameters, the chemical composition of the oceans, like e.g. seawater Mg/Ca, might also impact foraminiferal calcification. Hence, even though foraminifera are sensitive recorders of past changes in temperature and carbon chemistry, they are as organisms themselves also sensitive to changes in ocean chemistry: *Double Trouble*. In the following chapters I will try to create new insights on the impact of changing ocean conditions on foraminiferal calcification and investigate trace element incorporation as a function of carbonate system parameters.

In 1983, Sandberg proposed that the mineral phase of inorganic carbonates precipitated from seawater reflects Phanerozoic seawater chemistry (Sandberg, 1983). Shifts between so-called aragonite- and calcite seas are primarily caused by long-term changes in the ratio of $[Mg^{2+}]$ over $[Ca^{2+}]$ in seawater (i.e. Mg/Ca_{SW}; Hardie, 1996; Lowenstein et al., 2001; Dickson, 2002). Dominance of organisms producing calcite (e.g. rugose and tabulate corals) or aragonite (e.g. scleractinian corals and dasycladacean algae) follow these observed trends in Mg/Ca_{SW} (Stanley and Hardie, 1998; Stanley, 2006), but the response of foraminifera to changes in Mg/Ca_{SW} is only sparsely investigated (Martin, 1995). In **chapter 2**, '*The long-term impact of magnesium in seawater on foraminiferal mineralogy: mechanism and consequences*' fossil foraminiferal occurrences are analyzed in terms of their calcification strategy (e.g. comparing hyaline versus porcelaneous occurrences) during the Phanerozoic. High Mg/Ca values of seawater were observed to promote aragonite and high-Mg carbonate producing foraminifera, while low-Mg foraminifera are more abundant during intervals when seawater Mg/Ca is low. This is in line with the difference in nucleation fields for aragonite and calcite polymorphs in inorganic precipitation,

suggesting foraminifera, in spite of the tight control they exert on their calcifying fluid are still susceptible sea water chemistry.

Impact of seawater Mg/Ca on foraminiferal calcification is further explored in **chapter 3**, '*The impacts of seawater Mg/Ca and temperature on element incorporation in foraminiferal calcite*'. In this chapter, individual and combined impacts of seawater Mg/Ca and temperature on Mg incorporation in both hyaline (*Elphidium crispum*) and porcelaneous (*Quinqueloculina* sp.) foraminifera are investigated. We found that changing seawater Mg/Ca does not alter the slope of $Mg/Ca_{CALCITE}$ to temperature correlation for the two species studied here. Changes in seawater Mg/Ca will therefore only alter the absolute value of reconstructed temperature, a vital requirement for the method to reconstruct seawater Mg/Ca using $Mg/Ca_{CALCITE}$ of porcelaneous and hyaline foraminifera (Evans and Müller, 2012; Evans et al., 2015), and potentially also other marine calcifyers (Dickson, 2002).

Analyzing and comparing trends in element incorporation in hyaline and porcelaneous foraminifera may provide constrains on the differences between their calcification strategies. In **chapter 4**, '*Contrasting trends in element incorporation in hyaline and miliolid foraminifera*', we show results from eight lager benthic foraminiferal species (both hyaline and miliolid) cultured over a range of pCO_2. We observed no impact of changing carbonate chemistry on Mg, Sr and Na incorporation, while foraminiferal Zn/Ca and Ba/Ca increase with increasing pCO_2 (and thus decreasing $[CO_3^{2-}]$). We observed a strong dependency of incorporation between elements for hyaline foraminifera, i.e. foraminifera that incorporate more Mg, also incorporate more of the other studied elements. We propose that foraminifera transport elements to the site of calcification by Ca^{2+} channels, previously proposed in a trans-membrane transport model (TMT) by Nehrke et al. (2013), although the role of TMT to transport ions to the site of calcification is smaller in miliolids, since these species calcify in previously secluded seawater vacuoles.

Agglutinating foraminifera usually do not combine Ca^{2+} with CO_3^{2-} within a tightly controlled space, but collect and fixate particles within a cement. This cement is usually an organic matrix, and in some cases is known to be $CaCO_3$. In **chapter 5**, '*Combined impacts of ocean acidification and dysoxia on survival and growth of four agglutinating foraminifera*', we explore the isolated and combined impacts of dysoxia and ocean acidification on several species of agglutinating foraminifera. We found species-specific reactions to both stressors, but most species produced more chambers and survived better in the double stressor (dysoxia and ocean acidification) treatment. Furthermore, none of the species used in this culture study precipitated calcareous

cement, even though this was reported for at least one species (*Textularia tenuissima*), which may explain the absence of a response to lowered saturation state of the species studied here.

It is often challenging to decouple the impacts of different carbonate system parameters on trace element incorporation in foraminiferal carbonate when using 'standard' OA experiments. In **chapter 6**, '*Impacts of pH and [CO_3^{2-}] on the incorporation of Zn in foraminiferal calcite*', we cultured foraminifera in two different treatments, designed to decouple the effects of pH and [CO_3^{2-}] on incorporation of Zn. We found Zn incorporation to be exclusively governed by [CO_3^{2-}], due to the control it exerts on Zn speciation and therefore the amount of bioavailable Zn. These results show that foraminiferal Zn/Ca may be a useful proxy for two different parameters. First, if seawater [CO_3^{2-}] is known, this relation can be used to reconstruct seawater [Zn]. This would allow for unravelling of past seawater composition and reconstruction of past nutrient profiles using the global deep water Zn:Si relationship. Secondly, foraminiferal Zn/Ca might be used to reconstruct [CO_3^{2-}]. In combination with a proxy for other inorganic carbonate system parameters (e.g. $\delta^{11}B$ from foraminiferal calcite for seawater pH; Hönisch et al., 2009), $Zn/Ca_{CALCITE}$ can enable reconstruction of the complete carbon system and thereby, past atmospheric CO_2.

In **chapter 7**, *'Sulfur in foraminiferal calcite as a potential proxy for seawater carbonate ion concentration'*, we investigate sulfur in foraminiferal calcite as a potential proxy for sea water [CO_3^{2-}]. Due to lattice substitution, sulfate is hypothesized to substitute for carbonate in the crystal lattice, in theory leading to an increase in S/Ca with decreasing seawater [CO_3^{2-}]. We show $S/Ca_{CALCITE}$ calibrations for the hyaline species *Amphistegina gibbosa* and the miliolid *Marginopora vertebralis*, showing a decrease of resp. 21 and 19% per increase of 100 µm/kg [CO_3^{2-}]. In an accompanying culturing experiment, it was found that salinity does not have an effect on S/Ca in *A. lessonii*. Foraminifera increase their internal pH (De Nooijer et al., 2009), causing almost all inorganic carbon to be present in the form of CO_3^{2-}. However, since we observe a difference in amount of S incorporation over a range of pCO_2, the CO_3^{2-} to SO_4^{2-} ratio at the site of calcification must change. This suggest that internal pH is not elevated to a certain value, but probably increased with a fixed amount of units compared to the surrounding seawate

Chapter 2

The long-term impact of magnesium in seawater on foraminiferal mineralogy: Mechanism and consequences

Inge van Dijk, Lennart J. de Nooijer, Malcolm. B. Hart, and Gert-Jan. Reichart

DOI: 10.1002/2015GB005241

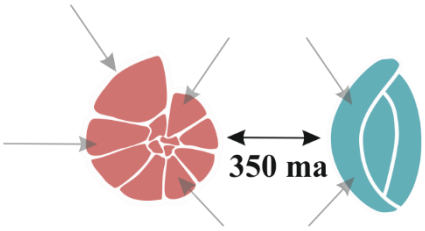

Abstract

Foraminifera are unicellular protists, primarily known for their calcium carbonate shells that provide an extensive fossil record. This record, ranging from Cambrian to present shows both major shifts and gradual changes in the relative occurrence of taxa producing different polymorphs of carbonate. Here we present evidence for coupling between shifts in calcite- versus aragonite-producing species and periods with, respectively, low and high seawater Mg/Ca throughout the Phanerozoic. During periods when seawater Mg/Ca is < 2 mol/mol, low-Mg calcite-producing species dominate the foraminiferal community. Vice versa, high-Mg calcite- and aragonite-producing species are more abundant during periods with relatively high seawater Mg/Ca. This alteration in dominance of the phase precipitated is due to selective recovery of groups producing the favorable polymorph after shifts from calcite to aragonite seas. In addition, relatively high extinction rates of species producing the mineral phase not favored by the seawater Mg/Ca of that time may be responsible for this alteration. These results imply that the current high seawater Mg/Ca will, in the long term, favor prevalence of high-Mg and aragonite-producing foraminifera over calcite-producing taxa, possibly shifting the balance toward a community in which calcite production is less dominant.

1. Introduction

In 1983, Sandberg proposed that the mineral phase of inorganic carbonates that precipitated from seawater reflects Phanerozoic seawater chemistry (Sandberg, 1983). Shifts between so-called aragonite and calcite seas are primarily caused by long-term changes in the ratio of $[Mg^{2+}]$ over $[Ca^{2+}]$ in seawater (Hardie, 1996; Lowenstein et al., 2001; Dickson, 2002) (i.e., Mg/Ca_{SW}). This ratio varies over geological timescales due to changes in the balance between weathering, oceanic crust production, dolomite formation, and rate of carbonate burial (Wilkinson and Algeo, 1989; Hardie, 1996; Berner, 2004; Holland, 2005; Arvidson et al., 2006; Farkaš et al., 2007; Arvidson et al., 2011). Dominance of organisms producing calcite (e.g., rugose and tabulate corals) or aragonite (e.g., corals and dasycladacean algae) as well as abiotically precipitated calcite and aragonite follows trends in Mg/Ca_{SW} (Stanley and Hardie, 1998; Stanley, 2006). The impact of Mg/Ca_{SW} on biogenic mineralogy can be explained by differences in affinity of Mg ions for calcite versus aragonite crystal surfaces (Reddy and Wang, 1980; Nancollas and Sawada, 1982; Falini et al., 1994; Fernandez-Diaz et al., 1996; De Choudens-Sánchez and Gonzalez, 2009). Magnesium ions adsorb relatively well to calcite surfaces compared to those of aragonite (Mucci and Morse, 1985), resulting in a relative decrease in calcite growth rate at high seawater $[Mg^{2+}]$ (Berner, 1975). The boundary between nucleation fields for inorganic aragonite and calcite lies at a Mg/Ca_{SW} of 2 mol/mol (Sun et al., 2015) and depends on temperature and pressure (Berner, 1975). Recently, it is shown that seawater sulfate concentrations have an (additional) effect on the seawater Mg/Ca threshold (Bots et al., 2011). Periods with $Mg/Ca_{SW} < 2$ (e.g., Devonian and Silurian) are associated with calcite-producing organisms and are therefore termed "calcite seas," whereas "aragonite seas" are defined by periods with $Mg/Ca_{SW} > 2$ and are characterized by dominance of aragonite and/or high-magnesium calcite producers (Dickson, 2004; Stanley, 2008) (e.g., Permian and Triassic). The biological mechanisms affected by changes in Mg/Ca_{SW} may include decreasing growth rates and increased energy costs for calcification by organisms producing an unfavored $CaCO_3$ crystal phase (Ries, 2010). Both of these biological impediments result in a dominance of calcite-producing organisms during periods with low Mg/Ca_{SW}, while favoring those precipitating aragonite when Mg/Ca_{SW} is high.

Although the relationship between Phanerozoic changes in seawater Mg/Ca and the evolutionary history of many marine calcifiers has been analyzed (Kiessling et al., 2008; Stanley, 2008; Porter, 2010), the response of foraminifera to changes in Mg/Casw is only sparsely investigated (Martin, 1995). Most low-Mg calcite

producing or hyaline taxa are known to actively control the amount of magnesium incorporated (Bentov and Erez, 2006; De Nooijer et al., 2014b). Since the Mg/Ca of the calcifying fluid is, in this case, dissimilar from that of ambient seawater, foraminifera might potentially be unaffected by changes in Mg/Ca_{SW}. High concentrations of seawater Mg^{2+}, however, may require allocation of more energy to maintain biomineralization and thereby link long-term changes in Mg/Ca_{SW} to the success of aragonite- versus calcite-producing foraminifera. Geological longevity, areal and depth distribution, composition of the tests (aragonite or calcite), and importance in the global carbon cycle, however, make foraminifera particularly suitable to study the interplay between seawater chemistry and biogenic mineralogy. Here we present an analysis of foraminiferal abundances through the Phanerozoic and relate their mineralogy to changes in Mg/Ca_{SW} and mass extinction events. Past shifts in dominance of calcite- versus aragonite-producing foraminifera serve as an analogue to evaluate future foraminiferal success under ongoing climate and environmental stress.

2. Methods

2.1. Foraminiferal Occurrences

Over Geological Timescales In order to investigate major trends in foraminiferal distribution, we analyzed foraminiferal occurrences in the Paleobiology database of Fossilworks (http://fossilworks.org). In general, we used the database in default mode, with some small exceptions, and this input data are listed in the supplementary data (supplementary Table S1). In short, we extracted 6270 collections with 37,586 species occurrences covering the last 500 Ma (Kiessling et al., 2015), when queried the database for Foraminferea, Foraminiferida, and Foraminifera (genus level or above). All foraminiferal species occurrences were grouped into ~5 Myr time bins ("Fossil Record 2 bin"). Occurrences were extracted from the database on a species level, excluding contributions with open nomenclature (aff., cf., "…," and "?") (Bengtson, 1988) which take into account different levels of uncertainty during the determination on species level. To estimate global foraminiferal abundances, the full geographical range was used. By enabling the database's "scale option" we also extracted composition and life habitat information of every species. The assignments of these mineralogical and ecological attributes were based on a number of sources reporting mineralogy and habitat preferences for the different foraminiferal (sub)orders (Loeblich and Tappan, 1984, 1988). The composition of the tests was aragonite or

calcite with low (LMC; 8%wt $MgCO_3$). So-called intermediate-Mg calcite (4–8%wt $MgCO_3$) was already labeled LMC by the authors of the database. This distinction coincides with known differences in biomineralization strategies (e.g., hyaline versus porcelaneous foraminifera, respectively (Hemleben et al., 1986; De Nooijer et al., 2009). Life habitat information was either planktonic or benthic (infaunal, semi-infaunal, and epifaunal). For 10.5% of all species present in the database, the $CaCO_3$ mineralogy is unknown or not recorded and was therefore excluded from further statistical analysis. Also, species which do not (actively) calcify, like agglutinated and naked foraminifera, or precipitate carbonate but opaline silica (order Silicolocilinida; Sen Gupta, 1999), for example, were not used for this analysis. Occurrences of species from collections older than 320 Ma were excluded from analysis due to scarcity of collections and consequently very low foraminiferal species occurrences (90% of the total occurrences. This could be due to a possible bias of Fossilworks toward planktonic foraminifera. However, when performing the analysis without the planktonic LMC group, we still observe the same general pattern for all the other groups (see Fig. S1 in the Supplementary Material).

2.2. Aragonite Versus Calcite Sea Events

Since different Mg/Casw reconstructions yield slightly different timings of calcite-aragonite sea events (Evans and Müller, 2012), we choose to define periods in which reconstructions (Stanley and Hardie, 1998; Farkaš et al., 2007) agree as the "true" calcite and aragonite sea events. To test whether occurrences of LMC versus aragonite/HMC producers are significantly different in these calcite and aragonite seas or before/after mass extinction events (Raup and Sepkoski Jr, 1982), two-way Student's t tests assuming equal variances were performed. We compared the average *p*(aragonite + HMC) between adjacent calcite and aragonite seas, as well as between all calcite and aragonite sea intervals combined. Finally, the three bins before and after three mass extinction events with student's t tests to determine whether these average occurrences were different. Our analyses include the end-Permian (252 Ma), end-Triassic (200 Ma), end-Cretaceous (65 Ma), and Paleocene Eocene Thermal Maximum (PETM; ~55 Ma) mass extinctions. Due to the resolution of our database, the end Cretaceous and PETM were regarded as one event, despite known differences in their causes and consequences. We in this case compared p(aragonite + HMC) of the three time bins before the end Cretaceous (65 Ma) with the three time bins after the PETM (55 Ma). All of the aforementioned events are associated with minor or major perturbations in marine inorganic chemistry (Hönisch et al., 2012; Hart et al.,

2014) and are characterized by a decrease in biodiversity, including that of foraminifera.

3. Results

3.1. Seawater Mg/Ca Reconstruction

Long-term patterns in Mg/Ca_{SW} can be reconstructed from model studies taking into account mid-ocean ridge spreading rates, weathering, and dolomite formation (Wilkinson and Algeo, 1989; Hardie, 1996). Over the last few decades, these reconstructions have been improved by, e.g., new insights in biochemical cycles. One of the most recent reconstructions (Farkaš et al., 2007; Figure 1) combines a model of coupled calcium, carbon, and magnesium global cycles (Wallmann, 2001; Hansen and Wallmann, 2003; Wallmann, 2004; Heuser et al., 2005) with reconstructed seafloor spreading rates based on $^{87}Sr/^{86}Sr$ (Veizer et al., 1999; Wallmann, 2004). The resulting reconstruction is in close agreement with a number of independent proxies for Mg/Ca_{SW}, including Mg/Ca of fluid inclusions (Lowenstein et al., 2001; Horita et al., 2002) and that of rudists (Steuber and Rauch, 2005) and echinoderms (Dickson, 2002). This relatively recent Mg/Ca_{SW} reconstruction is largely in agreement with those from earlier studies (Hardie, 1996), whereas deviations between models is likely caused by recent updates in the assumptions for the earlier models (Holland et al., 1996; Holland and Zimmermann, 2000; Horita et al., 2002). The model by Farkaš et al. (2007) also includes more recent data on global major elements cycling and refined estimates of seafloor spreading rates, resulting in slightly different $[Ca^{2+}]$ and $[Mg^{2+}]$ trends. The transitions between these calcite and aragonite seas deviate somewhat from those of the often-used reconstruction (Stanley and Hardie, 1998), which is therefore included in our discussion. This divided the past 500 Ma into two periods with a relatively low Mg/Ca_{SW} (end Cambrian to Devonian and end Triassic to mid-Cretaceous, CI and CII, respectively) and two with a relatively high Mg/Ca_{SW} (Carboniferous to end Triassic and mid-Cretaceous to recent, AII and AIII, respectively).

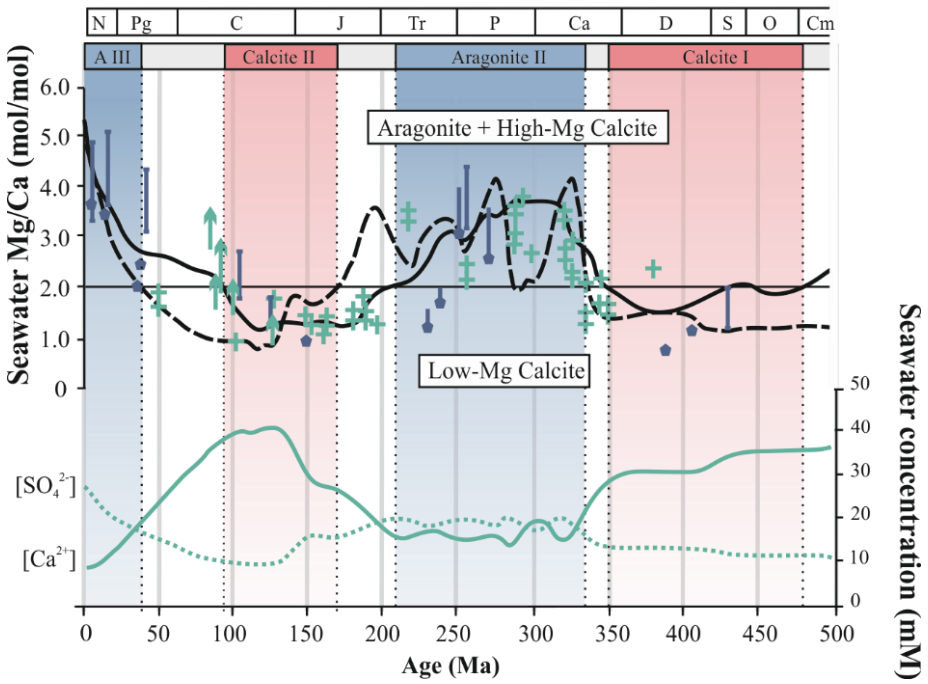

Figure 1. (top) Reconstruction of calcite (CI and CII) and aragonite sea (AII and AIII) intervals based on modeled seawater Mg/Ca reconstructions (solid line (Stanley and Hardie, 1998) and dashed line (Farkaš et al., 2007)), supported by Mg/Ca from fluid inclusions (bars (Lowenstein et al., 2001) and pentagons (Horita et al., 2002)) and that of echinoderm ossicles and rudists (arrows (Steuber and Rauch, 2005) and crosses (Dickson, 2002)'. The horizontal line divides calcite sea (Mg/Ca < 2) and aragonite sea (Mg/Ca > 2) intervals (Berner, 2004; Stanley, 2008). Accordingly, aragonite sea intervals are indicated by blue panels and calcite sea events with red panels. The grey panels indicate periods where the two models deviate in the timing of the division between calcite and aragonite seas. (bottom) Phanerozoic reconstruction of SO_4^{2-} (dotted line) and Ca^{2+} (solid line) concentrations over geological time (after Demicco et al., 2005). Cm = Cambrian, O = Ordovician, S = Silurian, D = Devonian, Ca = Carboniferous, P = Permian; Tr = Triassic, J = Jurassic, C = Cretaceous, Pg = Palaeogene, and N = Neogene.

3.2. The Response of Foraminifera to Changes in Mg/Ca_{SW}

Although it has been suggested that foraminifera are "sophisticated biomineralizers" and are, therefore, able to cope with relatively variable Mg concentrations in seawater (Stanley, 2008), there is a significant ($p < 0.01$) correlation between average seawater Mg/Ca of combined aragonite versus calcite sea events (CII versus AII + AIII) and the ratio between calcite- versus aragonite-producing foraminifera (Figure 2).

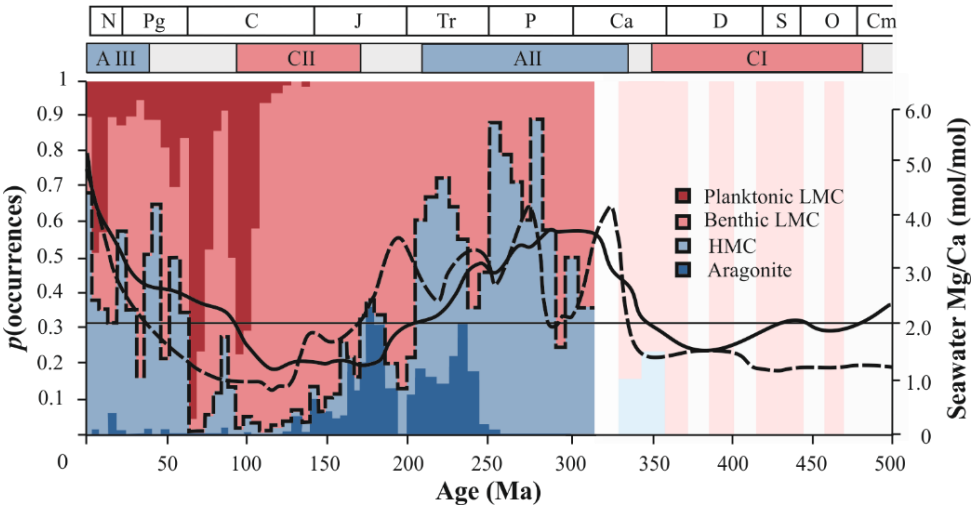

Figure 2. Proportional foraminiferal species occurrences through the Phanerozoic Era. The *p*(occurrences) is the number of times that a species of one of the four groups is present per time bin, relative to the other three groups. Low-Mg calcite-producing (LMC) benthic and planktonic foraminifera (light and dark red areas, respectively) and of high-Mg calcite (HMC) and aragonite foraminifera (light and dark blue areas, respectively) are divided by a dashed black line. The three mass extinction events (P-Tr, Tr-J, PETM, and C-Pg) are indicated by vertical dotted lines. Light shaded data before 320 Ma are not statistically supported due to a limited amount of foraminiferal occurrences in this part of the fossil record. Abbreviations as in Figure 1.

Aragonite sea species (taxa-producing aragonite or HMC) are more abundant during periods with high seawater Mg/Ca values. In periods with low Mg/Ca_{SW} values, there is an increase in abundance of LMC-producing taxa. However, after the shift from CII to AIII, there appears to be a lag in the response of the foraminiferal community.

Aragonite sea species only start to increase after the end Cretaceous and PETM, not directly when Mg/Ca_{SW} increases. Nevertheless, the effect of mass extinction events on the dominating foraminiferal mineralogy is less clear (Table 1).

Transition or Event	Δmean	T-value	d.f.	p-value
C/A*	0.394	9.85	20	<0.00
CII/AIII	0.306	4.91	10	<0.00
AII/CII	0.483	7.39	10	<0.00
End-Permian (252 Ma)	0.310	3.39	2	0.08
End-Triassic (200 Ma)	0.444	7.63	2	0.02
End-Cretaceous (65 Ma) and PETM (55 Ma)	0.411	3.07	2	0.09

Table 1. Changes in Aragonite versus Calcite Sea species over mass extinction events and aragonite/calcite sea intervals. Bold values are significant. Aragonite (AII and AIII) and Calcite (CII) sea intervals. Δmean is the difference between the means of the compared groups. *All Calcite sea periods versus all Aragonite sea periods = CII/(AII+AIII)

Only the end-Triassic extinction, coinciding with a transition from aragonite to calcite sea interval (AII/CII), correlates to a significant ($p < 0.05$) shift in abundance from aragonite to calcite sea species. Furthermore, first appearance of aragonite precipitating foraminifera, i.e., the orders Involutinida and Robertinida, occurs during aragonite sea II (approximately 250 Ma ago), while planktonic calcite precipitating foraminifera evolve during calcite sea II.

4. Discussion and Conclusion

4.1. Foraminiferal Trends are controlled by seawater Mg/Ca

Long-term trends in fossil foraminiferal occurrences are in line with fluctuations in Mg/Ca_{SW} and community changes of other marine calcifiers (Stanley and Hardie, 1998; Stanley, 2008; Porter, 2010). However, $[SO_4^{2-}]$ has an additional effect on preferential $CaCO_3$ polymorph formation due to its effect on the Mg/Ca threshold separating the nucleation fields for aragonite and calcite. Especially when $[SO_4^{2-}]$ decreases below <10 mM (Bots et al., 2011), the Mg/Ca threshold for preferential aragonite increases, resulting in an overall increase of calcite precipitated. Hence, high $[SO_4^{2-}]$ promotes the precipitation of aragonite, similar to high seawater Mg/Ca. Since

Phanerozoic [SO_4^{2-}] reconstructions (Demicco et al., 2005) show a covariation of [SO_4^{2-}] with seawater Mg/Ca, it is difficult to disentangle the contribution of these two controls. During biomineralization, however, the [SO_4^{2-}] of the calcifying fluid of a foraminifera is much lower than that of the surrounding seawater, as indicated by the low partition coefficient for sulfur (Berry, 1998; Chapter 7). This implies that despite geological fluctuations in [SO_4^{2-}], its effect on the boundary between nucleation fields for calcite versus aragonite precipitation is similar through time.

Nevertheless, periods with relatively low Mg/Ca_{SW} are dominated by calcite-producing foraminifera, whereas aragonite producers are found predominantly during periods with high Mg/Ca_{SW}. For other organisms, shifts in dominance of marine calcite and aragonite producers are explained by increased extinction and speciation rates after transitions of Mg/Ca_{SW}, or by adaptation to preferred mineralogy by switching from calcite to aragonite precipitation or vice versa (Stanley et al., 2002; Ries, 2004; Ries, 2010). For foraminifera, extinction and radiation seem more likely since there are significant differences in community composition before and after mass extinction events. Moreover, no foraminiferal species has yet been found to produce both calcium carbonate phases, nor have culturing experiments with varying Mg/Ca_{SW} (Segev and Erez, 2006; Mewes et al., 2014; Evans et al., 2015) suggested that foraminifera can change or adapt to another $CaCO_3$ phase, kinetically favored, e.g., coralline algae (Stanley et al., 2002) and echinoids, crabs, shrimps, and calcareous serpulid worms (Ries, 2004). Since foraminifera do not switch from calcite to aragonite production (or vice versa) as a response to changes in Mg/Ca_{SW}, they will eventually be calcifying at unfavorable Mg/Ca_{SW} conditions as a consequence of changing ocean chemistry. For other organisms, this is shown to negatively impact calcification through decreased growth rates and/or increased energy spent on calcification (Ries, 2010). Hyaline and porcelaneous foraminifera have different calcification strategies to produce their shells (Hemleben et al., 1986; De Nooijer et al., 2009; De Nooijer et al., 2014b). The costs involved in calcification are poorly constrained but will depend on biomineralization strategy (Zeebe and Sanyal, 2002). In case Mg^{2+} is selectively removed from the calcifying fluid (Bentov and Erez, 2006), increased seawater [Mg^{2+}] will likely increase energy requirements for calcification due to increased pumping rates. When calcification is driven by active, transmembrane transport of Ca^{2+} (Nehrke et al., 2013; De Nooijer et al., 2014b), the involved energy may also increase by Mg ions blocking selective Ca transporters. The latter may be overcome by, e.g., increasing the Ca transporter density, which will also increase the energy requirements when calcifying under high [Mg^{2+}].

4.2. Preferential Dissolution

Geological trends in fossil foraminiferal shells are potentially biased by preferential dissolution as a result of changes in seawater saturation state with respect to calcium carbonate. Saturation state (Ω) is the product of seawater carbonate and calcium concentrations ($[Ca^{2+}] \times [CO_3^{2-}]$), divided by the solubility product K_{sp}. This solubility product differs between aragonite (-log K_{sp} = 6.19) and low-Mg calcite (-log K_{sp} = 6.37) and therefore results in relatively poor preservation of aragonite shells compared to calcite ones. Such a preservation bias could have affected fossil occurrences of the different foraminiferal groups, thereby compromising our results, discussion, and conclusions. Although preferential dissolution may have affected foraminiferal taphonomy, it is unlikely to impact overall shifts in dominance of calcite versus aragonite producers since reconstructed seawater saturation states (Riding and Liang, 2005) are anticorrelated to changes in Mg/Ca_{SW}. Low Ω states co-occur with high Mg/Ca_{SW} on global and geological scales and vice versa. Even though periods with a low Ω may be reflected by increased aragonite dissolution and therefore decreased preservation, the opposite is found (Figure 2). Hence, the effect of elevated Mg/Ca_{SW} on aragonite production apparently outweighs any potential bias due to preferential dissolution. Depending on the magnitude of increased aragonite dissolution during periods with a low Ω, the observed correlation between Mg/Ca_{SW} and calcite versus aragonite foraminiferal species abundances might be stronger than reported here. However, we cannot account for postburial diagenetic change, which may also cause the preferential dissolution of aragonite and/or replacement by calcite.

4.3. The Effect of Mass Extinction Events

The importance of mass extinction events on the balance between calcite and aragonite producers, in general, has been analyzed by Kiessling et al. (2008), who proposed that major environmental perturbations rather than changes in ocean chemistry determine the dominance of calcite versus aragonite producers. This conclusion is based on a study also relying on fossil abundances and included a group "foraminifera + algae," representing a minor portion of the total species occurrences. In Kiessling et al.'s analysis, trends in the combination of all marine-calcifying organisms are mainly driven by mass extinction events, while Mg/Ca_{SW} seems to have a minor impact. This is seemingly in contrast with our results, which suggest the relation between long-term seawater chemical changes and evolution of calcifying organisms is not always straightforward. An explanation for these contrasting results

may point to the fact that different controls shape the evolution of marine calcifiers on different levels and/or that each group (e.g., corals, bivalves, and foraminifera) responds differently to changes in Mg/Ca_{SW}. It is therefore crucial to analyze the evolution of (and within) marine-calcifying groups in relation to seawater chemistry separately. It is likely that mass extinction events impact the mineralogy of marine calcifiers, in general, while within these orders, changes in seawater chemistry influence evolutionary success and extinction rates. When analyzing foraminiferal community shifts as a function of mass extinction events, only the end-Triassic event shows a significant shift from a high-Mg and aragonite-dominated community to one with more low Mg calcite-producing species. Due to differences in the causes, duration, and magnitude of all events analyzed, in combination with the resolution of our data, the impact of mass extinctions on overall foraminiferal community cannot be unambiguously assessed based on this data set. Nevertheless, for other major groups of calcifying organisms, mass extinction events play an important role in aragonite versus calcite dominance (Kiessling et al., 2008) mainly due to selective recovery of the organisms which precipitated the favored polymorph, which may also be the case for foraminifera.

4.4. First Occurrence, Extinction, and Recovery of Foraminiferal Taxa

The effect of ocean chemistry on foraminiferal evolution is likely caused by (1) timing of the first occurrences of newly formed taxa and (2) selective recoveries and extinctions of taxa before and after Mg/Ca_{SW} transitions and/or major carbon perturbations. This would explain, for instance, the observed lag of dominance by HMC and aragonite producers after the CII/AIII transition. The importance of Mg/Ca_{SW} on foraminiferal mineralogy is reflected by the first occurrences of newly evolved taxa, generally exhibiting the mineralogy which is favored by the seawater Mg/Ca of that time. For example, all taxa from the orders Involutinida and Robertinida produce aragonite shells and both orders originated in Aragonite sea II (at 303 and 250 Ma, respectively). After establishing their mineralogy, these taxa did not change their mineralogical preference within their calcification mechanism and continued producing aragonite, even during periods of lower Mg/Ca_{SW}. This was already suggested by Martin (1995) that Mg/Ca_{SW} plays a key role in determining the mineralogy of clades at their moment of origination (Porter, 2007; Porter, 2010). There might be an increased recovery or diversification of taxa producing the polymorph which is supported by seawater Mg/Ca. For instance, high Mg/Ca_{SW} could have played a part in the postextinction recovery by aragonitic trochospiral

Robertinida (genera Oberhauserella and Reinholdella) following the end-Triassic extinction (Fuchs, 1967, 1970; Clémence and Hart, 2013), which occurred during relatively high Mg/Ca_{SW}. In the Lower Jurassic, calcitic taxa (Lenticulina, Lingulina, Paralingulina, Nodosaria, Pseudonodosaria, etc.) gradually began to dominate the assemblage in the developing calcite II ocean (Copestake and Johnson, 2014), with the aragonitic taxa (especially Reinholdella and Epistomina) reduced to a low-diversity lineage throughout the mid–Late Jurassic and Early Cretaceous (Hart, 1984; Oxford et al., 2004; Hart et al., 2008). After the end-Cretaceous extinction event, occurrences of high-Mg foraminiferal taxa increased (Figure 2) and aragonitic pteropods and heteropods became a significant part of the oceanic plankton (Wall-Palmer et al., 2012) while seawater Mg/Ca rose to its current value. An example of the interplay between the mineralogy of newly originated taxa and selective recovery by subsequent changes in oceanic state can be found in the evolution of planktonic foraminifera. The early planktonic foraminifera, Conoglobigerina, were aragonite producers and evolved from aragonitic benthic ancestors in the high Mg/Ca_{SW} ocean of the Early Jurassic (Wernli, 1988; Wernli, 1995; Hart et al., 2003; Hart et al., 2012). This Conoglobigerina-Globuligerina-Favusella lineage appeared to be unsuccessful and did not diversify in the developing calcite II ocean and then became extinct in the mid-Cretaceous, after which the new calcite producing taxa became highly diverse and successful. These new calcite-producing planktonic foraminifera emerged in the Early Cretaceous, and their evolution can be traced throughout the Cretaceous, despite a number of significant changes in the foraminiferal community at oceanic anoxic events (BouDagher-Fadel et al., 1997; Hart, 1999; Premoli Silva and Slite, 1999; Hart et al., 2002).

4.5. Consequences for (Future) Foraminifera

Currently, high seawater Mg/Ca favors occurrence of organisms producing aragonite and high-Mg calcite (e.g. Stanley and Hardie, 1998; Stanley, 2006). Following fossil alterations in dominant foraminiferal mineral phases, all extant low-Mg calcite-producing foraminifera, including all planktonic species, are currently living in an ocean that is not favorable to the mineral phase of their shells. Ongoing anthropogenic CO_2 emissions and subsequent ocean acidification are currently resulting in a major marine carbon perturbation by decreasing seawater pH and Ω, which will likewise hamper marine calcification (Ilyina and Zeebe, 2012; Van de Waal et al., 2013) as it did in the geological past (e.g. Hönisch et al., 2012). Since ongoing oceanic CO_2 uptake will cause seawater to become undersaturated with respect to aragonite sooner

than it will be for calcite, organisms producing aragonite and high-Mg calcite (scleractinian corals, echinoderms, and some foraminiferal taxa) are generally thought to be most vulnerable to ocean acidification (Orr et al., 2005). However, foraminiferal species producing this polymorph of carbonate (i.e., aragonite or HMC) are supported by the current high seawater Mg/Ca. Even though they may be relatively vulnerable to ongoing ocean acidification, subsequent recovery and diversification may favor their long-term success. Our results highlight the potential role of seawater Mg/Ca as a possible controller on the success of calcite versus aragonite producers in a changing ocean. We suggest that on longer timescales, high-Mg calcite- and aragonite-producing foraminifera dominance will not be negatively impacted by ongoing ocean acidification due to rapid recovery and diversification after the event, which will be perhaps even at the expense of low-Mg calcite-producing foraminifera.

Acknowledgments

This research is funded by the NIOZ Royal Netherlands Institute for Sea Research and the Darwin Centre for Biogeosciences project "Double Trouble: Consequences of Ocean Acidification— Past, Present and Future—Evolutionary changes in calcification mechanisms." The data set ("Taxonomic occurrences of to 600 Foraminferea, Foraminiferida, and Foraminifera recorded in Fossilworks, the Evolution of Terrestrial Ecosystems database, and the Paleobiology Database") used in this study is freely available at http://fossilworks.org. The input parameters necessary to reproduce the results are also available in the supporting information. This is a Paleobiology Database publication.

Supplementary Material Chapter 2

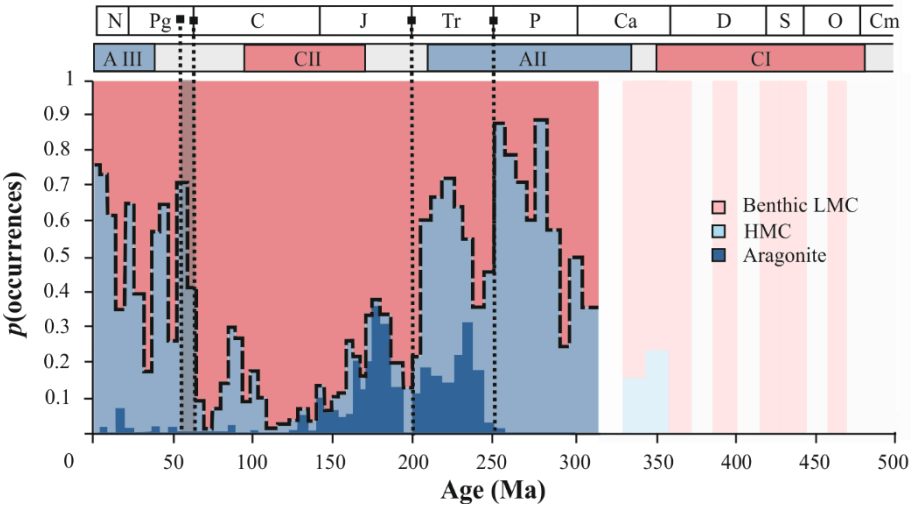

Figure S1. Proportional foraminiferal species occurrences through the Phanerozoic Era. *p*(occurrences) is the number of times that a species of one of the four groups is present per timebin, relative to the other three groups. Calcite producing benthic foraminifera (light red area) and of HMC and aragonite foraminifera (light and dark blue areas resp.) are divided by a dashed black line. The three mass extinction events (P-Tr, Tr-J, PETM and C-Pg) are indicated by vertical dotted lines. Light shaded data before 320 Ma is not statistically supported due to a limited amount of foraminiferal occurrences in this part of the fossil record. Accordingly, aragonite sea intervals are indicated by blue panels and calcite sea events with red panels. The grey panels indicate periods where the two models deviate in the timing of the division between calcite- and aragonite seas. Cm=Cambrian; O=Ordovician; S=Silurian; D=Devonian; Ca=Carboniferous; P=Permian; Tr=Triassic; J=Jurassic; C=Cretaceous; Pg=Palaeogene; N=Neogene.

Table S1. Division of taxa in mineralogy groups into mineralogy (aragonite, high- and low-Mg calcite) and/or life habitat (benthic or planktonic) based on their assignment in Paleobiology Database Fossilworks (http://Fossilworks.org). In order to compress the data we only listed the genera.

Aragonite producers
Angulodiscus, Arenovidalina, Auloconus, Aulotortus, Coronipora, Diplotremina, Duostomina, Epistomina, Hoeglundina, Involutina, Lamarckina, Lamelliconus, Neotrocholina, Raphconilia, Reinholdella, Semiinvoluta, Tethysocarnia, Triasina, Trocholina, Trochonella, Variostoma.
High-Mg producers
Abriolina, Acervulina, Affinetrina, Agathammina, Altinerina, Alveolina, Alveolinella, Ammovertella, Archaias, Articulina, Austrotrillina, Baisalina, Borelis, Broeckina, Calcitornella, Chubbina, Cisalveolina, Cornuspira, Costifera, Cucurbita, Cycloforina, Dentostomina, Derventina, Fabularia, Fallotia, Fasciolites, Flintina, Galeanella, Glomalveolina, Gsollbergella, Gypsina, Hauerina, Hechtina, Hedraites, Hemigordiopsis, Hemigordius, Hoyenella, Hydrania, Idalina, Istriloculina, Kamurana, Keramosphaerina, Lacazina, Lachlanella, Lamarmorella, Larrazetia, Marginopora, Massilina, Meandrospira, Meandrospiranella, Miliolechina, Miliolinella, Miliolipora, Moesiloculina, Multidiscus, Murciella, Murgella, Neoangulodiscus, Nodobaculariella, Nodophthalmidium, Nubecularia, Nubeculinella, Nummofallotia, Nummoloculina, Opertorbitolites, Ophthalmidium, Orbitolites, Orthotrinacria, Orthovertella, Ovalveolina, Palaeomiliolina, Paraophthalmidium, Penarchaias, Peneroplis, Planiinvoluta, Praealveolina, Praerhapydionina, Pseudedomia, Pseudorhapydionina, Pseudorhipidionina, Pseudotaberina, Pseudotriloculina, Pyrgo, Quinqueloculina, Raadshoovenia, Raadshovenia, Rectocornuspira, Rhapydionina, Scandonea, Schlumbergerina, Scythiloculina, Senalveolina, Siculocosta, Sigmoilina, Sigmoilinita, Sigmoilopsis, Simplalveolina, Sinuloculina, Sinzowella, Siphonaperta, Siphonofera, Solenomeris, Sorites, Sphaerogypsina, Spirolina, Spiroloculina, Spirophthalmidium, Taberina, Trepeilopsis, Triloculina, Turriglomina, Vertebralina, Vidalina, Vinelloidea.
Planktonic low-Mg producers
Archaeoglobigerina, Cassigerinella, Chiloguembelina, Dentoglobigerina, Dicarinella, Favusella, Globigerina, Globigerinelloides, Globigerinita,

Globigerinoides, Globoconella, Globoquadrina, Globorotalia, Globorotaloides, Globotruncana, Globotruncanella, Globoturborotalita, Guembelitria, Hastigerina, Hedbergella, Heterohelix, Marginotruncana, Neogloboquadrina, Orbulina, Praeglobotruncana, Praeorbulina, Pseudoguembelina, Pulleniatina, Rotalipora, Rugoglobigerina, Sigalia, Sphaeroidinellopsis, Tenuitella, Truncorotaloides, Turborotalia.
Benthic low-Mg producers
Abadehella, Acervoschwagerina, Advenella, Aeolisaccus, Afghanella, Alabamina, Aljutovella, Alpinophragmium, Alpinoschwagerina, Ammonia, Amphistegina, Anderssonites, Angulogerina, Anomalinoides, Anulofusulinella, Archaediscus, Archaesphaera, Armenina, Assilina, Astacolus, Asterigerina, Asteroarchaediscus, Astrononion, Aubignyna, Austrocolomia, Baggina, Bartramella, Beedeina, Benshiella, Berthelinella, Biseriella, Bisphaera, Bitubulogerina, Biwaella, Bojarkaella, Bolivina, Bolivinita, Botuloides, Boultonia, Bradyina, Brizalina, Brunsia, Buccella, Buchnerina, Bulimina, Buliminella, Bullopora, Calcarina, Caligella, Calvezina, Cancellina, Cancris, Carpenteria, Cassidulina, Cassidulinoides, Caucasina, Ceratobulimina, Chalaroschwagerina, Changmeia, Chrysalogonium, Chusenella, Cibicidella, Cibicides, Cibicidoides, Citharina, Citronites, Climacammina, Codonofusiella, Colaniella, Conicospirillina, Conorbella, Coryphostoma, Crenulosepta, Cribroelphidium, Cribrogenerina, Cribrononion, Cribrosphaeroides, Cryptoseptida, Cuniculinella, Cycloclypeus, Cymbaloporetta, Dagmarita, Daixina, Darbyella, Darvasella, Darvasites, Darvasoschwagerina, Daviesina, Deckerella, Dentalina, Dentalinopsis, Dictyoconoides, Diplosphaerina, Discocyclina, Discorbinella, Discorbis, Dunbarinella, Dunbarula, Dutkevitchia, Dutkevitchites, Dyocibicides, Earlandia, Earlandinita, Elphidium, Endostaffella, Endotaxis, Endoteba, Endotebanella, Endothyra, Endothyranella, Endothyranopsis, Eoendothyranopsis, Eofusulina, Eoguttulina, Eoparafusulina, Eoparastaffella, Eopolydiexodina, Eoschubertella, Eostaffella, Eotextularia, Eotuberitina, Eowaeringella, Eozellia, Epistominella, Eponides, Eulepidina, Falsopalmula, Fissurina, Florilus, Frondicularia, Frondina, Frumentella, Fursenkoina, Fusiella, Fusulina, Fusulinella, Gallowayinella, Gandinella, Gavelinella, Gavelinopsis, Geinitzina, Geinitzinita, Gifuella, Gifuelloides, Glabratella, Glandulina, Globivalvulina, Globobulimina, Globocassidulina, Globoendothyra, Globulina, Glomodiscus, Grigelis, Grillina, Grovesella, Guttulina, Gyroidina, Gyroidinoides, Hanzawaia, Heterolepa, Heterostegina, Hoeglundina, Homotrema, Howchinia, Hyalinonetrion,

Ichthyofrondina, Ichthyolaria, Inyoschwagerina, Islandiella, Jigulites, Kahlerella, Kahlerina, Kanmeraia, Kansanella, Klamathina, Kriptoseptida, Kubergandella, Laevidentalina, Lagena, Lagenoglandulina, Langella, Lantschichites, Lasiodiscus, Laxifusulina, Leeina, Leella, Lenticulina, Lepidocyclina, Lepidolina, Lepidorbitoides, Leptotriticites, Likharevites, Lingulina, Lingulogavelinella, Lingulonodosaria, Lockhartia, Loeblichia, Lunucammina, Maklaya, Marginulina, Marginulinopsis, Mediocris, Melonis, Mesoschubertella, Metadoliolina, Millerella, Miniacina, Minojapanella, Miscellanea, Misellina, Mississippina, Moellerites, Mohlerina, Monodiexodina, Monotaxinoides, Montiparus, Mucronina, Mufushanella, Multiseptida, Nagatodarvasiella, Nanicella, Nankinella, Nanlingella, Neoarchaediscus, Neoconorbina, Neodutkevitchia, Neoendothyra, Neoeponides, Neofusulinella, Neoschwagerina, Neostaffella, Neothailandina, Nibelia, Nigribaccinus, Nipponitella, Nodoinvolutaria, Nodosaria, Nodosinella, Nodosinelloides, Nonion, Nonionella, Nonpseudofusulina, Notorotalia, Nummulites, Oberhauserella, Occidentoschwagerina, Ogbinella, Omphalocyclus, Omphalotis, Oolina, Operculina, Orbitoides, Oridorsalis, Orobias, Ozawainella, Pachyphloia, Palaeofusulina, Palaeospiroplectammina, Palaeotextularia, Palmula, Pamirina, Paraboultonia, Paracolaniella, Parafusulina, Paraglobivalvulina, Paraleeina, Paralingulina, Parareichelina, Pararotalia, Paraschwagerina, Parastaffella, Parastaffelloides, Parathurammina, Paratikhinella, Parazellia, Perigondwania, Permodiscus, Pisolina, Planoarchaediscus, Planoendothyra, Planorbulina, Planorbulinella, Planospirodiscus, Planostegina, Planularia, Planulina, Plectofusulina, Plectogyra, Plectostaffella, Pleurostomella, Pojarkovella, Polydiexodina, Polymorphina, Postendothyra, Praeobsoletes, Praepseudofusulina, Praesiderolites, Praeskinnerella, Pravitoschwagerina, Profusulinella, Protelphidium, Protonodosaria, Protriticites, Pseudoammodiscus, Pseudochusenella, Pseudodoliolina, Pseudodunbarula, Pseudoendothyra, Pseudofusulina, Pseudofusulinella, Pseudofusulinoides, Pseudokahlerina, Pseudolangella, Pseudolituotuba, Pseudonodosaria, Pseudophragmina, Pseudopolymorphina, Pseudoreichelina, Pseudoschwagerina, Pseudosiderolites, Pseudostaffella, Pseudotristix, Putrella, Pyramidulina, Pyrulina, Quasiendothyra, Quasifusulina, Quasifusulinoides, Ramulina, Rauserella, Rauserites, Rectoglandulina, Rectostipulina, Reichelina, Reitlingerina, Reussella, Robertina, Robuloides, Robulus, Robustoschwagerina, Rosalina, Rotalia, Rotorbinella, Rugosochusenella, Rugosofusulina, Ruzhenzevites, Sagrina, Saracenaria, Schagonella, Schellwienia, Schubertella, Schubertina, Schwagerina, Schwageriniformis, Seminovella, Septabrunsiina, Septoglobivalvulina, Shuguria,

Sichotenella, Siderolites, Sigmomorphina, Siphogenerina, Siphonina, Skinnerella, Skinnerina, Sphaeroschwagerina, Sphaerulina, Spireitlina, Spirillina, Spiroclypeus, Staffella, Stensioeina, Stewartina, Stilostomella, Subaljutovella, Sumatrina, Svratkina, Syzrania, Tetrataxis, Tezaquina, Thailandina, Thompsonella, Tikhinella, Toriyamaia, Trifarina, Tristix, Triticites, Tuberitina, Tumulotriticites, Turrispirillina, Uralodiscus, Uvigerina, Vaginulina, Vaginulinopsis, Valvulinella, Valvulineria, Verbeekina, Verella, Vicinesphaera, Virgulina, Wanganella, Wedekindellina, Xiaoxinzhaiella, Yabeina, Yangchienia, Zellerella, Zellerina

Chapter 3

The impacts of seawater Mg/Ca and temperature on element incorporation in foraminiferal calcite

Lennart J. de Nooijer, Inge van Dijk, Takashi Toyofuku and Gert-Jan Reichart

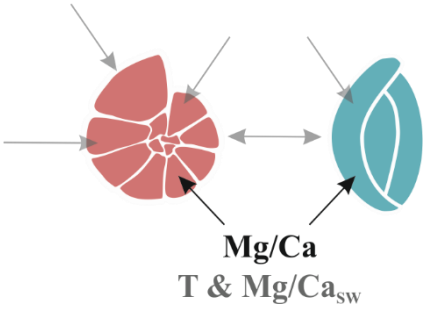

Abstract

On geological timescales, oceanic [Mg^{2+}] and [Ca^{2+}] vary with changing rates of weathering, seafloor spreading and dolomite formation. Accurate reconstruction of the ratio between [Mg^{2+}] and [Ca^{2+}] in seawater (Mg/Ca_{SW}), may potentially be reconstructed using foraminiferal Mg/Ca ratios. For this approach, species with contrasting Mg-incorporation mechanisms from the same paleoceanographic samples need to be compared. Since both temperature and seawater Mg/Ca impact foraminiferal Mg/Ca, successful reconstruction of Mg/Ca_{SW} requires quantification of both these parameters independently on foraminiferal Mg/Ca, as well as their combined effect on Mg-incorporation. Here we present the combined and isolated impacts of temperature and Mg/Ca_{SW} on Mg incorporation in two model species, the benthic foraminifers *Elphidium crispum* and *Quinqueloculina* sp. using controlled growth experiments. Specimens of these two species were kept at four different temperatures (ranging from 10 to 27 °C) and three Mg/Ca_{SW}'s (3.4, 6.4 and 8.5 mol/mol), resulting in 12 experimental conditions. Newly grown calcite was analyzed for a number of elements (Na, Mg and Sr) by laser ablation-ICP-MS. Results show that although the Mg/Ca varied by more than an order of magnitude between species, the sensitivity of Mg incorporation with respect to temperature was not impacted by Mg/Ca_{SW}. These results allow for an improved accuracy in the reconstruction of past Mg/Ca_{sw} based on foraminifera with contrasting Mg/Ca.

1. Introduction

Foraminiferal calcite element concentrations are popular tools to reconstruct past seawater conditions and thereby serve as the basis of many paleoclimate reconstructions. Incorporation of magnesium (Mg) into their test (i.e. shell) calcite is a function of ambient temperature (Nürnberg et al., 1996; Elderfield and Ganssen, 2000; Anand et al., 2003) and can hence be used in fossil specimens to derive past seawater temperatures (Hastings et al., 1998; Lear et al., 2000). Salinity and carbonate ion concentration additionally impact foraminiferal Mg/Ca (Nürnberg et al., 1996; Rosenthal et al., 1997; Yu and Elderfield, 2008; Dueñas-Bohórquez et al., 2009; Dueñas-Bohórquez et al., 2011), but in many environmental settings, these influences are relatively small or can be accounted for using other proxies, e.g. B/Ca for saturation state (Yu and Elderfield, 2007) and Na/Ca for salinity (Wit et al., 2013; Allen et al., 2016).

The ratio of $[Mg^{2+}]$ over $[Ca^{2+}]$ in seawater (Mg/Ca_{SW}) has a significant effect on the foraminiferal Mg/Ca (Segev and Erez, 2006) and thus needs to be corrected for when reconstructing seawater temperature from periods with a different Mg/Ca_{SW} than that of today (~5). Due to changes in the balance between rates of weathering, seafloor spreading and dolomite formation, Mg/Ca_{sw} changes over geological timescales (Hardie, 1996; Holland and Zimmermann, 2000; Steuber and Veizer, 2002; Berner, 2004; Farkaš et al., 2007). Due to the relatively long residence times of Ca^{2+} and Mg^{2+} (~1 and ~13 Ma, respectively; Broecker et al., 1982), changes in this ratio are notable over timescales >1 Ma. For example, Mg/Ca_{SW} during the early Cretaceous was close to 1 (Hardie, 1996; Farkaš et al., 2007) and application of uncorrected Mg/Ca-T calibrations would thus greatly underestimate seawater temperatures at that time (e.g. Hasiuk and Lohmann, 2010; Evans and Müller, 2012).

When applying Mg/Ca as a temperature proxy to foraminifera older than ~1 Ma, a correction factor based on reconstructed Mg/Ca_{SW} is often applied (e.g. Lear et al., 2000; Billups and Schrag, 2002; Tripati et al., 2005; Evans et al., 2015). This approach assumes that the sensitivity of the relation between foraminiferal Mg/Ca and seawater temperature remains constant. Although several studies have quantified the sensitivity of foraminiferal Mg/Ca as a function of both temperature (Nürnberg et al., 1996; Lea et al., 1999; Toyofuku et al., 2000) and Mg/Ca_{SW} (Segev and Erez, 2006; Raitzsch et al., 2010), the synergistic effects of those parameters remains to be investigated.

Here we present results from a culturing study using two benthic species with contrasting calcification mechanism: the perforate *Elphidium crispum*, precipitating

calcite with a low Mg content (~5 mmol/mol; Allison et al., 2010) and the miliolid *Quinqueloculina* sp. (Mg/Ca = ~140 mmol/mol; Toyofuku et al., 2000). Mg incorporation in the former increases exponentially with temperature (e.g. Nürnberg et al., 1996; Nürnberg, 2015), whereas it increases linearly with temperature in miliolid foraminifera (Toyofuku et al., 2000; Wit et al., 2012). The difference in absolute Mg content between these two species is a consequence of the different biomineralization strategies between perforate and miliolid foraminifera (Debenay et al., 1998; Erez, 2003; Bentov and Erez, 2006; De Nooijer et al., 2009). In our culturing experiment, seawater temperature and Mg/Ca_{sw} were varied independently to quantify the effect of these two parameters combined as well as separated. Newly formed calcite was also analyzed for Na- and Sr- concentrations to quantify the impact of temperature and Mg/Ca_{SW} on incorporation of these elements.

2. Methods

2.1 Culture set-up

Culturing experiments were conducted at the Japan Agency for Marine-Earth Sciences and Technology (JAMSTEC), Japan. Different species of shallow benthic foraminifera were collected from Morito-kaigan rocky shore (N 35°15'57.6", E 139°34'14.9"), Hayama, Miura peninsula, Kanagawa, Japan in October 2012. Upon return in the laboratory, specimens of *Elphidium crispum* and *Quinqueloculina* sp. were isolated from sieved sediment (>125 µm). To monitor chamber addition, single specimens were photographed at 50x magnification using a Zeiss Stemi 2000-C microscope with an Axiocam ERc 5s camera (Zeiss, Germany). After photographing, single specimens were placed in 20 ml vials with screw caps to avoid evaporation and minimize changes in salinity and carbonate chemistry. Vials were filled with the three different media (Table 1) and placed in incubators with three different temperatures (17, 22 and 27 °C) with a 12 hour dark-light cycle for 100 days. This resulted in specimens which were cultures in nine different conditions. After termination of the culturing experiment on day 100, the foraminifera were photographed again. Specimens were then rinsed three times with ultrapure water (18.2 Ω), once with NaOCl (5%) for 15 minutes and again three times with ultrapure water to remove any remaining salts and organic matter at the test surface. Prior to laser ablation-ICP-MS analysis, specimens were dried overnight at 45°C.

Artificial seawater (ASW) was prepared by mixing salts (KANTO Chemicals Co. Inc., Japan) according to Kester et al. (1967) corresponding to the average chemical composition of seawater. Gravimetric salts and volumetric salts (excluding $MgCl_2*6H_2O$) were dissolved in 2,000 and 1,000 gram, respectively, of ultrapure water before combining with the other salts to avoid precipitation of $CaCO_3$, $CaSO_4$, $SrCO_3$ or $SrSO_4$. Seawater Mg/Ca was altered by changing the amount of $MgCl_2*6H_2O$, resulting in ASW with different $[Mg^{2+}]$. The reduction in $[Cl^-]$ was compensated by addition of NaCl. Seawater element composition was determined by ICP-MS (X-series, Thermo Fisher). Analytical precision was 0.4% for Mg/Ca and Na/Ca and 0.5% Sr/Ca. Seawater Mg/Ca ratios produced were 3.43, 6.40 and 8.55 (± 0.05) mmol/mol (Table 1). Salinities of the culture media were determined using a VWR CO310 salinometer at the beginning and end of the experiments and ranged from 35.0 to 35.3.

Element	**ASW1**	**ASW2**	**ASW3**
Ca	9.31 (±0.09)	8.88 (± 0.23)	9.39 (± 0.14)
Mg	31.9 (± 0.3)	56.7 (± 1.3)	80.1 (± 1.1)
Na	533 (± 4)	481 (± 12)	452 (± 6)
Sr	0.159 (± 0.001)	0.152 (± 0.003)	0.161 (±0.003)
Mg/Ca (mol/mol)	3.43 (± 0.01)	6.40 (± 0.02)	8.55 (± 0.05)
Na/Ca (mol/mol)	57.3 (± 0.2)	54.2 (± 0.1)	48.1 (± 0.3)
Sr/Ca (mmol/mol)	17.1 (± 0.1)	17.1 (± 0.1)	17.1 (± 0.1)

Table 1: element composition of the prepared culture media. All concentrations are in mmol/Kg seawater, standard deviations in parentheses (n=9).

Incubated specimens were fed the green algae *Chlorella*, which was cultured in natural seawater (NSW). To avoid contamination of seawater with NSW Mg/Ca ratio (~5.2 mmol/mol) when adding the algae cells to the culture vials, the *Chlorella* cells were centrifuged for 5 minutes at 3000 rpm and dissolved in the three ASWs (Table 1) at 17 °C.

2.2 Calcite element analyses

Element composition of the newly formed calcite (expressed as $Na/Ca_{CALCITE}$, $Mg/Ca_{CALCITE}$, etc.) was determined by Laser Ablation-Inductively Coupled Plasma-Mass Spectrometry (LA-ICP-MS) at Utrecht University (Reichart et al., 2003). This system consists of a Lambda Physik Excimer laser system with GeoLas 200Q optics. Ablation was performed in a helium atmosphere at a pulse repetition of 6 Hz, energy density of ~ 1 J/cm^2 and a spot diameter of 40 or 60 µm until the test wall was completely penetrated, usually lasting 30-50 seconds. Ablated particles were measured using a sector field ICP-MS (Element2, Thermo Fisher). Scanned masses included ^{23}Na, ^{24}Mg, ^{26}Mg, ^{27}Al, ^{43}Ca, ^{44}Ca, ^{55}Mn and ^{88}Sr. Calibration and standardization was done using a NIST SRM 610 glass (values from Jochum et al., 2012) that was ablated using a higher laser fluency of ~5 J/cm^2. Using a different energy density between foraminiferal calcite and glass standard has been shown to not affect the analyses (Dueñas-Bohórquez et al., 2009). Analytical precision (relative standard deviation (RSD) of all NIST610 measurements) was 3% for ^{26}Mg, 5% for ^{23}Na and 3% for ^{88}Sr The obtained time resolved counts were blank subtracted, internally standardized to ^{43}Ca and calibrated using data reduction software (Glitter) to obtain depth profiles (Fig. 1) and calculate the single chamber $Mg/Ca_{CALCITE}$, $Na/Ca_{CALCITE}$ and $Sr/Ca_{CALCITE}$ etc.

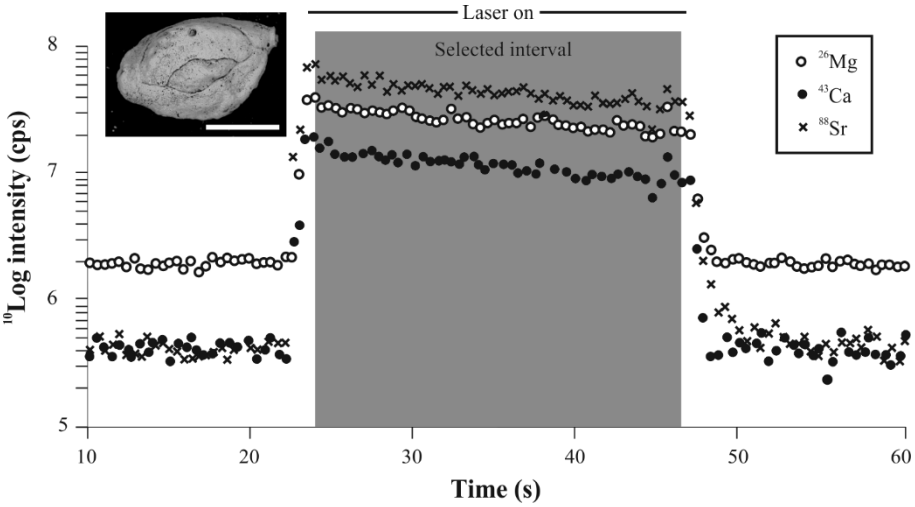

Figure 1. Representative example of a laser ablation profile for ^{26}Mg (white circles), ^{43}Ca (black circles) and ^{88}Sr (crosses) for *Quinqueloculina* sp. Scale bar at inset: 500 µm.

In total 86 chambers were analysed, 39 for *Quinqueloculina* sp. and 47 for *E. crispum*. For *Quinqueloculina* sp., 2 measurements were discarded due to short ablation profiles and related high element concentrations. The remaining 84 single laser spot measurements used for calculating average element concentrations were relatively evenly dispersed over the 12 experimental conditions. We calculated the standard deviation (SD) and relative standard deviation (RSD) per treatment. The partition coefficient (D) of an element (E) between seawater and foraminiferal calcite is expressed as $D_E = (E/Ca_{CALCITE})/(E/Ca_{SW})$.

3. Results

3.1 Foraminiferal Mg/Ca

Obtained $Mg/Ca_{CALCITE}$ increased with temperature and Mg/Ca_{SW} in both species (Table 2).

ASW	**T**	**n**	**Na/Ca (mmol/mol)**	**D_{Na} ($*10^{-3}$)**	**^{26}Mg/Ca (mmol/mol)**	**D_{Mg} ($*10^{-3}$)**	**Sr/Ca**	**D_{Sr}**
***Quinqueloculina* sp. (n=37)**								
1	10	2	3.8±2.9	0.03± 0.05	120.1±2.1	35.0± 0.6	3.4±1.0	0.16± 0.06
1	17	8	4.8±0.5	0.08± 0.01	130.5±4.1	38.3± 1.3	2.9±0.1	0.17± 0.01
1	22	4	4.8±0.9	0.08± 0.02	133.9±7.1	39.3± 2.3	3.3±0.6	0.19± 0.04
1	27	2	5.5±0.2	0.10± 0.00	142.5±1.1	41.9± 0.4	3.0±0.2	0.18± 0.01
2	10	6	6.5±2.0	0.12± 0.04	132.0±4.1	20.6± 0.6	3.0±0.1	0.17± 0.01
2	17	5	3.8±0.9	0.07± 0.02	138.3±3.1	21.6± 0.5	3.3±0.8	0.19± 0.05
2	22	1	5.3	0.10	139.8	21.80	3.5	0.21
2	27	2	5.6±0.04	0.10± 0.01	147.2±1.1	23.0± 0.2	3.1±0.1	0.18± 0.005
3	10	1	6.4	0.13	138.4	16.30	3.7	0.22
3	17	2	6.4±0.4	0.14± 0.01	142.8±0.1	16.8± 0.1	3.8±0.9	0.22± 0.05
3	22	1	5.1	0.11	153.3	18.00	3.0	0.17
3	27	3	4.9±1.7	0.10± 0.03	154.4±3.1	18.2± 0.4	3.1±0.4	0.18± 0.02

Elphidium crispum (n=47)								
1	10	1	4.3	0.08	2.19	0.64	2.30	0.13
1	17	8	6.9±1.7	0.12± 0.03	3.03±0.86	0.89± 0.25	2.6±0.2	0.15± 0.01
1	22	7	7.8±1.6	0.14± 0.03	4.06±0.63	1.19± 0.19	2.0±0.4	0.12± 0.02
1	27	2	8.4±0.2	0.15± 0.00	4.81±0.05	1.42± 0.01	2.3±0.7	0.14± 0.04
2	10	3	7.9±0.8	0.15± 0.01	3.28±1.16	0.51± 0.18	1.5±0.1	0.08± 0.01
2	17	4	8.8±1.8	0.16± 0.03	4.71±0.87	0.74± 0.14	2.7±0.5	0.16± 0.03
2	22	9	6.7±1.8	0.12± 0.03	6.21±1.30	0.97± 0.20	2.6±0.5	0.15± 0.03
2	27	0	n.m.	n.m.	n.m.	n.m.	n.m.	n.m.
3	10	0	n.m.	n.m.	n.m.	n.m.	n.m.	n.m.
3	17	7	6.1±1.4	0.13± 0.03	8.29±1.59	0.97± 0.19	2.4±0.4	0.14± 0.02
3	22	6	8.0±2.2	0.17± 0.05	9.27±2.38	1.09± 0.28	2.5±0.3	0.15± 0.02
3	27	0	n.m.	n.m.	n.m.	n.m.	n.m.	n.m.

Table 2. Average element to calcium ratio and partition coefficient per condition of *Quinqueloculina* sp. and *Elphidium crispum*. Standard deviations in parentheses.

In *Quinqueloculina* sp., $Mg/Ca_{CALCITE}$ increased with temperature and was approximately 30 times higher than in *E. crispum*, for which the $Mg/Ca_{CALCITE}$ increases with temperature. For $Mg/Ca_{CALCITE}$ measurements on chambers from *E. crispum* obtained from one condition, the average standard deviation (n=12) is 1.1 mmol/mol, corresponding to an average relative standard deviation (RSD) of 18%. For *Quinqueloculina* sp., the average standard deviation for the $Mg/Ca_{CALCITE}$ values within one treatment (with 12 treatments in total) is 3.8 mmol/mol, corresponding to an average RSD of 1.6%. A multiple linear regression analysis for the $Mg/Ca_{CALCITE}$ of *Quinqueloculina* sp. as a function of both temperature and Mg/Ca_{SW} (Fig. 2) shows that the $Mg/Ca_{CALCITE}$ of this species is best described by:

(**1**) $Mg/Ca_{Quinqueloculina} = 1.02(\pm0.11)*T + 2.87(\pm0.34)*Mg/Ca_{sw} +102.6(\pm2.8)$

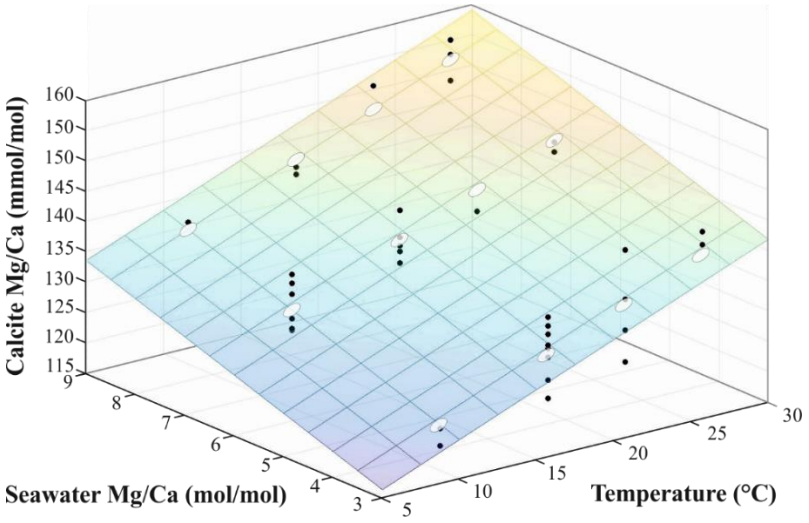

Figure 2. Measured Mg/Ca$_{CALCITE}$ (mmol/mol) for *Quinqueloculina* sp. as a function of Mg/Ca$_{sw}$ (mol/mol) and temperature (°C). The plane is based on equation 1, the transparent ellipses indicate the modelled Mg/Ca$_{CALCITE}$ for the experimental conditions (i.e. above/below the clusters of measured Mg/Ca$_{CALCITE}$ are situated).

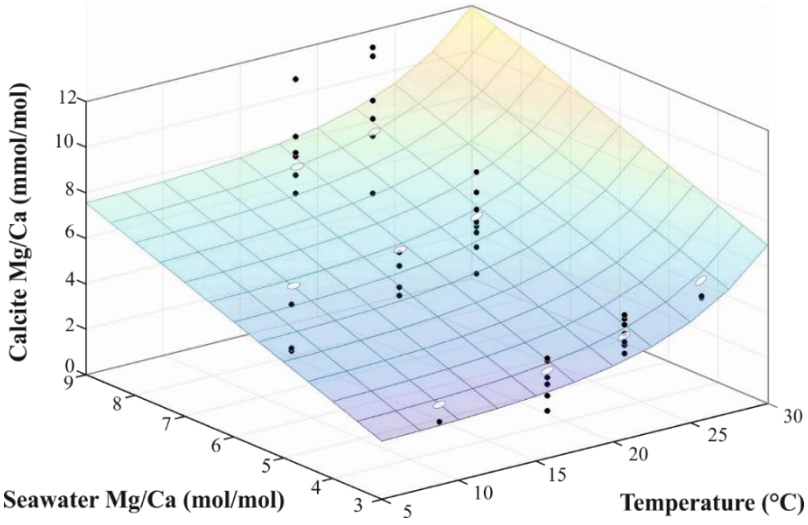

Figure 3. Measured Mg/Ca$_{CALCITE}$ (mmol/mol) for *E. crispum* as a function of Mg/Casw (mol/mol) and temperature (°C). The plane is based on equation 2, the transparent ellipses indicate the modelled Mg/Ca$_{CALCITE}$ for the experimental conditions (i.e. above/below the clusters of measured Mg/Ca$_{CALCITE}$ are situated).

The reported uncertainties associated with this multiple regression (Equation 1) represent the 95% confidence intervals and are based on the least sum of squares. R^2 value for this regression analysis is 0.82, $p<0.001$ (n=37). A linear regression model is chosen since this provides the highest correlation coefficient when relating foraminiferal Mg/Ca to seawater Mg/Ca (Hasiuk and Lohmann, 2010).

For *Elphidium crispum*, the multiple linear regression (Fig. 3) results in the equation:

2) $Mg/Ca_{Elphidium} = 10^{(0.0729\ (\pm0.054)*T\ -\ 1.54(\pm1.41))} + 0.831(\pm0.98)*Mg/Ca_{sw}$

The reported uncertainties associated with this multiple regression (**2**) represent the 95% confidence intervals and are based on the least sum of squares. R^2 value for this regression analysis is 0.67, $p<0.001$ (n=47). Contrary to the regression model for *Quinqueloculina* sp. (Fig. 1), an exponential regression was chosen for the Mg/Ca_{cc} as a function of temperature since this describes the relation between these two parameters best for low-Mg, rotalid species (e.g. Anand et al., 2003; Toyofuku et al., 2011). The relation between Mg/Ca_{cc} of low-Mg calcite and Mg/Ca_{sw} is assumed to be linear, as described previously (Segev and Erez, 2006; Raitzsch et al., 2010; Mewes et al., 2014).

3.2 Foraminiferal Na/Ca and Sr/Ca

For *Elphidium crispum*, average $Na/Ca_{CALCITE}$ was 7.3 mmol/mol (±1.8 SD) and 5.9 mmol/mol (±3.7 SD) for *Quinqueloculina* sp. (Table 2). For neither species, these values did not vary with Mg/Ca_{SW}, and nor were they correlated to temperature (Fig. 4). Since $[Na^+]$ varied between conditions due to the addition of NaCl (Table 1; from 57 to 48 mol Na/ mol Ca), the foraminiferal sodium content is expressed as the partition coefficient (D_{Na}), equaling $(Na/Ca_{CALCITE})/(Na/Ca_{SW})$. $Sr/Ca_{CALCITE}$ were slightly higher in *Quinqueloculina* sp., 3.4 mmol/mol (±1.6 SD), than in *E. crispum*, 2.4 mmol/mol (±0.46 SD), showing no clear trend with temperature, nor with Mg/Ca_{SW} (Fig. 5), which is in contrast to findings of Mewes et al. (2015), reposting a linear increase of $Sr/Ca_{CALCITE}$ with increasing $Mg/Ca_{CALCITE}$. When comparing species, however, incorporation of Sr in foraminiferal calcite showed an approximately 1.5 times higher Sr/Ca in *Quinqueloculina* sp. than in *E. crispum*.

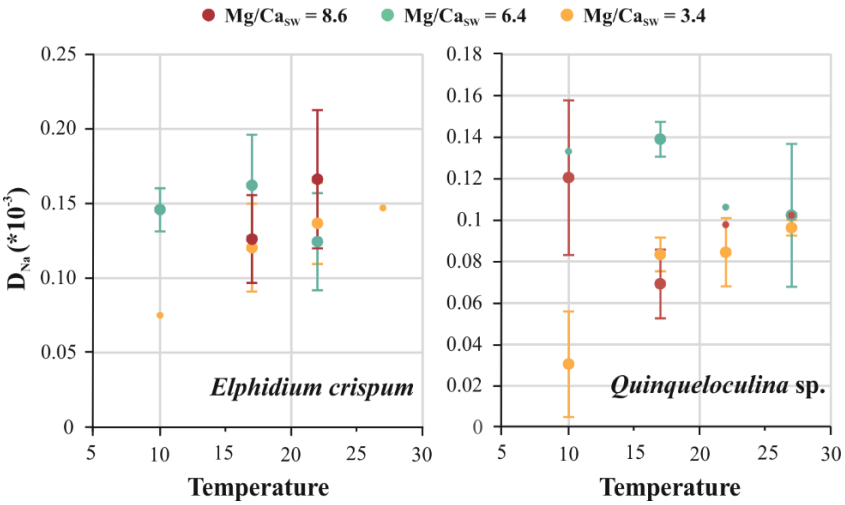

Figure 4. Partition coefficient of Na (D_{Na}) in *E. crispum* (left) and *Quinqueloculina* sp. (right) versus seawater temperature. Different seawater Mg/Ca are indicated by different colors. Small spots indicate single laser ablation measurements.

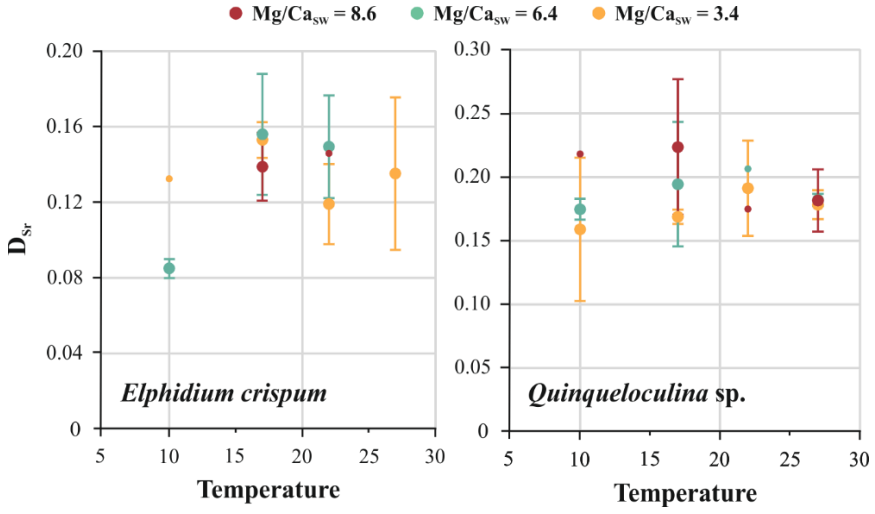

Figure 5. Partition coefficient of Sr (D_{Sr}) in *E. crispum* (left) and *Quinqueloculina* sp. (right). Different seawater Mg/Ca are indicated by different colors. Small spots indicate single laser ablation measurements.

4. Discussion

4.1 Sr and Na incorporation in hyaline and miliolid foraminifera

The obtained D_{Na} are similar for both species and not related to temperature or Mg/Ca_{SW} (Fig. 5). The ratios are in the same range as those reported for cultured specimens of the benthic *Ammonia tepida* (Wit et al., 2013) and the planktonic G*lobigerinoides sacculifer* and *Orbulina universa* cultured at a similar salinity (Delaney et al., 1985). Previously reported Sr/Ca for most foraminiferal species are lower than those reported here, ranging from 1.3 to 1.5 in field collected planktonic species (e.g. Friedrich et al., 2012) and from 0.80 to 1.0 in core-top derived specimens of the benthic *Oridorsalis umbonatus* (Dawber and Tripati, 2012). These differences are mainly caused by the relatively high $[Sr^{2+}]$ in our culture media. When expressing the Sr/Ca as partition coefficient (D_{Sr}), we obtain partition coefficients of 0.13 for *E. crispum* and 0.19 for *Quinqueloculina* sp. Similar D_{Sr} were also found in cultured specimens of *Elphidium williamsoni* (0.13-0.16; Allison et al., 2011), *Ammonia* spp. (0.17; Dueñas-Bohórquez et al., 2011; De Nooijer et al., 2014a) and the planktonic *G. sacculifer* (0.15; Dueñas-Bohórquez et al., 2011). Comparable to the D_{Sr} reported here for *Quinqueloculina* sp. (0.19), Sr partitioning in the high-Mg secreting miliolid species *Marginopora vertebralis* and *Amphisorus hemprichii* cultured at similar conditions were 0.14 to 0.21 (Raja et al., 2005).

The impact of Mg/Ca_{SW} on incorporation of elements other than Mg in the species studied here is negligible (Fig. 4 and 5). This means that past changes in Mg/Ca_{SW} do not affect calibrations for $Na/Ca_{CALCITE}$ as a function of salinity (Wit et al., 2013) and $Sr/Ca_{CALCITE}$ as a function of Sr/Ca_{SW} (Elderfield and Ganssen, 2000; Raitzsch et al., 2010; Dueñas-Bohórquez et al., 2011). Seawater temperature has no significant impact on Na- and Sr-incorporation over the ranges studied here, which is in line with previous studies on Sr incorporation in foraminiferal calcite (e.g. Russell et al., 2004; Dissard et al., 2010).

4.2 Magnesium in foraminifera as a function of temperature and seawater Mg/Ca

The relation between $Mg/Ca_{CALCITE}$ of low-Mg foraminifera and seawater temperature is generally described by an exponential function (e.g. Nürnberg et al., 1996; Lea et al., 1999; Anand et al., 2003; Toyofuku et al., 2011; Wit et al., 2012). The sensitivity (exponential constant) for the calibrations of most of these species vary between 0.05

and 0.10. The sensitivities for the specimens of *E. crispum* grown at Mg/Ca_{SW} of 3.4 – 8.6 are similar, suggesting that the sensitivity of Mg incorporation as a function of temperature is independent of Mg/Ca_{SW} in this species. Partition coefficients (D_{Mg}) calculated from the calcite Mg/Ca and seawater Mg/Ca, i.e. $(Mg/Ca_{CALCITE})/(Mg/Ca_{SW})$, in *E. crispum* are between 0.0005 and 0.014.

In species in which magnesium is incorporated at high concentrations (>100 mmol/mol Mg/Ca), $Mg/Ca_{CALCITE}$ increases linearly with temperature (Toyofuku et al., 2000; Toyofuku and Kitazato, 2005). Sensitivity for *Quinqueloculina* sp. varies between 0.81 and 1.2 (increase in mmol Mg/mol Ca per °C), whereas sensitivity for other species vary between 1.6 and 2.9. Consequently, the y-axis intercept for *Quinqueloculina* sp. (Fig. 2) lies between 100 and 130 mmol/mol, while those previously reported are in the range of 65-90 mmol/mol (Toyofuku et al., 2000; Toyofuku and Kitazato, 2005). Results from the multiple linear regression indicate that the impact of temperature on Mg incorporation in this species is independent of that of Mg/Ca_{SW}. Calculated partition coefficients for Mg are in the range of 0.015 and 0.045, increasing significantly with decreasing Mg/Ca_{SW}.

For both species, Mg/Ca_{SW} has a clear impact on the amount of Mg incorporated in the foraminiferal calcite. Across the temperature range studied here, the increase in $Mg/Ca_{CALCITE}$ for every increase of 1 mol/mol in Mg/Ca_{SW} is 0.59 and 3.8 mmol/mol for *E. crispum* and *Quinqueloculina* sp., respectively (Fig. 2 and 3; equations 1 and 2). In both species, this equals an increase in $Mg/Ca_{CALCITE}$ of 2-3% per 1 mol/mol increase in Mg/Ca_{SW}. These results show that despite very different absolute $Mg/Ca_{CALCITE}$ values, and despite different temperature sensitivities, the relative response to changes in Mg/Ca_{SW} are similar for these two species. They are also comparable to the relative increase in $Mg/Ca_{CALCITE}$ with changing Mg/Ca_{SW} in *Amphistegina lobifera* and *A. lessonii* (Segev and Erez, 2006) and *Heterostegina depressa* (Raitzsch et al., 2010). The general differences between calibrations presented here for the high-Mg/Ca miliolid and low-Mg perforate species is in line with the general difference in calcification strategy between these groups (Hemleben et al., 1986; De Nooijer et al., 2009).

4.3 Paleoceanographic implications

When using foraminiferal calcite for paleoceanographic reconstructions past ~1 Myr ago, deviations in Mg/Ca_{SW} from current day ratios need to be accounted for. Existing models for past changes in Mg/Ca_{SW} show that in the Miocene, for example, ratios

were 3-4 mol/mol (Hardie, 1996; Stanley and Hardie, 1998; Farkaš et al., 2007) and could have been as low as 1-2 mol/mol in the Paleocene (Stanley and Hardie, 1998; Berner, 2004). Using fossil foraminiferal $Mg/Ca_{CALCITE}$ for paleotemperature estimates from these periods thus requires application of a correction factor. Using two species with contrasting $Mg/Ca_{CALCITE}$ may provide the opportunity to circumvent the use of a correction factor based on modelled Mg/Ca_{SW} using their respective calibrated correlations to both temperature and Mg/Ca_{SW}. It is assumed in this approach, however, that the sensitivities of $Mg/Ca_{CALCITE}$ remain constant over the range of Mg/Ca_{SW} studied. Our results show that this is the case and that combining $Mg/Ca_{CALCITE}$ of low-Mg and miliolid foraminifera can be used to accurately reconstruct past seawater temperature and Mg/Ca_{SW}.

When using a modelled past seawater Mg/Ca_{SW} to correct for $Mg/Ca_{CALCITE}$-based seawater temperatures (for example when only perforate foraminifera are available), it has been argued that a power, instead of a linear function should be applied to correct fossil $Mg/Ca_{CALCITE}$ (Hasiuk and Lohmann, 2010; Evans and Müller, 2012). The reason for this is the non-linear relation between D_{Mg} and Mg/Ca_{SW} previously found (e.g. Delaney et al., 1985; Segev and Erez, 2006; Raitzsch et al., 2010). In our results, however, the partition coefficient for Mg did not change notably with Mg/Ca_{SW} in *E. crispum*, reflected by the $Mg/Ca_{CALCITE}$-Mg/Ca_{SW} correlation passing the origin closely (Fig. 3). For *Quinqueloculina*, the correlation between D_{Mg} and Mg/Ca_{SW} is almost equally well described by a power and linear function ($R^2 = 0.98$ versus 0.92). This suggests that when using these species, the offset in past Mg/Ca_{SW} when using a power function-based correction factor versus a linear-based factor is very small.

On short timescales (i.e. <1 Ma), salinity is the environmental parameter most likely biasing Mg/Ca-based temperature reconstructions. Our results show that on these timescales, $Mg/Ca_{CALCITE}$ and $Na/Ca_{CALCITE}$ can be combined to simultaneously and accurately reconstruct salinity and temperature, either using pooled and dissolved specimens or at the resolution of a single foraminiferal chamber using LA-ICP-MS. The sensitivity of $Mg/Ca_{CALCITE}$ to salinity has been reported to be approximately the equivalent of ~1 °C reconstructed temperature for a change in 2 salinity units (Lea et al., 1999; Kısakürek et al., 2008; Dissard et al., 2010; Hönisch et al., 2013). Nürnberg et al. (1996) reported a higher sensitivity (~2 °C reconstructed temperature increase for every salinity unit increase), but this result was based on a limited number of measurements. Possibly, the effect of salinity on Mg/Ca is caused by overgrowth of a

phase rich in Mg after burial of the test in the sediment (e.g. Hoogakker et al., 2009) and/ or differential rates of dissolution (Hönisch et al., 2013).

5. Conclusions

Incorporation of Mg in the benthic perforate foraminifer *Elphidium crispum* and the miliolid *Quinqueloculina* sp. increases as a function of both temperature and seawater Mg/Ca. The sensitivity of this increase with temperature does not change as a function of seawater Mg/Ca over the ranges studied here. The overall difference in Mg/Ca and the sensitivity of their increase with temperature between the two species results from the difference in biomineralization strategies between perforate and miliolid species, likely as a difference in the balance between transmembrane ion transport- and seawater-derived Mg^{2+}. The combined seawater Mg/Ca-temperature calibration shows that the cumulative impacts of these two parameters on foraminiferal Mg/Ca are similar to the individual impacts on Mg-incorporation**.**

Chapter 4

Contrasting trends in element incorporation in hyaline and miliolid foraminifera

Inge van Dijk, Lennart J. De Nooijer and Gert-Jan Reichart

DOI:10.5194/bg-2016-402

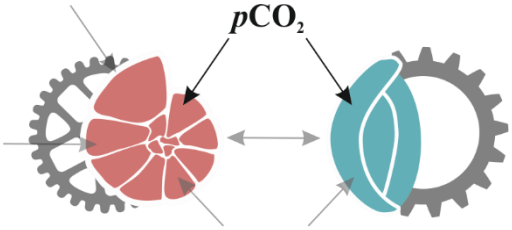

Abstract

We analyzed trends in element incorporation between hyaline (perforate) and miliolid (imperforate) foraminifera in order to investigate processes involved in calcification affecting element incorporation into foraminiferal carbonate. For both groups, we observed similar trends in element incorporation with pCO_2, suggesting there is some mechanisms to transports ions to the site of calcification are similar for both calcification pathways, although the impact might be different across species. A previously published trans-membrane transport model assumes foraminifera utilize Ca^{2+} channels to transport calcium to the site of calcification. These channels are somewhat a-specific, leading to (accidental) transport of other free ions. By modelling the activity of free ions as a function of pCO_2, we observed that speciation of some elements (like Zn and Ba) are heavily influenced by the formation of carbonate complexes. This leads to an increase in availability of free Zn and Ba with increasing pCO_2, which leads to more transport to the site of calcification and subsequently incorporation in the foraminiferal shell. We further observed that incorporation of the trace elements studied here is positively correlated between the hyaline test building species. This could be due to dissimilar activity and/or selectivity of calcium channels between species, perhaps due to differences in size. For miliolid calcification, part of the calcium is obtained not only through channels but by also included seawater vesicles, which leads to similar element to calcium ratios between species and element partitioning which is more in line with inorganic carbonates.

1. Introduction

On the broadest taxonomic scale, calcareous foraminifera, cosmopolitan unicellular protists, produce tests using either one of two fundamentally different mechanisms. These calcification strategies reflect the evolutionary separation of foraminiferal groups dating back to the Cambrian diversification, from where the imperforate miliolids and perforate hyaline foraminifera, developed independently (Pawlowski et al., 2003). The calcification process of the latter group has been studied more extensively than that of the miliolids (De Nooijer et al., 2014b). Although many aspects of perforate calcification remain unsolved, there is consensus that chamber formation takes place extracellularly, but within a (semi-) enclosed space, generally termed the site of calcification (SOC). The first layers of calcite precipitate on an organic matrix (the POS or primary organic sheet) that serves as a template for the calcite layer that forms the chamber wall (Hemleben et al., 1977; Erez, 2003). To promote calcification, foraminifera furthermore need to remove Mg ions and/or protons (Zeebe and Sanyal, 2002) from the seawater entering the SOC. Many larger benthic foraminifera are hyaline species although the amount of Mg in their shells is often more than 10 times higher than that of planktonic and small benthic hyaline species, hence covering a large range in Mg/Ca values.

The calcification strategy of porcelaneous foraminifera is less well studied, which may be partly explained by their limited application in paleoceanography. Porcelaneous foraminifera use a different mode of calcification (Berthold, 1976; Hemleben et al., 1986; Debenay et al., 1998; De Nooijer et al., 2009) and produce shells without pores (hence, the term imperforate) consisting of tablets or needles (Debenay et al., 1998; Erez, 2003; Bentov and Erez, 2006). These calcitic needles (2-3µm) are precipitated intracellularly (Berthold, 1976), after which they are transported out of the foraminifer to form a new chamber (Angell, 1980). At the outer and inner layers of these chambers, the needles are arranged along the same orientation so that they form an optically homogenous surface, giving it a shiny (hence the term 'porcelaneous') appearance. In general the Mg/Ca values of the shells of porcelaneous foraminifera are high.

Remarkably, despite this large biological control, incorporation of minor and trace elements still reflects environmental conditions, in both hyaline and porcelaneous foraminiferal shells. For instance, the Mg/Ca of foraminiferal shells is primarily determined by seawater temperature (Allen and Sanders, 1994; Nürnberg et al., 1996) and seawater Mg/Ca (Chapter 3; Segev and Erez, 2006; Evans et al., 2015). After

correcting for the effect of the latter (if necessary) the use of foraminiferal Mg/Ca has been validated by its wide application as paleothermometer (Elderfield and Ganssen, 2000; Lear et al., 2000). Insight in vital effects (Erez, 2003) and inter-specific differences in trace element incorporation (Bentov and Erez, 2006; Toyofuku et al., 2011; Wit et al., 2012) is needed for making the Mg/Ca thermometer more robust. Systematic offsets between different species, interdependence of trace elements incorporated (Langer et al., in press.) and the different response of element incorporation on element speciation (Chapter 6; Keul et al., 2013b; Wit et al., 2013), potentially provides useful clues for determining which processes play an important role in the biomineralization pathways.

Here we present the results from a controlled growth experiment for which we used several (intermediate- and high-Mg) hyaline and miliolid species and an inter-species comparison of trace elements. We assessed the impact of bio-calcification on element incorporation as a function of pCO_2 in order to contrast the impact of different calcification strategies. During foraminiferal calcification, incorporation of certain elements or fractionation of certain isotopes is shown to depend on the carbonate system, e.g. $U/Ca_{CALCITE}$ (Russell et al., 2004; Keul et al., 2013b) and $Zn/Ca_{CALCITE}$ to $[CO_3^{2-}]$ (Marchitto et al., 2000; Chapter 6) and $\delta^{11}B$ to pH (Sanyal et al., 1996). Species-specific differences in partitioning and fractionation most likely primarily reflect differences in calcification strategy. Offsets are largest between hyaline and miliolid species, due to their fundamentally different calcification strategies (see for a summary, Toyofuku et al., 2011). Differences in chemical composition and their dependency on environmental variables can hence be used to identify key processes in miliolid and hyaline calcification. We cultured eight benthic foraminiferal species (4 hyaline and 4 porcelaneous) under four different pCO_2 conditions, analyzing incorporation of Mg, Sr, Na, Zn and Ba. Results are combined and compared with literature data, to identify processes involved in calcification.

2. Methods

2.1 Foraminiferal collection

Large samples of macroalgae (*Dictyota* sp.) were collected in November 2015 at a depth of 2-3 meters in Gallows Bay, St. Eustatius (N 17°28'31.6", W62°59'9.4"). Salinity was ~34 and temperature was ~29°C at the site of collection. The collected macroalgae were transported to the laboratory at the Caribbean Netherlands Science

Institute (CNSI), where they were placed in a 5 L aquarium with aerated and unfiltered seawater. From this stock, small amounts of algae and debris were gently sieved over a 90 and 600 µm mesh to carefully dislodge foraminifera. Several species of foraminifera were picked from the resulting 90-600 µm fraction. Living specimens of hyaline foraminifera *Asterigerina carinata* (d'Orbigny, 1839), *Amphistegina gibbosa* (d'Orbigny, 1839), *Heterostegina antillarum* (d' Orbigny, 1839) and *Planorbulina acervalis* (Brady, 1884), as well as porcelaneous species *Marginopora vertebralis* (Quoy & Gaimard, 1830), *Laevipeneroplis bradyi* (Cushman, 1930), *Archaias angulatus* and *Peneroplis pertusus* (Forskål, 1775) characterized by yellow cytoplasm and pseudopodial activity, were selected for the culturing experiments.

2.2 Culture set-up

We used an adapted version of the culture set-up descripted in Chapter 7. In short, four barrels each containing 100 L of seawater (5µm filtered), were connected to a Li-Cor CO_2/H_2O analyzer (LI-7000), to regulate the CO_2 level in the barrels' head space. The set levels were maintained by addition of CO_2 and/ or CO_2-scrubbed air according to the monitored pCO_2. The set-points for pCO_2 were 350 (A), 450 (B), 760 (C) and 1400 (D) resulting in four batches of seawater differing only in their inorganic carbon chemistry. Salinity (34.0±0.2) was monitored with a salinometer (VWR CO310). The fluorescent compound calcein (Bis[N,N-bis(carboxymethyl)aminomethyl]-fluorescein) was added to the culture media (5 mg/L seawater) to enable determination of newly formed chambers during the culture experiment (Bernhard et al., 2004). Short-term exposure (<three weeks) to calcein has no detectable impact on the physiology of benthic foraminifera (Kurtarkar et al., 2015), and the presence of calcein has no effect on the incorporation of Mg and Sr in foraminiferal calcite (Dissard et al., 2009). Culture media was stored air-free in portions of 250 ml in Nalgene bottles with teflon lined caps at 4°C until further use. Foraminifera were divided over the different treatments in duplicate and placed in 70 ml Falcon ® tissue bottles with gas-tight caps in a thermostat set at 25°C (Fig. 1).

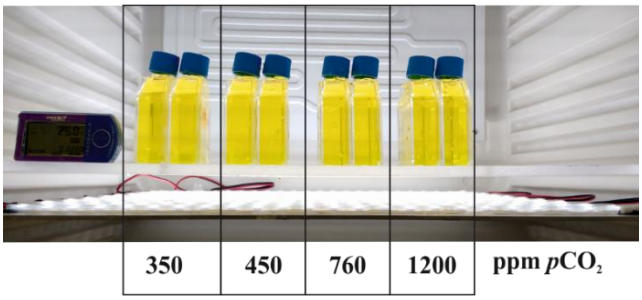

Figure 1. Photograph of the culture set-up with temperature logger and LED shelf. Treatment with corresponding set-points are A=350, B=450 ppm, C=760 ppm, D=1200 ppm. Yellow color is caused by calcein added to the culture media.

The thermostat was monitored by a temperature logger (Traceable Logger Trac, Maxi Thermal), monitoring the temperature every minute. The average temperature over the whole experiment was 25±0.2°C. To create uniform light conditions, the thermostat was equipped with two LED shelves, which resulted in high light conditions 12 hr/12hr. Culture media was replaced every four days, to avoid build-up of organic waste and to obtain stable seawater element concentrations and carbon chemistry. Foraminifera were fed after every water change with 0.5 ml of concentrated freeze-dried *Dunaliella salina* cells, pre-diluted with the corresponding treatment seawater. After 21 days, the experiment was terminated. Foraminifera were rinsed three times with de-ionized water, dried at 40°C and stored in micropaleontology slides until further analysis at the Royal Netherlands Institute for Sea Research (NIOZ).

2.3 Analytical methods

2.3.1 Seawater carbon parameters

At the start and termination of the experiment, 125 ml samples of the seawater at each of the different experimental conditions were collected to analyze dissolved inorganic carbon (DIC) and total alkalinity (TA) on a Versatile INstrument for the Determination of Titration Alkalinity (VINDTA) at the CNSI. Using the measured DIC and TA values and the software CO2SYS v2.1, adapted to Excel by Pierrot et al. (2006) the other carbon parameters (including $[CO_3^{2-}]$ and $\Omega_{CALCITE}$) were calculated (Table 1). For this we used the equilibrium constants for K1 and K2 of Mehrbach et al. (1973), refitted by Dickson and Millero (1987).

Treatment	Set-point	Measured		Calculated CO2SYS		
	pCO_2 ppm	TA µmol/kg	DIC µmol/kg	$[CO_3^{2-}]$ µmol/kg	pH (total scale)	$\Omega_{CALCITE}$
A	**350**	2302.8±8.2	2007.5±10.7	211.2	8.04	5.1
B	**450**	2305.2±5.8	2021.3±12.5	204.1	8.02	4.9
C	**760**	2304.4±0.9	2100.8±13.4	153.3	7.86	3.7
D	**1200**	2300.3±0.7	2201.4±4.1	92.7	7.61	2.2

Table 1. Carbon parameters (TA= Total alkalinity, n=2, DIC=Dissolved Inorganic Carbon, n=2) with (relative) standard deviation of the culture water per treatment of the pCO_2 experiment. CO2SYS was used to calculate seawater carbonate ion concentration, calcite saturation state and pH from measured TA and DIC.

3.2 Seawater element concentrations

At the start and end of the experiment and during replacement of the culture media, subsamples were collected in duplo using 50 ml LDPE Nalgene bottles and immediately frozen at -80^{0}C. After transportation to the NIOZ, melted samples were acidified with 3 times Quartz distilled HCl to pH ~1.8 and the seawater composition of the samples was analyzed on an Element 2 sector field double focusing mass spectrometer (SF-ICP-MS) run in medium resolution mode. IAPSO Standard Seawater was used as a drift monitor. Analytical precision (relative standard deviation) was 3% for Ca, 4% for Mg, 1% Na, 1% for Sr and 5% Ba. We obtained average values of 5.25±0.06 mol/mol for Mg/Ca, 44.6±0.6 mol/mol Na/Ca, 8.63±0.05 mol/mol for Sr/Ca, and 9.04±0.47 for µmol/mol Ba/Ca.

A subsample was analyzed using a commercially available pre-concentration system, SeaFAST S2. With the SeaFAST system elements with low concentrations can be pre-concentrated to values above detection limit of the SF-ICP-MS. Accordingly, we measured Cd, Pb U, B, Ti, Mn, Fe, Co, Ni, Cu, and Zn. In short, 10ml of sample was mixed with an ammonium acetate buffer to pH 6.2 and loaded on a column containing NOBIAS chelating agent. After rinsing the column with a diluted ammonium acetate buffer the metals were eluted in 750 µl of quartz distilled 1.5 M HNO_3 before being quantified on the SF-ICP-MS. Here we use the Zn data only, as this was analyzed in the foraminifera well. Analytical precision (relative standard deviation) was 5% for

Zn. We obtained average values 15.3±0.5 µmol/mol for Zn/Ca for all treatments. Although these values are clearly above natural open ocean values, the concentrations are very uniform between treatments and when comparing start and end of the experiments. The contamination with Zn might hence have occurred already when filling the culture setup with the waters from the bay adjacent to the culture facility and the concentration was well below values considered toxic (Nardelli et al., 2016).

2.3.3 Cleaning methods

After termination of the experiment, foraminiferal shells were cleaned following an adapted version of Barker et al. (2003). Per treatment duplicate, all foraminifera were transferred to 10 ml PE vials. To each vial, 10 mL 1% H_2O_2 solution (buffered with 0.5M NH_4OH) was added to remove organic matter. The vials were heated for 10 minutes in a water bath at 95 °C, and placed in an ultrasonic bath for 30 seconds (degas mode, 80kHz, 50% power), after which the oxidizing reagent was removed. These steps (organic removal procedure) were repeated five times. Foraminiferal samples were rinsed five times with ultrapure water, after which the vials were stored overnight in a laminar flow cabinet at room temperature to dry. Dried foraminifera were placed on double sided tape on LA-ICP-MS stubs. Pictures were taken of individual foraminifera with a ZEISS Axioplan 2 fluoresence microscope equipped with appropriate excitation and emission optics and a ZEISS Axiocam MRc 5 camera, to assess the number of chambers added during the experiment based on the incorporation of calcein.

2.3.5. LA-ICP-MS

Element concentrations of individual fluorescent chambers were analyzed by Laser Ablation-ICP-MS (Reichart et al., 2003). To determine foraminiferal element concentrations, the laser system (NWR193UC, New Wave Research) at the Royal NIOZ was equipped with a 2-volume cell 2 (New Wave Research), characterized by a wash-out time of 1.8 seconds (1% level) and hence allowing detection of variability of obtained element to Ca ratios within chamber walls. Single chambers were ablated in a helium environment using a circular laser spot with a diameter of 80 µm (*M. vertebralis*) or 60 µm (other species). We ablated all calcein-stained chambers twice, except for the first 1-2 chambers that formed during the experiment to avoid contamination of calcite of chambers formed prior to the experiments that may be overlapped by the first labelled chambers (Fig.2).

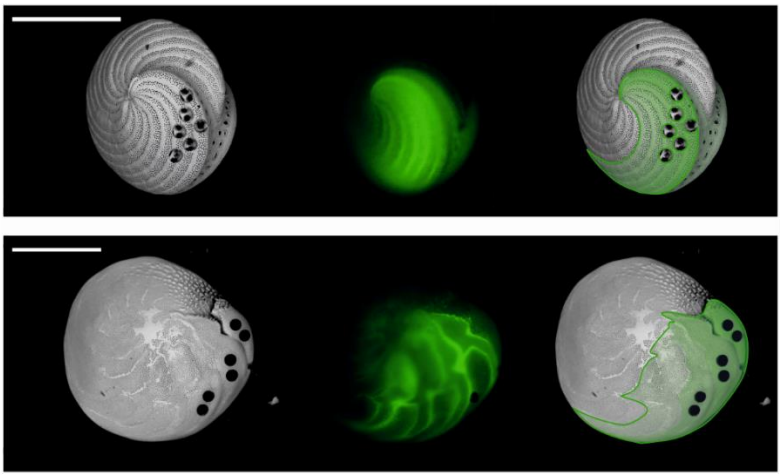

Figure 2. SEM (left) and fluorescence microscope (middle) photographs of *A. angulatus* (top series) and *A. gibbosa* (bottom series) to assess newly formed chambers for laser ablation (right). Scale bar = 500 µm.

All foraminiferal samples were ablated with an energy density of 1±0.1 J/cm^{-2} and a repetition rate of 6 Hz. The resulting aerosol was transported on a helium flow through an in house build smoothing device, being mixed with a nitrogen flow (2 L/min), before entering the quadrupole ICP-MS (iCAP-Q, Thermo Scientific). Monitored masses included ^{7}Li, ^{11}B, ^{23}Na, ^{24}Mg, ^{25}Mg, ^{27}Al, ^{43}Ca, ^{44}Ca, ^{66}Zn, ^{88}Sr and ^{137}Ba. Contrary to ^{67}Zn and ^{68}Zn, ^{66}Zn is free of interferences when measuring calcium carbonate and SRM NIST glass standards (Jochum et al., 2012). Potential contamination or diagenesis of the outer or inner layer of calcite was excluded by monitoring the Al signal. At the start of each series, we analyzed SRM NIST612 and NIST610 glass standard in triplicate (using an energy density of 5±0.1 J/cm-2), JCt-1 (coral carbonate) and two in-house standards, namely NFHS (NIOZ Foraminifera House Standard; for details see Mezger et al., 2016) and the Iceland spar NCHS (NIOZ Calcite House Standard). We further analyzed JCp-1 (Giant clam) and MACS-3 (Synthetic Calcium Carbonate) at the start of each series, and to monitor drift after every ten samples. All element to calcium ratios were calculated with an adapted version of the MATLAB based program SILLS (Guillong et al., 2008). SILLS was modified to evaluate LA-ICP-MS measurements on foraminifera, allowing import of Thermo Qtegra software sample list, laser data reduction and laser LOG files. Major adaptions include improved automated integration and evaluation of (calibration and

monitor) standards, quality control report of the monitor standards and export in element to calcium ratios (mol/mol). Calibration was performed against the MACS-3 carbonate standard, with ^{43}Ca as an internal standard and we used the multiple measurements of MACS-3 for a linear drift correction. Relative analytical precision (relative standard deviation (RSD) of all MACS-3 analyses) is 3% for ^{23}Na, 3% for ^{24}Mg, 3% for ^{25}Mg, 4% for ^{66}Zn, 3% for ^{88}Sr and 3% for ^{137}Ba. In total, 961 analyses were performed on 251 specimens covering eight species cultured in four experimental conditions (see Table 2 for specifics).

Species	**n LA(n specimens)**			
	A: 350 ppm	**B: 450ppm**	**C: 760 ppm**	**D: 1200 ppm**
A. angulatus	62(19)	72(21)	76(21)	51(14)
M. vertebralis	48(14)	49(15)	57(18)	33(11)
A. gibbosa	106(28)	126(32)	75(18)	59(15)
L. bradyi	21(5)	38(13)	27(5)	16(4)
A. carinata	12(2)	14(1)	19(4)	5(1)
P. pertusus	-	12 (2)	-	11 (2)
H. antillarum	-	12 (1)	-	14 (2)
P. acervalis	-	8 (2)	-	-
Total	187(49)	331(87)	254(66)	189(49)

Table 2. Total number of LA-ICP-MS measurements per species, per treatment (A-D).

We calculated the standard deviation (SD), RSD and standard error (SD/√n; SE) per treatment. The partitioning coefficient (D) of an element (E) between seawater and foraminiferal calcite is expressed as $D_E = (E/Ca_{CALCITE})/(E/Ca_{SW})$. Partition coefficients, element versus calcium ratio and growth parameters were statistically compared with different experimental parameters (such as pCO_2 or $[CO_3^{2-}]$) using a two-sided T-test with 95% confidence levels. This also allows for the calculation of 95% confidence intervals over the average per treatment. Pairwise comparisons were made for per E/Ca per species and culture conditions using ANOVA. Groups that showed significant difference were assigned different letters. When comparing partition coefficients to other studies, E/Ca_{SW} data was, in some studies, not measured. In these cases, we used average seawater E/Ca_{SW} to calculate D_E (see also supplementary Table S1).

3. Results

3.1 Inter-species differences in element incorporation

In Table 2 we present all the elemental data for the eight species investigated in this controlled pCO_2 culture experiment. $Mg/Ca_{CALCITE}$ of Mg in hyaline species varies between 25.9-141.3 mmol/mol Mg/Ca. In contrast, $Mg/Ca_{CALCITE}$ of miliolid species ranges from 121.3-149.3 mmol/mol. This large spread in foraminifera E/Ca of hyaline species is also observed for Sr (1.7-3.1 mmol/mol), Na (3.4-19.5 mmol/mol), Zn (9.0-97.0 µmol/mol) and Ba (2.7-20.1 µmol/mol), while miliolids only vary over a narrow range (Sr = 2.0-2.2 mmol/mol; Na = 3.8-5.8 mmol/mol; Zn = 53.0-140.8 µmol/mol; Ba = 18.0-29.0 µmol/mol). When comparing Mg incorporation to that of the other elements studied here (Ba, Zn, Sr and Na) between species (treatment B; supplementary Table S1), we observe a positive relation between D_{Sr} ($p<0.0025$), D_{Na} ($p<0.0005$), D_{Ba} ($p<0.05$) and D_{Zn} ($p<0.005$) for hyaline species (Table 4). In general hyaline species are enriched similarly in all elements (Fig. 3). Compared to porcelaneous species, the hyaline shell building species which incorporate the most Mg (>100 mmol/mol Mg/Ca) incorporate more Na, and Sr, while incorporating less Zn and Ba. Element incorporation across miliolid species is less variable than observed for hyaline species and in general partition coefficients for these species seem closer to inorganic values. Including data from literature (both culture and field calibrations; see supplementary Table S2), preferable in which both Mg/Ca and at least one other element (Na, Sr, Ba or Zn) is measured, shows that the relation based on the Caribbean species studied here is also more general applicable when including more species ($D_{Sr} = p<0.005$); $D_{Na} = p<0.0005$); $D_{Ba} = p<0.005$; $D_{Zn} = p<0.01$), even though this compiled data (labeled 'All studies' in Table 4) covers a wide range in environmental and experiment conditions (see supplementary Table S2 for details).

3.2 Element/Ca as a function of ocean acidification

In both porcelaneous and hyaline species we find an increase of $Zn/Ca_{CALCITE}$ and $Ba/Ca_{CALCITE}$ with pCO_2, while foraminiferal Sr/Ca, Mg/Ca and Na/Ca remain similar across the experimental conditions (Fig. 4 and Table 5).

D_E versus D_{Mg}		R^2	p-value
D_{Na}	This study	0.97	<0.0005
	All studies	0.95	<0.0005
D_{Sr}	This study	0.90	<0.0025
	All studies	0.53	<0.005
D_{Zn}	This study	0.88	<0.005
	All studies	0.80	<0.01
D_{Ba}	This study	0.58	<0.05
	All studies	0.56	<0.005

Table 4. R^2 and p-values of linear trendline of D_E versus D_{Mg} of all hyaline species of this studies and compiled literature studies (all studies).

Species	Zn/Ca		Ba/Ca	
	R^2	p-value	R^2	p-value
M. vertebralis	0.99	<0.0005	0.81	<0.025
A. angulatus	0.95	<0.0025	0.99	<0.0005
L. bradyi	0.98	<0.0005	0.97	<0.0025
A. carinata	0.98	<0.001	0.94	<0.005
A. gibbosa	0.99	<0.0005	0.98	<0.001

Table 5. Regression and p-values of foraminiferal Zn/Ca and Ba/Ca versus pCO_2 values of different species (Fig. 4).

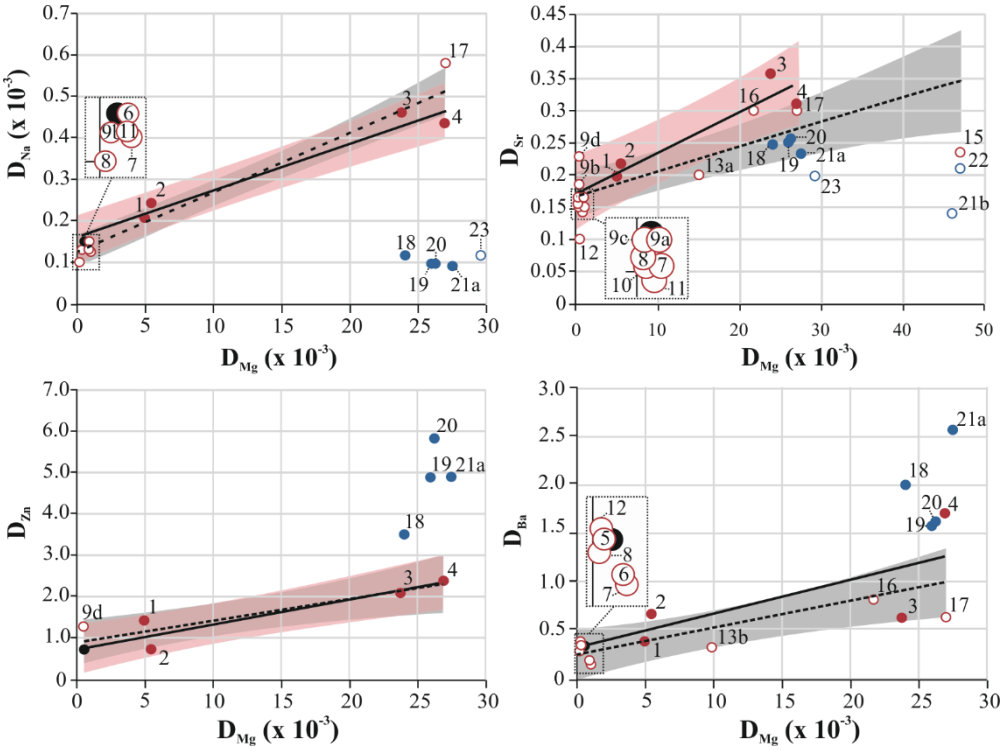

Hyaline species
- **This study**

1 Amphistegina gibbosa
2 Asterigerina carinata
3 Planorbulina acervalis
4 Heterostegina antillarum

- **Other studies**

5 Uvigerina spp.
6 Globigernoides ruber
7 Globigerinoides sacculifer
8 Neogloboquadrina pachyderma
9a Ammonia tepida

Other studies (continued)
9b Ammonia tepida
9c Ammonia tepida
9d Ammonia tepida
10 Cibicidoides wuellerstorfi
11 Elphidium crispum
12 Oridorsalis umbonatus
13a Amphistegina lessonii
13b Amphistegina lessonii
14 Amphistegina lobifera
15 Neorotalia calcar
16 Heterostigina depressa
17 Operculina ammonoides

Milliolid species
- **This study**

18 Peneroplis pertusus
19 Laevipeneroplis bradyi
20 Archaias angulatus
21a Marginopora vertebralis

- **Other studies**

21b Marginapora vertebralis
22 Amphisorus hemprichii
23 Quinqueloculina sp.

Figure 3. Partition coefficient of Na, Sr, Zn and Ba versus D_{Mg} of hyaline (red symbols) and miliolid (blue symbols) species in this study (closed symbols) and other studies (open symbols). Black lines represent trendlines (solid = this study; dashed = all studies). The 95% confidence intervals are indicated in pink (this study) and grey (all studies), which sometimes overlap. Black dots represent the in-house NFHS carbonate standard, consisting of planktonic foraminifera. Numbers correspond to species analyzed (supplementary Table S2).

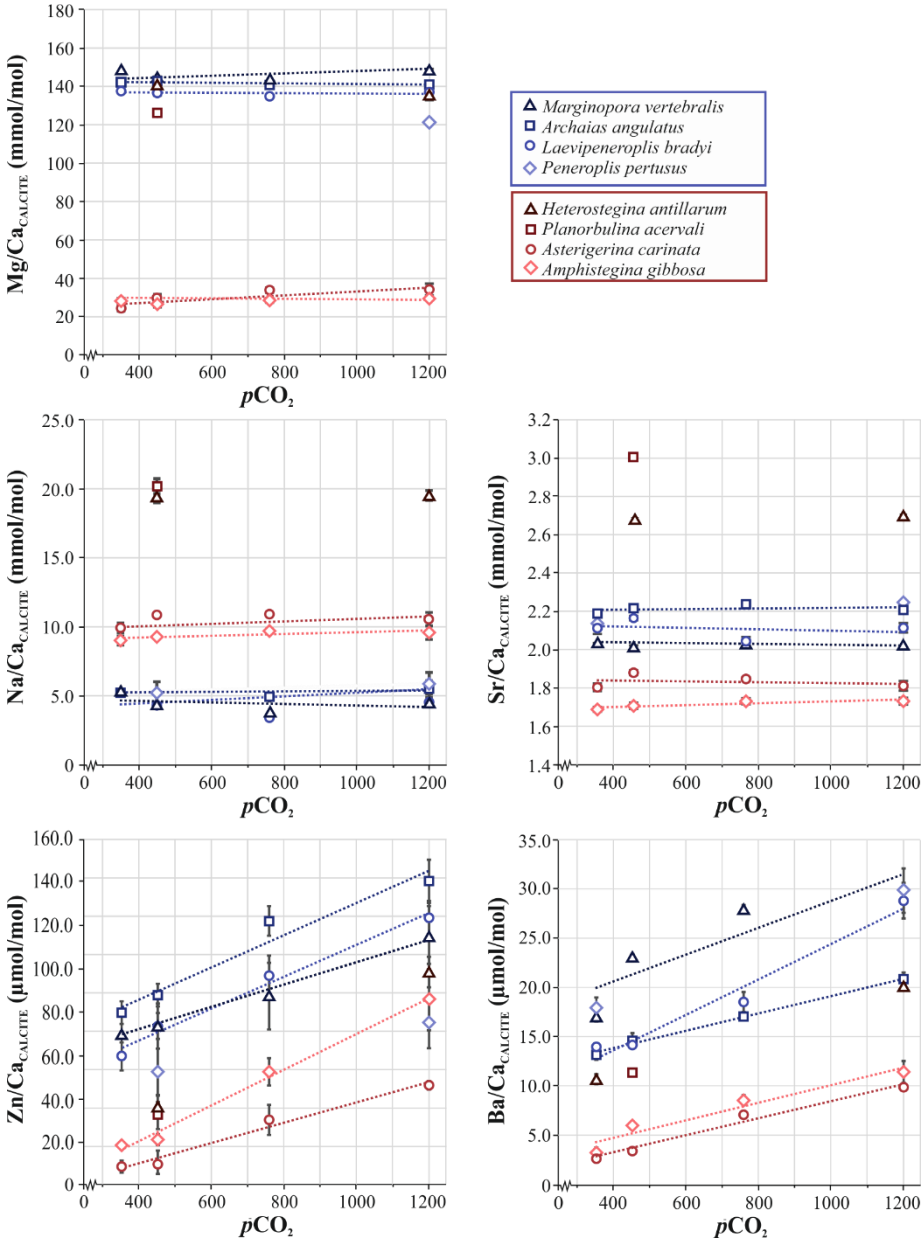

Figure 4. Element to Ca ratios (±SE) of different species of foraminifera over a range of pCO$_2$ values. In some cases, the error bar is smaller than the symbol. Miliolid species in blue (triangles = *M. vertebralis*; squares = *A. angulatus*; circles = *L. bradyi*; squares = *P. pertusus*) and hyaline species in red (triangles = *H. antillarum*; squares = *P. acervalis*; circles = *A. carinata;* diamonds = *A. gibbosa*).

Sensitivity of both foraminiferal Zn/Ca and Ba/Ca to changes in seawater pCO_2 differs between the studied porcelaneous and hyaline species. When pCO_2 changes from 350 to 1200 ppm, Zn/Ca of hyaline foraminifera increase by a factor of 3.7 (*A. carinata*) or 4.5 (*A. gibbosa*) while miliolid foraminiferal Zn/Ca increases only by 1.3 (*M. vertebralis*), 1.8 (*A. angulatus*) and 2.1 (*L. bradyi*). Also sensitivity of foraminiferal Ba/Ca to the same change in pCO_2 shows a similar pattern, with Ba/Ca of hyaline species increasing by a factor of 3.6 (*A. carinata*) or 3.7 (*A. gibbosa*), while miliolid species increase Ba/Ca only with a factor of 1.8 (*M. vertebralis*), 1.6 (*A. angulatus*) or 2.1 (*L. bradyi*).

4. Discussion

4.1 Trends in element incorporation

Both miliolid and hyaline foraminifera promote calcification by increasing their internal pH (De Nooijer et al., 2009). Still, they might use different mechanisms to take up the ions (Ca^{2+} and CO_3^{2-}) necessary for chamber formation, which is reflected in the different trends observed here. Element incorporation in hyaline foraminifera is highly interdependent, i.e. species with increased Mg content also incorporate more Sr, Na, Ba and Zn (Fig. 3). This observation suggests that uptake of all these elements is controlled by the same process, which may be the transmembrane transport of calcium ions to the site of calcification. Such transport likely involves Ca^{2+} channels (Nehrke et al., 2013), capable of transferring other ions, like e.g. Mg, Sr and Na (Hess and Tsien, 1984; Allen and Sanders, 1994; Sather, 2005). This may result in an interdependence between all these elements studied such as observed here for the hyaline species if the selectivity for Ca^{2+} of these channels vary between species. In contrast, miliolid species, building porcelaneous shells show much less inter-species variation in element incorporation and ratios between incorporated elements is thus relatively similar between species (Fig. 3). This may be explained by calcification from an internal reservoir, such as intracellular vacuoles containing (modified) seawater (Hemleben et al., 1986; Erez, 2003; Bentov et al., 2009). The fact that the Mg partitioning in this foraminiferal group is similar to the inorganic partition coefficient may indicate that the carbonate is directly precipitated from seawater, without major removal of Mg^{2+} ions. The relative similarity in partition coefficients of other elements between miliolid species are generally in line with an inorganic-like calcite precipitation, with only minor alteration of the elemental composition of the calcifying fluid by ion channels.

4.2 Effect of ocean acidification on Element/Ca

For neither miliolid nor hyaline species, foraminiferal Mg/Ca, Na/Ca and Sr/Ca systematically change with pCO_2. The impact of pH (and/or $[CO_3^{2-}]$) on $Mg/Ca_{CALCITE}$ and $Sr/Ca_{CALCITE}$ in foraminifera has been the subject of discussion (e.g., Elderfield et al., 1996; Dissard et al., 2010). In low-Mg benthic species, both $Mg/Ca_{CALCITE}$ and $Sr/Ca_{CALCITE}$ do not seem to depend on inorganic carbon system parameters, e.g. pH or $[CO_3^{2-}]$ (Allison et al., 2011; Dueñas-Bohórquez et al., 2011). However, for several planktonic species pH does influence $Mg/Ca_{CALCITE}$ and $Sr/Ca_{CALCITE}$ (Lea et al., 1999; Russell et al., 2004; Evans et al., 2016). The effect of pH on $Sr/Ca_{CALCITE}$ might be explained via increased growth rates due to pH-associated changes in $[CO_3^{2-}]$ (Dissard et al., 2010). However, due to the limited experimental set-up, we are not able to disentangle the effects of the different carbon parameters in this study. Still, here we show that incorporation of Mg, Sr and Na of the selected larger benthic hyaline and miliolid foraminifera are not significantly impacted when cultured over a range of pCO_2 and thus $[CO_3^{2-}]$ and pH values. Observed offsets in studies using acid titration (Lea et al., 1999; Russell et al., 2004; Dueñas-Bohórquez et al., 2011; Evans et al., 2016) to alter the carbonate system might be related to changes in alkalinity rather than pCO_2 or DIC. In the experimental setup here alkalinity was kept constant between the different treatments, but pH, DIC and carbonate ion concentration varied as a function of pCO_2.

In contrast, foraminiferal Zn/Ca and Ba/Ca are significantly impacted by pCO_2 for all species studied here (Table 5; Fig. 4). Although Hönisch et al. (2011) suggested that the impact of carbonate chemistry on Ba incorporation is negligible, their data does suggest a trend over the same interval in pH as studied here. In hyaline foraminifera, Zn/Ca and Ba/Ca increases more as a function of pCO_2 (factor of 3.7-4.5 and 3.6-3.7, respectively when pCO_2 increases from 350 to 1200 ppm) compared to the miliolid species (1.3-2.1 and 1.6-2.1 times, respectively). In the culture set-up used, increasing pCO_2 increases DIC, reduces pH and thereby decreases seawater $[CO_3^{2-}]$. Speciation of Zn, Ba and also other elements, like U (Keul et al., 2013b), is primarily controlled by seawater $[CO_3^{2-}]$. Using the PHREEQC (Parkhurst and Appelo, 1999) and the standard llnl database, the speciation of all elements studied here (Mg, Na, Sr, Zn and Ba) for our different seawater treatments were modelled. We observed a decrease of free ions (Zn^{2+} and Ba^{2+}) and an increase in Ba and Zn carbonate complexes ($BaCO_3^0$ and $ZnCO_3^0$), with increasing pCO_2 (Fig. 5), while the activity of Mg^{2+}, Na^+ and Sr^{2+} remained unaffected. This suggests that element incorporation in foraminiferal calcite might be depending on the bioavailability of free ions, which in the case of Ba and Zn, changes with pCO_2.

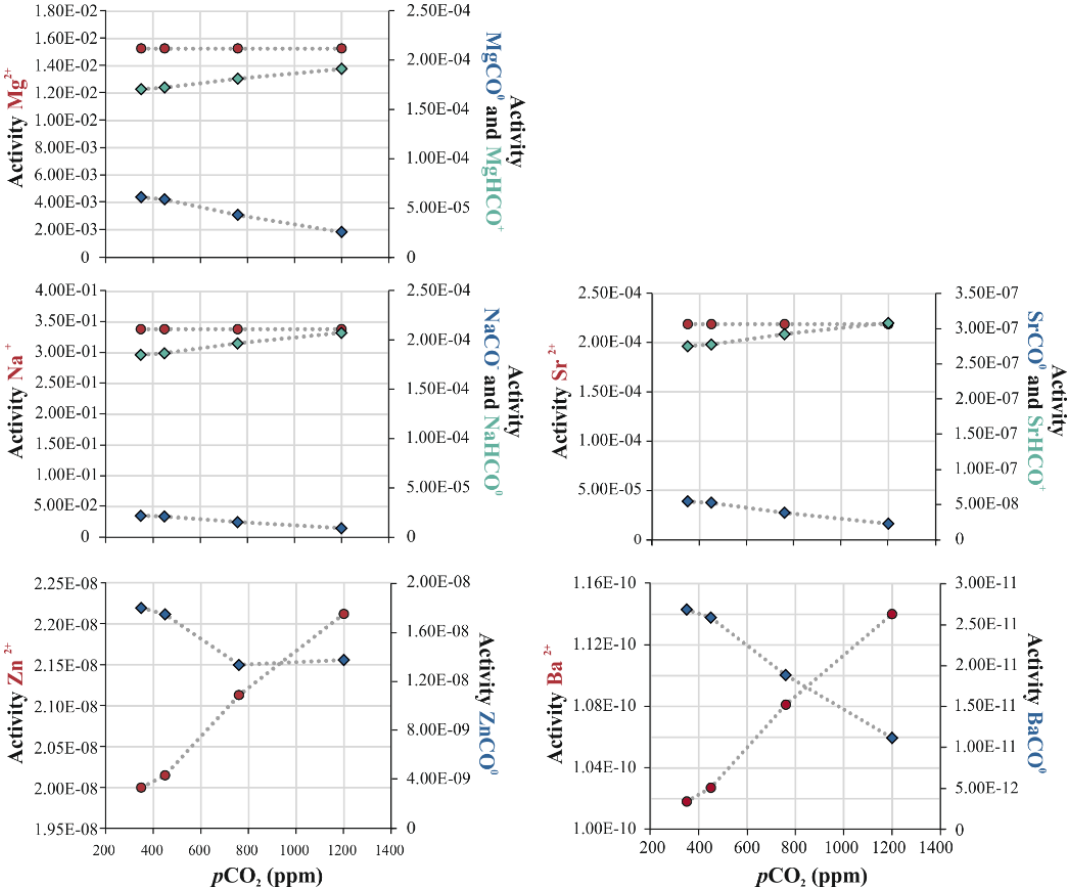

Figure 5. Speciation of Mg, Na, Sr, Zn and Ba in the different seawater treatments modelled in PHREEQC (Parkhurst and Appelo, 1999). Activities of free ions (red) and element (E)-carbonate complexes (ECO_3 = blue diamonds and $EHCO_3$ = green diamonds).

4.3 Speciation in the foraminiferal microenvironment

During inorganic precipitation, carbonate complexes (e.g. $MgCO_3^0$) are easily incorporated into the calcite crystal lattice. However, foraminifera build their test from ions available at the site of calcification, which is well separated from the surrounding seawater (De Nooijer et al., 2009). During calcification, Ca^{2+} is proposed to be transported from seawater to the SOC via ion channels (Nehrke et al., 2013). This so-called trans-membrane transport (TMT) through Ca^{2+} channels has also been found

for other marine organisms, including coccolithophores (Gussone et al., 2006). These Ca^{2+} channels may not discriminate perfectly between Ca ions and elements like Sr and Ba (Allen and Sanders, 1994), causing accidental transport of these elements into the SOC. How much of a certain element will enter the SOC in this way, depends on 1) the selectiveness of the channels and the characteristics of the transported ions, 2) the element to calcium ratio in the foraminiferal microenvironment and 3) the concentration gradient between seawater and the SOC. For instance, ions such as Mg^{2+} are heavily fractionated against during TMT, which is reflected by the low D_{Mg} found in most species. The large range in Mg/Ca values in hyaline species suggests that TMT plays an important, but also variable, role in calcification of these species. The availability of some free ions, like Ba and Zn, changes as a function of pCO_2 due to the formation of carbonate complexes (Fig. 5). When Zn and Ba form stable complexes with carbonate ions they are no longer available for (sporadic) transport through the Ca^{2+} channels, decreasing the availability at the site of calcification and subsequently, incorporation into the foraminiferal calcite (Fig. 6).

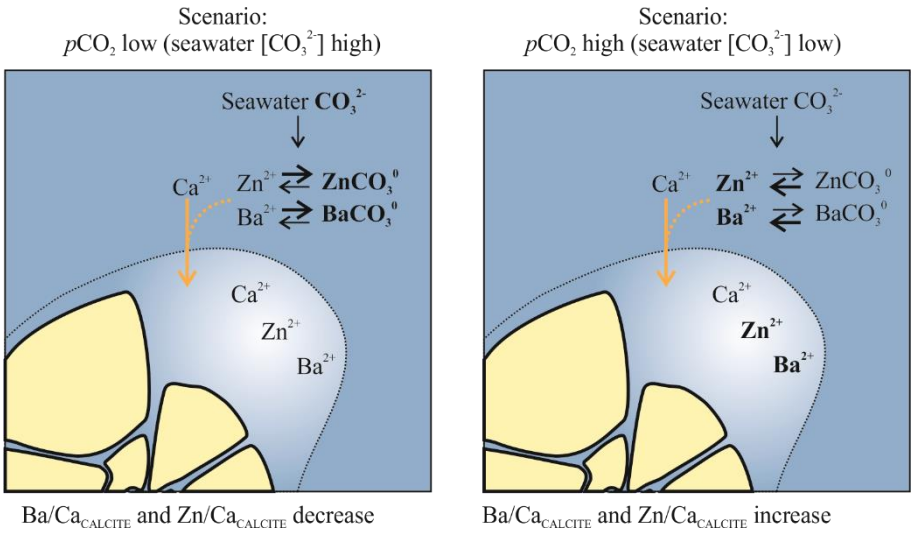

Figure 6. Schematic of incorporation of Zn and Ba during foraminiferal calcification under low (left panel) and high (right panel) pCO_2 conditions. Amount of free ions (e.g. Zn^{2+} and Ba^{2+}) is influenced by speciation due to changing [CO_3^{2-}]. Increases in availability of elements, e.g. due to a shift in chemical speciation, are indicated in bold. Orange arrow indicates transport of Ca^{2+} through channel, with the associated accidental transport of Zn^{2+} and Ba^{2+}.

In summary, the amount of Zn and Ba available at the site of calcification is proportional to the concentration of the ratio between Ca^{2+} and free Zn^{2+} and Ba^{2+} in the foraminiferal microenvironment. In turn, the amount of free Zn and Ba ions in seawater is controlled by their respective concentration in seawater concentration, as well as $[CO_3^{2-}]$. Foraminiferal Mg/Ca, Na/Ca and Sr/Ca is not detectably affected by $[CO_3^{2-}]$, since these elements do not form carbonate complexes over the range of $[CO_3^{2-}]$ studied here.

4.4 Element incorporation in hyaline species

Between hyaline species, we observe simultaneous increases in all elements incorporated and this trend is confirmed when including published data for other species compiled from previous studies (Fig. 4 and supplementary Table S2). Interestingly, the two hyaline species that are most enriched in all elements studied (Mg, Na, Sr, Zn and Ba) are also the foraminiferal species with the largest average adult test size (*H. antillarum* and *P. acervalis*) for which data is available (this study). The other hyaline species, *A. carinata* and *A. gibbosa*, have considerably smaller maximum shell sizes and lower Mg/Ca, Sr/Ca, etc. values.

Two processes involving these calcium channels could possibly explain the observed size trend in hyaline species. First, larger foraminifera have a smaller surface area to volume ratio and, therefore, proportionally less Ca^{2+} channels, assuming the density of these channels per surface area remains similar. This would imply that fewer channels need to transport more ions for a given volume of $CaCO_3$ precipitated, which may in turn, possibly reduce selectivity between Ca^{2+} and other divalent cations. Secondly, a larger foraminifer will need more overall Ca^{2+} compared to smaller species for the production of a single new chamber, since the volume of the chamber walls increases with the size of the individual. This increased uptake of Ca^{2+} from the microenvironment around the foraminifer, may cause a lower concentration of Ca^{2+} in the direct surroundings of the foraminifer compared to the other ions, which may subsequently translate into an increased transport of ions other than Ca^{2+} to the site of calcification.

A consequence of these hypotheses is that juvenile or smaller adults should have lower partition coefficients than fully grown adults. Although some studies have shown a size effect for several elements (e.g. Elderfield et al., 2002), other studies show no major effect of size on element partitioning (e.g. Friedrich et al., 2012; Evans and Müller, 2013). The moderate trend observed within species, in comparison to the large

differences observed here between species, may indicate that species control channel density per surface area as a function of average shell size of the species. Alternatively, the maximum size of a species may be accompanied by a difference in their calcification mechanism (e.g. the relative contribution of TMT in element uptake) explaining inter-species differences in element partitioning. From an evolutionary point of view the latter explanation seems more likely.

4.5 Mechanisms for element uptake in miliolid foraminifera

In contrast to hyaline species, the miliolid species build porcelaneous shells that show much less inter-species variation in element composition (Fig. 3). While hyaline species calcify in a (semi-)enclosed space, miliolids precipitate their calcite intracellularly in vesicles in which they promote calcification by increasing pH (De Nooijer et al., 2009). This suggests that these species calcify directly from seawater (Ter Kuile and Erez, 1987). The fact that the element partitioning is (marginally) closer to the inorganic partition coefficients (e.g. Mucci and Morse, 1983; Ishikawa and Ichikuni, 1984) in this foraminiferal group might reflect that the carbonate is directly precipitated from intracellular seawater, without major alteration of the original [Mg^{2+}]. The relative similarity in partition coefficients between different porcelaneous shell building species is in line with primarily inorganic precipitation, with only minor alteration of the elemental composition of the calcifying fluid by ion channels.

However, the observed correlation between pCO_2 and Ba and Zn (Fig. 4) suggests that Ca channels still play a (modest) role in supplying Ca^{2+} to the miliolid SOC. The contribution of Ca^{2+} through TMT is likely smaller than in hyaline species, since they already obtain calcium by including seawater in their calcification vesicle prior to calcite precipitation. The considerably smaller flux of transmembrane Ca^{2+} compared to perforate species explains the observed lower sensitivity of e.g. foraminiferal Zn/Ca and Ba/Ca to changes in seawater [CO_3^{2-}] in miliolid species (Fig. 4). This approximately 2 times lower sensitivity of porcelaneous foraminifera compared to hyaline species suggests that miliolid foraminifera acquire half of the necessary Ca^{2+} through Ca-channels, and the other half directly from vacuolized seawater. Element incorporation in miliolid foraminifera will therefore be mainly governed by their respective concentrations in seawater, and to a lesser extent by the selectivity for Ca^{2+}/ permeability for other ions during TMT.

5. Conclusions

Trends in element incorporation in larger benthic foraminifera can be explained by a combination of differences in calcification strategy and seawater chemistry. Carbonate ion concentration in seawater determines bioavailability of some ions (e.g. Zn^{2+} and Ba^{2+}), which are transported through Ca-channels to the site of calcification. For hyaline foraminifera, we observed increased element incorporation for larger species compared to smaller species, which can be explained by more intense activity of these channels and the relative concentration in seawater during calcification. For miliolid foraminifera, only half of the needed Ca is acquired through these Ca^{2+} channels, while the other half is obtained by including small vesicles of seawater, leading to element partitioning to be more in line with inorganic calcite.

Acknowledgments

This research is funded by the NIOZ – Royal Netherlands Institute for Sea Research and the Darwin Centre for Biogeosciences project "*Double Trouble*: Consequences of Ocean Acidification – Past, Present and Future –Evolutionary changes in calcification mechanisms" and the program of the Netherlands Earth System Science Center (NESSC). Great thanks to all participants of the 2015 foraminifera culture expedition at the CNSI, St. Eustatia (Jelle Bijma and Gernot Nehrke from the AWI, Brett Metcalfe (VU), Alice Webb (NIOZ), Esmee Geerken (NIOZ) and Didier de Bakker (NIOZ/IMARES). This study would not have been possible without Steven van Heuven and Bob Koster, who designed and constructed the pCO_2 set-up. Furthermore, we would like to thank Kirsten Kooijman for supplying *Dunaliella salina* cultures, Patrick Laan and Karel Bakker for seawater analysis and Mariëtte Wolthers for providing technical support with PHREEQC. Lastly, we thank Jan-Berend Stuut (NIOZ) for the usage of the Hitachi TM3000 SEM (NWO grant 822.01.008 and ERC grant 311152).

Supplementary Material Chapter 4

Table S1. Overview of element to Ca ratios in foraminiferal calcite (AVG=average; SE=standard error) and partition coefficients D_E, with D_E of ambient conditions (treatment B) in bold. Letters ([a] to [d]) indicate (per species per E/Ca) groups that are statistical different (one-way ANOVA).

Species	pCO_2	Mg/Ca mmol/mol		Na/Ca mmol/mol		Sr/Ca mmol/mol		Zn/Ca µmol/mol		Ba/Ca µmol/mol	
		Avg ±SE	D_{Mg} ($*10^{-3}$)	Avg ±SE	D_{Na} ($*10^{-3}$)	Avg ±SE	D_{Sr}	Avg ±SE	D_{Zn}	Avg ±SE	D_{Ba}
Porcelaneous species											
A. angulatus	**350**	139.4 ±0.6[a]	26.6	5.2 ±0.1[a]	0.12	2.2 ±0.02[a]	0.25	80.0 ±5.1[a]	5.3	13.2 ±0.5[a]	1.5
	450	137.7 ±0.5[b]	**26.3**	4.3 ±0.1[b]	**0.10**	2.2 ±0.01[a]	**0.26**	88.1 ±5.2[b]	**5.8**	14.6 ±0.5[b]	**1.6**
	760	137.4 ±0.7[b]	26.2	4.9 ±0.1[c]	0.11	2.2 ±0.01[a]	0.26	122.6 ±7.0[c]	8.1	17.0 ±0.6[b]	1.9
	1200	138.6 ±1.1[a]	26.4	5.4 ±0.2[a]	0.12	2.2 ±0.02[a]	0.26	140.8 ±9.9[d]	9.3	20.9 ±0.2[c]	2.3
M. vertebralis	**350**	147.7 ±0.6[a]	28.2	4.8 ±0.1[a]	0.11	2.0 ±0.01[a]	0.23	70.0 ±10.1[a]	4.6	17.0 ±0.5[a]	1.9
	450	144.2 ±0.8[b]	**27.5**	4.1 ±0.1[b]	**0.09**	2.0 ±0.01[a]	**0.23**	74.0 ±10.6[b]	**4.9**	23.1 ±0.5[b]	**2.6**
	760	143.0 ±0.6[a]	27.3	3.8 ±0.1[a]	0.09	2.0 ±0.01[a]	0.23	87.7 ±15.5[c]	5.8	27.9 ±0.6[c]	3.1
	1200	148.3 ±0.5[b]	28.3	4.5 ±0.2[c]	0.10	2.0 ±0.01[a]	0.23	115.6 ±15.3[d]	7.6	30.1 ±0.2[d]	3.3
L. bradyi	**350**	137.8 ±1.3[a]	26.3	5.2 ±0.2[c]	0.12	2.1 ±0.03[a]	0.24	60.0 ±6.5[a]	4.0	14.0 ±0.5[a]	1.5
	450	136.2 ±0.7[a]	**26.0**	4.3 ±0.1[b]	**0.10**	2.2 ±0.01[b]	**0.25**	73.8 ±6.0[b]	**4.9**	14.2± 0.5[a]	**1.6**
	760	134.4 ±1.2[b]	25.6	3.4 ±0.1[a]	0.08	2.0 ±0.02[c]	0.24	97.5 ±9.4[c]	6.4	18.5± 0.6[b]	2.1
	1200	136.9 ±1.1[a]	26.1	6.2 ±0.2[d]	0.14	2.1 ±0.02[a]	0.24	124.2 ±7.8[d]	8.2	28.8± 0.2[c]	3.2
P. pertusus	**350**										
	450	126.1 ±1.8[a]	**24.0**	5.2 ±0.3[a]	**0.12**	2.1 ±0.07[a]	**0.25**	53.0 ±10.8[a]	**3.5**	18.0 ±0.5[a]	**2.0**
	760										
	1200	121.3 ±1.0[a]	23.1	5.8 ±0.2[a]	0.13	2.2 ±0.02[a]	0.26	75.5 ±11.9[b]	5.0	29.8 ±0.2[b]	3.3

Table S1 continued

Hyaline species											
Species	**pCO_2**	**Mg/Ca mmol/mol**		**Na/Ca mmol/mol**		**Sr/Ca mmol/mol**		**Zn/Ca µmol/mol**		**Ba/Ca µmol/mol**	
		Avg ±SE	**D_{Mg} ($*10^{-3}$)**	**Avg ±SE**	**D_{Na} ($*10^{-3}$)**	**Avg ±SE**	**D_{Sr}**	**Avg ±SE**	**D_{Zn}**	**Avg ±SE**	**D_{Ba}**
H. antillarum	**350**										
	450	141.3 ±0.3[a]	**26.9**	19.4 ±0.5[a]	**0.44**	2.7 ±0.02[a]	**0.31**	36.0 ±14.7[a]	**2.4**	10.7 ±0.5[a]	**1.2**
	760										
	1200	136.9 ±1.6[a]	26.1	19.5 ±0.4[a]	0.44	2.7 ±0.02[a]	0.31	97.0 ±18.3[b]	6.4	20.1 ±0.2[b]	2.2
P. acervalis	**350**										
	450	139.1 ±1.2	**26.5**	19.5 ±0.7	**0.46**	3.1 ±0.02	**0.36**	31.6 ±6.6	**2.1**	11.3 ±0.5	**1.3**
	760										
	1200										
A. carinata	**350**	23.6 ±1.5[a]	4.5	9.9 ±0.4[a]	0.22	1.8 ±0.02[a]	0.21	9.0 ±2.6[a]	0.6	3.2 ±0.5[a]	0.4
	450	28.5 ±2.4[b]	**5.4**	10.8 ±0.1[a]	**0.24**	1.9 ±0.01[a]	**0.22**	10.9 ±5.5[a]	**0.7**	6.0 ±0.5[b]	**0.7**
	760	33.1 ±1.2[b]	6.3	10.9 ±0.2[a]	0.24	1.8 ±0.01[a]	0.21	30.7 ±7.0[b]	2.0	8.5 ±0.6[c]	0.9
	1200	33.5 ±3.1[b]	6.4	10.6 ±0.5[a]	0.24	1.8 ±0.03[a]	0.21	46.4 ±2.1[b]	3.1	11.4 ±0.2[d]	1.3
A. gibbosa	**350**	27.8 ±0.5[a]	5.3	9.0 ±0.1[a]	0.20	1.7 ±0.01[a]	0.20	19.0 ±1.8[a]	1.3	2.7 ±0.5[a]	0.3
	450	25.9 ±0.6[b]	**4.9**	9.2 ±0.1[a]	**0.21**	1.7 ±0.02[a]	**0.20**	21.5 ±2.5[b]	**1.4**	3.4 ±0.5[a]	**0.4**
	760	28.2± 0.7[a]	5.4	9.7±0. 1[b]	0.22	1.7 ±0.02[a]	0.20	52.8 ±6.1[c]	3.5	7.1 ±0.6[b]	0.8
	1200	28.7± 0.6[a]	5.5	9.6±0. 1[b]	0.21	1.7 ±0.02[a]	0.20	85.8 ±11.3[d]	5.7	9.9 ±0.2[c]	1.1

Table S2. Measured calcitic element (E) to calcium ratio, calculated partition coefficients and experimental/field conditions. Reported E/Ca are reported either as a range of values (min-max), or as average values. 'Study type' refers to core-top/sediment trap calibrations (1) or culture experiment (2). AVG indicates average, 'n.m.' means not measured or not reported and Ch. means Chapter. For a number of (field) studies, seawater element concentrations are not measured, but are here calculated ('*') to obtain an average partition coefficient (D_E). Assumed concentrations at salinity of 35 are 10.3 mmol/kg for Ca, 0.469 mol/kg for Na, 528 mmol/kg for Mg, 0.0909 mmol/kg or Sr and 0.101 µmol/kg for Ba.

Mg/Ca								
#	**Species**	**E/Ca (mmol/mol)**		**D_E ($*10^{-3}$)**	**T (^{0}C)**	**S**	**Study type**	**Ref.**
		calcite	**seawater**					
5	*Uvigerina spp.*	0.75–2.5	5126*	0.32	1.6-20	n.m.	1	[1]
6	*Globigerinoides ruber*	3.5-5.5	5126*	0.89	20-26	n.m.	1	[2]
7	*Globigerinoides sacculifer*	5.2	5126*	1	26	36	2	[3]
8	*Neogloboquadrina pachyderma*	0.75–1.05	5126*	0.175	-2	32.6 - 33.6	1	[4]
9a	*Ammonia tepida*	2-7	5158	0.895	25	32.2	2	[5]
9b	*Ammonia tepida*	1.3–2.2	5080	0.345	20.0	32.5	2	[6]
9c	*Ammonia tepida*	1-3	5100-5300	0.505	18.0	35.0	2	[7]
9d	*Ammonia tepida*	2.1	5565	0.40	25	35.2	2	Ch.6
10	*Cibicidoides wuellerstorfi*	0.98–1.40	5126*	0.23	2.9-3.4	n.m.	1	[8]
11	*Elphidium crispum*	4.3	5126	0.84	25	n.m.	2	Ch.3
12	*Oridorsalis umbonatus*	1–3	5300	0.38	1.1-3.6	n.m.	1	[9]
13a	*Amphistegina lessonii*	68–86	5126*	15	21-29	n.m.	1	[10]
13b	*Amphistegina lessonii*	40-60	5200	9.85	24	35	2	[11]
14	*Amphistegina lobifera*	50-70	5200	11.3	24	35	2	[11]
15	*Neorotalia calcar*	214-267	5126*	47	21-29	n.m.	1	[10]
16	*Heterostegina depressa*	110 – 140	5200-6200	21.7	18.0	35.0	2	[7]

Mg/Ca (continued)								
#	**Species**	**E/Ca (mmol/mol)**		**D_E ($*10^{-3}$)**	**T (^{0}C)**	**S**	**Study type**	**Ref.**
		calcite	**seawater**					
17	*Operculina ammonoides*	141	5330	27	24	37	2	[12]
21b	*Marginopora vertebralis*	213 – 255	5126*	46	21 – 29	n.m.	1	[10]
22	*Amphisorus hemprichii*	224 – 256	5126*	47	21 – 29	n.m.	1	[10]
23	*Quinqueloculina* sp.	150.9	5126	29.4	25	n.m.	2	Ch.3
Sr/Ca								
#	**Species**	**E/Ca (mmol/mol)**		**D_E ($*10^{-3}$)**	**T (^{0}C)**	**S**	**Study type**	**Ref.**
		calcite	**seawater**					
7	*Globigerinoides sacculifer*	1.35	8.83*	0.15	26	36	2	[3]
8	*Neogloboquadrina pachyderma*	1.36–1.40	8.83*	0.155	-2	32.6 –3.6	1	[4]
9a	*Ammonia tepida*	1.2–1.9	9.47	0.165	25	32.2	2	[5]
9b	*Ammonia tepida*	1.4–2.0	9.27	0.185	20.0	32.5	2	[6]
9c	*Ammonia tepida*	1.35	4.6 – 15.6	0.165	18.0	35.0	2	[7]
9d	*Ammonia tepida*	1.36	5.91	0.23	25	35.2	2	Ch. 6
10	*Cibicidoides wuellerstorfi*	1.29–1.36	8.83*	0.15	2.9 – 3.4	n.m.	1	[8]
11	*Elphidium crispum*	2.4	17.1	0.14	25	n.m.	2	Ch. 3
12	*Oridorsalis umbonatus*	0.8–1.00	8.72	0.1	1.1-3.6	n.m.	1	[9]
13a	*Amphistegina lessonii*	1.6–1.9	8.83*	0.2	21-29	n.m.	1	[10]
15	*Neorotalia calcar*	1.9–2.2	8.83*	0.235	21-29	n.m.	1	[10]
16	*Heterostegina depressa*	2.56	4.8 – 17.8	0.3	18.0	35.0	2	[7]
17	*Operculina ammonoides*	2.56	8.42	0.3	24	37	2	[12]
21b	*Marginopora vertebralis*	0.6–1.8	8.83*	0.14	21-29	n.m.	1	[10]
22	*Amphisorus hemprichii*	1.8 – 1.9	8.83*	0.21	21–29	n.m.	1	[10]
23	*Quinqueloculina* sp.	3.4	17.1	0.19	25	n.m.	2	Ch. 3

Na/Ca								
#	**Species**	**E/Ca (mmol/mol)**		**D_E ($*10^{-3}$)**	**T (^{0}C)**	**S**	**Study type**	**Ref.**
		calcite	**seawater**					
6	*Globigerinoides ruber*	5.9 – 7.6	45.5*	0.15	n.m.	n.m.	1	[13]
7	*Globigerinoides sacculifer*	5.5 – 6.0	45.5*	0.125	n.m.	n.m.	1	[14]
8	*Neogloboquadrina pachyderma*	4.5 – 5.2	45.5*	0.1	n.m.	n.m.	1	[14]
9b	*Ammonia tepida*	6.12	47.8	0.13	20.0	32.5	2	[6]
11	*Elphidium crispum*	7.3	52.7	0.13	25	n.m.	2	Ch.3
17	*Operculina ammonoides*	24	41.6	0.58	24	37	2	[12]
23	*Quinqueloculina* sp.	5.9	52.7	0.11	25	n.m.	2	Ch.3
Zn/Ca								
#	**Species**	**E/Ca (mmol/mol)**		**D_E ($*10^{-3}$)**	**T (^{0}C)**	**S**	**Study type**	**Ref.**
		calcite	**seawater**					
9d	*Ammonia tepida*	89.0	66	1.3	25	35.2	2	Ch.6
Ba/Ca								
#	**Species**	**E/Ca (mmol/mol)**		**D_E ($*10^{-3}$)**	**T (^{0}C)**	**S**	**Study type**	**Ref.**
		calcite	**seawater**					
5	*Uvigerina spp.*	1.9-4.7	4.6-13.1	0.33	n.m.	n.m.	1	[15]
6	*Globigerinoides ruber*	0.7–1.0	3.3-4.0	0.18	n.m.	n.m.	1	[16]
7	*Globigerinoides sacculifer*	0.65-2.17	4.4-15	0.145	22-39	36.7	2	[17]
8	*Neogloboquadrina pachyderma*	1.4-1.6	5.4 – 5.5	0.275	0	n.m.	1	[18]
10	*Cibicidoides wuellerstorfi*	1.8-4.4	4.5 – 13.5	0.36	n.m.	n.m.	1	[15]
13b	*Amphistegina lessonii*	10-40	50 - 90	0.32	25	32.5	2	[19]
16	*Heterostegina depressa*	30-90	50 - 90	0.81	25	32.5	2	[19]
17	*Operculina ammonoides*	0.3-13.5	15 - 19	0.62	24	37	2	[12]

References Table S2

1. Elderfield, H., et al., Calibrations for benthic foraminiferal Mg/Ca paleothermometry and the carbonate ion hypothesis. Earth and Planetary Science Letters, 2006. 250(3): p. 633-649.
2. Babila, T.L., Y. Rosenthal, and M.H. Conte, Evaluation of the biogeochemical controls on B/Ca of Globigerinoides ruber white from the Oceanic Flux Program, Bermuda. Earth and Planetary Science Letters, 2014. 404: p. 67-76.
3. Dueñas-Bohórquez, A., et al., Effect of salinity and seawater calcite saturation state on Mg and Sr incorporation in cultured planktonic foraminifera. Marine Micropaleontology, 2009. 73(3–4): p. 178-189.
4. Hendry, K.R., et al., Controls on stable isotope and trace metal uptake in Neogloboquadrina pachyderma (sinistral) from an Antarctic sea-ice environment. Earth and Planetary Science Letters, 2009. 278(1): p. 67-77.
5. De Nooijer, L.J., et al., Variability in calcitic Mg/Ca and Sr/Ca ratios in clones of the benthic foraminifer Ammonia tepida. Marine Micropaleontology, 2014. 107: p. 32-43.
6. Wit, J.C., et al., A novel salinity proxy based on Na incorporation into foraminiferal calcite. Biogeosciences, 2013. 10(10): p. 6375-6387.
7. Dueñas-Bohórquez, A., et al., Independent impacts of calcium and carbonate ion concentration on Mg and Sr incorporation in cultured benthic foraminifera. Marine Micropaleontology, 2011. 81(3-4): p. 122-130.
8. Yu, J., et al., Determination of multiple element/calcium ratios in foraminiferal calcite by quadrupole ICP-MS. Geochemistry, Geophysics, Geosystems, 2005. 6(8).
9. Dawber, C. and A. Tripati, Relationships between bottom water carbonate saturation and element/Ca ratios in coretop samples of the benthic foraminifera Oridorsalis umbonatus. Biogeosciences, 2012. 9(8): p. 3029-3045.
10. Raja, R., et al., Magnesium and strontium compositions of recent symbiont-bearing benthic foraminifera. Marine Micropaleontology, 2005. 58(1): p. 31-44.
11. Segev, E. and J. Erez, Effect of Mg/Ca ratio in seawater on shell composition in shallow benthic foraminifera. Geochemistry, Geophysics, Geosystems, 2006. 7(2).

12. Evans, D., et al., Mg/Ca-temperature and seawater-test chemistry relationships in the shallow-dwelling large benthic foraminifera Operculina ammonoides. Geochimica et Cosmochimica Acta, 2015. 148: p. 325-342.
13. Ni, Y., et al., A core top assessment of proxies for the ocean carbonate system in surface-dwelling foraminifers. Paleoceanography, 2007. 22(3).
14. Bian, N. and P.A. Martin, Investigating the fidelity of Mg/Ca and other elemental data from reductively cleaned planktonic foraminifera. Paleoceanography, 2010. 25(2).
15. Lea, D. and E. Boyle, Barium content of benthic foraminifera controlled by bottom-water composition. Nature, 1989. 338: p. 751-753.
16. Lea, D.W. and E.A. Boyle, Barium in planktonic foraminifera. Geochimica et Cosmochimica Acta, 1991. 55(11): p. 3321-3331.
17. Lea, D.W. and H.J. Spero, Assessing the reliability of paleochemical tracers: Barium uptake in the shells of planktonic foraminifera. Paleoceanography, 1994. 9(3): p. 445-452.
18. Hall, J.M. and L.H. Chan, Ba/Ca in Neogloboquadrina pachyderma as an indicator of deglacial meltwater discharge into the western Arctic Ocean. Paleoceanography, 2004.
19 De Nooijer, L.J., (Personal Communications) Ba incorporation in benthic foraminifera, in prep.

Chapter 5

Combined impacts of ocean acidification and dysoxia on survival and growth of four agglutinating foraminifera

Inge van Dijk, Joan M. Bernhard, Lennart J. de Nooijer, Gernot Nehrke, Johannes C.Wit and Gert-Jan Reichart

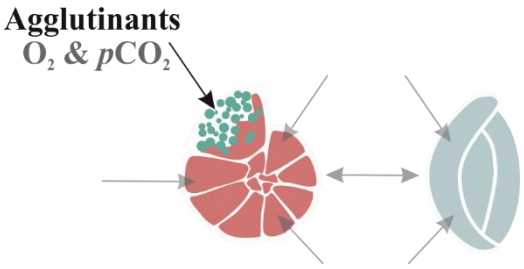

Abstract

Agglutinated foraminifera create a shell by assembling particles from the sediment and comprise a significant part of the foraminiferal fauna. Despite their high abundance and diversity, their response to environmental perturbations and climate change is relatively poorly studied. Here we present results from a culture experiment with different species of agglutinating foraminifera incubated in artificial substrate and exposed to different pCO_2 conditions, in either dysoxic or oxic settings. We observed species-specific reactions (i.e., reduced or increased chamber formation rates) to dysoxia and/or acidification. While chamber addition and/or survival rates of *Miliammina fusca* and *Trochammina inflata* were negatively impacted by either dysoxia or acidification, respectively, *Textularia tenuissima* and *Spiroplectammina biformis* had the highest survivorship and chamber addition rates with combined high pCO_2 (2000 ppm) and low O_2 (0.7 ml/l) conditions. The differential response of these species indicates that not all agglutinating foraminifera are well adapted to conditions induced by predicted climate change, which may result in a shift in foraminiferal community composition.

1. Introduction

Anthropogenic activities are rapidly increasing atmospheric carbon dioxide (CO_2) levels, causing increased dissolved seawater [CO_2] and a subsequent decrease in the ocean's pH and saturation state with respect to calcium carbonate (Doney et al., 2009; Feely et al., 2009). This pH decline in Earth's seawater has been termed "ocean acidification" (OA) and progressing CO_2 emissions are predicted to result in aragonite undersaturation of high latitude-surface seawater in the year 2050 (IPCC, 2007). At the same time, the extent of oxygen minimum zones (OMZ) have been increasing since the 1960s (Stramma et al., 2008a; Stramma et al., 2008b; Stramma et al., 2010) due to climate change (IPCC, 2014) and enhanced ongoing eutrophication (Rabalais et al., 2010; Rabalais et al., 2014). Several marine organisms produce skeletons and shells composed of calcium carbonate, a process that is generally believed to be impacted by ongoing acidification (Riebesell et al., 2000; Orr et al., 2005; Hoegh-Guldberg et al., 2007; Comeau et al., 2009; Keul et al., 2013a). Additionally, since most marine organisms are aerobic, increasing dysoxia may further challenge marine fauna (Stramma et al., 2010). Studies that combine these two stressors (anoxia and OA), so-called dual-stressor studies, are less numerous in the literature until recently (Gobler et al., 2014; Hernroth et al., 2015; Jakubowska and Normant, 2015), even though they can serve as more realistic analogues for future scenarios.

Foraminifera are protists and conspicuous members of microbial marine ecosystems, with representatives in pelagic as well as benthic habitats, occurring from the tropics to poles and from estuaries to hadal zones (Sen Gupta, 1999). Over the last decades, most studies on the relation between stress and foraminifera were performed on the calcium carbonate precipitating taxa (e.g., Weinkauf et al., 2013; Prazeres et al., 2016) and have revealed species-specific reactions to either OA (Kuroyanagi et al., 2009; Manno et al., 2012; Keul et al., 2013a; Doo et al., 2014), dysoxia (Bernhard and Reimers, 1991; Alve, 1995; Alve and Bernhard, 1995; Bernhard et al., 1997; Geslin et al., 2004; Langlet et al., 2014) or combined stressors in less common dual-stressor studies (Dissard et al., 2010; Schmidt et al., 2014; Wit et al., 2016). Uthicke et al. (2013) even suggest that foraminifera might go extinct due to ongoing ocean acidification.

Agglutinating taxa, which build a test (shell) by affixing particles within a matrix of organic compounds or one consisting of calcium carbonate (Bender and Hemleben, 1988), comprise a large portion of many benthic communities (Gooday et al., 1996; Gooday et al., 2000). In this study we analyze the response of selected agglutinating

foraminiferal species to experimentally-induced dysoxia and acidification. The use of artificial sediments allows us to estimate chamber addition rate and characterization of the cement type (carbonate versus non-carbonate). Comparing the response of non-calcareous agglutinating foraminifera to OA with that of calcifying species may allow us to distinguish impacts of reduced calcite saturation state on the calcification process, especially regarding the impacts on metabolism that are not directly linked to calcification. Thus, we can determine the physiological response of foraminifera to environmental stress, without a potential bias from calcium carbonate dissolution. Previous experiments with agglutinating foraminifera in artificial sediment were designed to analyze chamber addition rates, cement characteristics and grain-size selection of selected agglutinating foraminifera (Bender and Hemleben, 1988).

2. Methods

2.1 Foraminiferal collection

2.1.1 *Miliammina fusca* and *Trochammina inflata*

Sediments were recovered from a salt marsh near South Cape Beach, Mashpee MA, USA (N 41°33' 7.9", W70°30'54.4"). Sediments were sieved over a 1-mm mesh sieve to remove macrofauna and stored at Woods Hole Oceanographic Institution (WHOI; Woods Hole, Massachusetts, U.S.A) in containers coupled to a recirculating seawater drip system at room temperature. To obtain foraminifera, sediment from these marsh stocks were sieved over a 90-µm sieve, using artificial seawater (Instant Ocean®, Spectrum Brands, Vicksburg, VA, USA). Living specimens of two species of foraminifera were picked (*Trochammina inflata*, *Miliammina fusca*) from the >90-µm fraction at room temperature and then stored in Petri dishes containing artificial seawater in a thermostat at 15 °C until use in the experiment.

2.1.2 *Spiroplectammina biformis* and *Textularia tenuissima*

During R/V *Endeavor* cruise EN-524 (May 2013), sediment from boxcores was taken at a site called the Mudpatch located on the continental shelf (~80-m depth; approximately N 41°0'0.0", E 70°0'0.0"; Bothner et al., 1981). The surface ~2 cm of sediments was siphoned off the remainder of the boxcore and sieved in different fractions (i.e., <90, 90-125, 125-300, 300-500 µm), maintained at 7 ºC and transported to WHOI. These sediments were installed in a recirculating seawater drip system

housed in a climate room maintained at 7 ºC (±0.1). Foraminiferal stocks were fed weekly with a mixture of *Dunaliella tertiolecta* and *Isochrysis galbana* algae (e.g. Filipson et al., 2010). Prior to isolation of specimens, sediments from the <90 µm fraction were sieved over a 63-µm screen. Using ice packs and trays of ice to minimize temperature fluctuations, living specimens of two species that were abundant in these samples, *Spiroplectammina biformis* and *Textularia tenuissima*, were picked from the >63-µm fraction; these were stored in Petri dishes containing sediment and seawater at 7°C until start of the experiment.

2.2 Experimental set-up

The experimental set-up was identical to that described in Wit et al. (2016), except our experiment did not include the 4000 ppmv CO_2 treatment. In short, the experiment was conducted in a darkened climate-controlled room maintained at 7ºC (±0.1). The experimental set-up consisted of five Biospherix C-Chamber incubators controlled by a Biospherix ProCO_2 and/or ProO_2 controller(s) with sensors controlling the internal carbon dioxide and oxygen concentrations by adding CO_2 and/or nitrogen gas in these incubators (Fig.1).

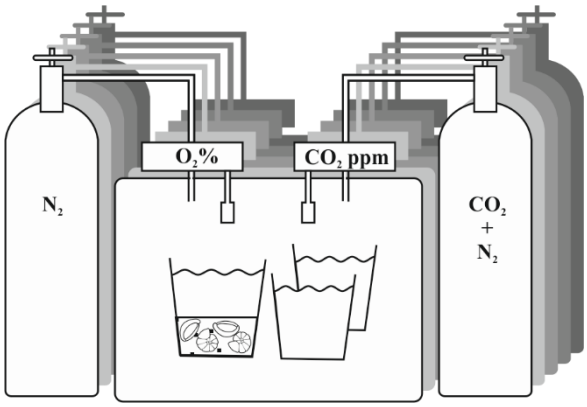

Figure 1. Schematic depicting the five incubators, coupled to N_2 and/or 10,000 ppm CO_2 premix (1% CO_2 + 99% N_2) to maintain stable oxygen and/or carbon dioxide concentrations inside each individual chamber. For this experiment, each incubator included one vessel containing artificial substrate and foraminifera and two vessels containing seawater for equilibration. All vessels were open, allowing for the seawater to be in equilibrium with the overlying air. Foraminifera, incubator size, and substrate depth are not to scale.

One incubator was programmed as a present-day "control" (I), with ambient concentrations of CO_2 (400 ppm) and O_2 (7.1 ml/L). The control was maintained in the laboratory at ambient pCO_2 (397±44 ppm), which was monitored with Qubit infrared CO_2 analyzer (QuBit Systems; Ontario Canada) calibrated with a N_2 gas blank and a standard gas of 1036 ppmv CO_2 in N_2 (McIntyre-Wressnig et al., 2013). Another incubator was programmed as a "Pre-industrial" treatment (IV), which used a CO_2 sensor and controller plumbed to N_2 to obtain pCO_2 (275 ppm) below current ambient concentrations. The other three controllers were set in such a way that these incubators mimicked either dysoxia (0.7 ml/L), acidification (2000 ppm CO_2) or a combination of these conditions. In sum, the design had five different treatments: Control (I), Dysoxia (II), Ocean Acidification (III; OA), Dual-stressor (IV; combined dysoxia and OA) and Pre-industrial (V). Incubators III and V where not coupled to O_2 controllers; the slightly lower O_2 concentrations were due to dilution of O_2 by the added premixed CO_2 gas (Table 1). The culture artificial seawater (salinity = 35), was placed in the different climate chambers four weeks prior to the start of the experiment, to ensure the culture water was in equilibrium with the CO_2 and O_2 levels inside each controlled incubator.

2.3 Artificial substrate

The artificial substrate consisted only of soda glass spheres (1-110 µm), normally used for sand abrasive blasting, so that newly formed chambers were composed of carbonate-free particles, allowing characterization of the adhesive (i.e., organic, calcitic or aragonitic). To clean the artificial substrate prior to the experiment, spheres were placed in a beaker with ultrapure HCl (8 M) and the beaker was placed in an ultrasonic bath for 1 hour and subsequently left standing overnight. The glass spheres were rinsed 5 times with deionized water and placed in the ultrasonic bath during every rinse. After the final rinse, spheres were dried in a laminar-flow hood.

2.4 Foraminiferal incubation

We used CellTracker™ (Life Technologies) to distinguish between living and dead specimens (Fig. 2) with a Leica MZ FLIII epifluorescence stereomicroscope with appropriate excitation and emission optics for the particular probe (see below). These fluorogenic probes cause living cells to fluoresce after proper incubation, and are more suitable for foraminifera than the conventional Rose bengal (protein) staining method

due to the long duration proteins remain postmortem (Bernhard 1988) and hence stain the foraminifera even after cell death. CellTracker™ Orange CMTMR (1 µM final concentration in seawater; 546(±10) nm excitation; 560 nm longpass emission) was used to select living specimens for the experiment, ensuring a living population at the start of incubations.

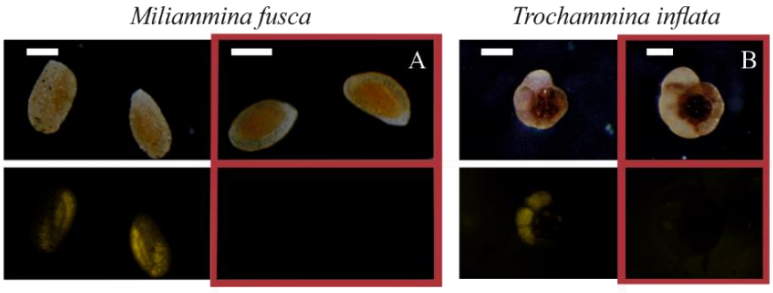

Figure 2. Series of paired light micrographs of CellTracker™ Orange CMTMR incubated specimens of *M. fusca* (A) and *T. inflata* (B). Top row = reflected light micrographs; bottom row = epifluorescence micrographs. Red outline indicates dead specimens (specimens do not fluoresce). Scale bars = 200 µm.

Living specimens of *T. inflata* and *M. fusca* were divided among the different treatments in vessels containing 120 ml seawater equilibrated with the corresponding pCO_2 (see Table 1) and one centimeter of artificial substrate (i.e., glass spheres). Due to limited numbers, living specimens of *S. biformis* and *T. tenuissima* were added to two of the treatments, namely the Control (I) and Dual-Stressor (IV) treatments.

Foraminifera were fed weekly a mix of concentrated *Dunaliella tertiolecta* and *Isochrysis galbana* (Filipsson et al., 2010). Half of the culture water was replaced weekly with equilibrated seawater from the same incubator; the experiment was terminated after 10 weeks. Approximately 24 hours prior to termination of the experiment, CellTracker™ Green CMFDA (Life Technologies) was added to each vessel to distinguish between living (fluorescent) and dead specimens (e.g., Bernhard et al., 2006). Contents of each culture vessels were sieved over a 63-µm mesh to remove most of the artificial substrate. Foraminifera were recovered from the >63-µm fraction and analyzed for survivorship. Living (i.e., fluorescent) and dead (non-fluorescent) foraminifera were stored separately in 4% formalin until further analysis.

Treatment: **Scenario:**	**I** **Control**		**II** **Dysoxia**		**III** **OA**		**IV** **Dual-stressor**		**IV** **Pre-industrial**	
***p*CO$_2$ (ppm)**	400		400		2000		2000		275	
Oxygen (ml/L)	7.1		0.7		5.9		0.7		4.9	
Start/End	**S**	**E**	**S**	**E**	**S**	**E**	**S**	**E**	**S**	**E**
M. fusca	63	48	63	62	63	52	73	67	73	72
T. inflata	57	57	50	47	30	29	45	44	45	45
S. biformis	32	32	-	-	-	-	25	21	-	-
T. tenuissima	25	18	-	-	-	-	25	23	-	-

Table 1. Number of specimens of different agglutinating foraminiferal species at the start of the experiment (S; i.e., introduced) and after harvesting (E; i.e., recovered). Average recovery was 92%. OA = Ocean acidification.

2.5 Analytical methods

2.5.1 Carbon parameters

At the start of the experiment, after the equilibration period of four weeks, we removed 18 ml of seawater (8 ml for dissolved inorganic carbon (DIC); 10 ml for total alkalinity (TA) analyses) from every treatment and replenished the volume with pre-equilibrated seawater from the same incubator, as described in Wit et al. (2016). TA was determined by automated Gran titrations of 1-ml samples, standardized using certified reference materials obtained from Dr. A. Dickson (Scripps Institution of Oceanography). DIC concentrations were determined manometrically on ~ 5 ml samples, using an automated vacuum extraction system. Other carbon parameters were calculated by using the DIC and TA values and the software CO2SYS v2.1, adapted to Excel by Pierrot et al. (2006; Table 2). With the equilibrium constants for K1 and K2 of Mehrbach et al. (1973), refitted by Dickson and Millero (1987) and assuming a [Ca^{2+}] of 10.3 mmol/Kg seawater (Riley and Tongudai, 1967) we were able to estimate [CO_3^{2-}], pH and calcite saturation state ($\Omega_{CALCITE}$) and compare calculated atmospheric CO_2 values to the set values of the CO_2 controller. Calculated *p*CO_2 approximates the set-points of the CO_2 controllers (Table 2).

Treatment: Scenario:		**I Control**	**II Dysoxia**	**III OA**	**IV Dual-stressor**	**IV Pre-industrial**
***p*CO$_2$ (ppm)**		400	400	2000	2000	275
Oxygen (ml/L)		7.1	0.7	5.9	0.7	4.9
Measured	**DIC (µmol/kg)**	2059.1 ±3.1	2171.1 ±1.2	2198.0 ±1.3	2381.4 ±2.4	1908.0 ±0.8
	TA (µmol/kg)	2183.2 ±4.2	2294.5 ±0.04	2163.61 ±3.0	2349.34 ±1.2	2124.63 ±0.02
Calculated	***p*CO$_2$ (ppm)**	471.11	511.13	1691.74	1748.26	247.63
	[CO$_3^{2-}$] (µmol/kg)	95.62	98.16	30.75	35.00	147.64
	pH (total scale)	8.06	8.05	7.52	7.55	8.30
	$\Omega_{CALCITE}$	2.28	2.34	0.73	0.83	3.52

Table 2. Measured (dissolved inorganic carbon (DIC) and total alkalinity (TA) with standard deviation) and calculated (*p*CO$_2$, [CO$_3^{2-}$] and pH) carbon parameters of all treatments.

2.5.2 Quantifying growth parameters

Scanning electron microscope (SEM) images of all foraminifera were taken with a tabletop Hitachi TM3000 to assess newly formed chambers. In addition to survival rates (section 2.4), we determined several growth parameters per species per treatment, namely chamber addition rate, % specimens grown and % deformation. Newly formed chambers were easily recognized because they consist of aggregated artificial sediment (glass spheres). The average number of new chambers per species is defined as the average chamber addition rate. The number of specimens that added any new chambers compared to the total number of incubated specimens, was expressed as percentage specimens grown (i.e., proportion of specimens that added any glass spheres). Specimens that showed deformation abnormalities in test formation (e.g., change in axis of growth; Fig. 3) were counted and divided by the total number of specimens in each treatment (% deformation). To evaluate relations between oxygen content and/or ocean acidification and growth parameters, we calculated p-values using two-sided T-tests and 95% confidence interval of the slopes.

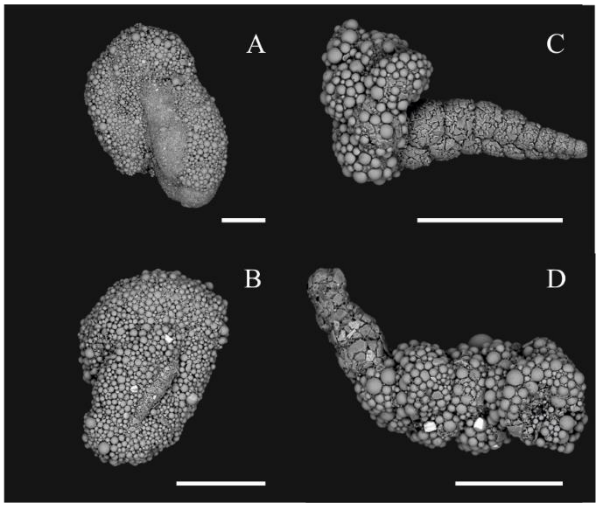

Figure 3. SEM micrographs of deformed specimens of *M. fusca* (A and B), *T. tenuissima* (C) and *S. biformis* (D). Scale bars = 200 µm.

2.5.3 Characteristics of agglutinant adhesives

Additional specimens (~3-5 tests per species) of the four species used in this experiment (*T. inflata*, *M. fusca* , *S. biformis* and *T. tenuissima*) were tested for carbonate cement by adding a drop of HCl (1M) on an air-dried test. This simple procedure represents a quick test to indicate whether dissolution of calcium carbonate occurs. Tests that showed bubbling upon contact with HCl, might have (traces of) carbonate in the adhesive and/or aggregated carbonate particles. Previously, X-ray diffraction was applied to infer foraminiferal cement mineralogy using, in many cases, whole specimens (Wood, 1948; Murray, 1973; Jørgensen, 1977), and later Raman spectroscopy on single grains (Robert and Murray, 1995). Interpretations of these results, however, may be hampered by detrital grains being non-quartz and carbonate rich, because the carbonate particle signal might obscure the adhesive signal. Our culturing methods ensured no incorporation of carbonate particles, and therefore the sole source of a carbonate signal, if detected, was from the adhesive. Hence, to independently verify results from the HCl test, we used confocal Raman microscopy as a method that also offers a high spatial resolution (< 1 µm) (Nehrke and Nouet, 2011), this way separating mineralogy of the adhesive and the aggregated particles. Additional measurements were made using an EDX detector coupled to a benchtop electron microscope (Phenom XL).

3. Results

3.1 Survival and chamber-addition rates

All foraminiferal species used in this culture experiment (except for *T. inflata*) utilized the available artificial substrate to build new chambers (Table 3 and Fig. 4). The proportion of deformed tests (i.e., change in the growth axis) showed no clear relationship among different treatments; for all species, on average, the control treatment had a slightly lower amount of deformations (21%) than in the dual-stressed treatment (24%). These data are insufficient to analyze statistically, but indicate no clear impact of the treatments on malformations in test development.

3.1.1 *T. inflata*

No specimens of this species grew any new chambers in any treatment for the duration of the experiment. Survival rates were, in general, low (≤14.9%), and no specimens survived the OA and Pre-industrial treatments. Survival rates under hypoxic conditions (Dysoxia; 14.9%), even in combination with ocean acidification (Dual-stressor; 13.6%) were higher than that of the Control (5.9%).

3.1.2 *T. tenuissima* and *S. biformis*

Survival rates of *T. tenuissima* and *S. biformis* were zero in the Control (even though ~11 and 47%, respectively, build new chambers), but specimens did survive the Dual-stressor treatment (8.7 and 9.5% for *T. tenuissima* and *S. biformis*, respectively). For both species, the percentage of specimens that grew chambers was highest in the Dual-stressor treatment. Furthermore, both species also had higher chamber addition in the Dual-stressor treatment compared to that of the Control treatment. For *T. tenuissima*, chamber-addition rates increased by a factor of 3.5 from an average of 1.7 in Control to an average of 5.9 chambers in Dysoxia + OA. For *S. biformis*, chamber-addition rates increased from an average of 3.9 (Control) to an average of 8.9 (Dysoxia + OA), which is more than a 2-fold increase. For *S. biformis*, this rate equated to nearly one chamber per week in the Dual-stressor treatment.

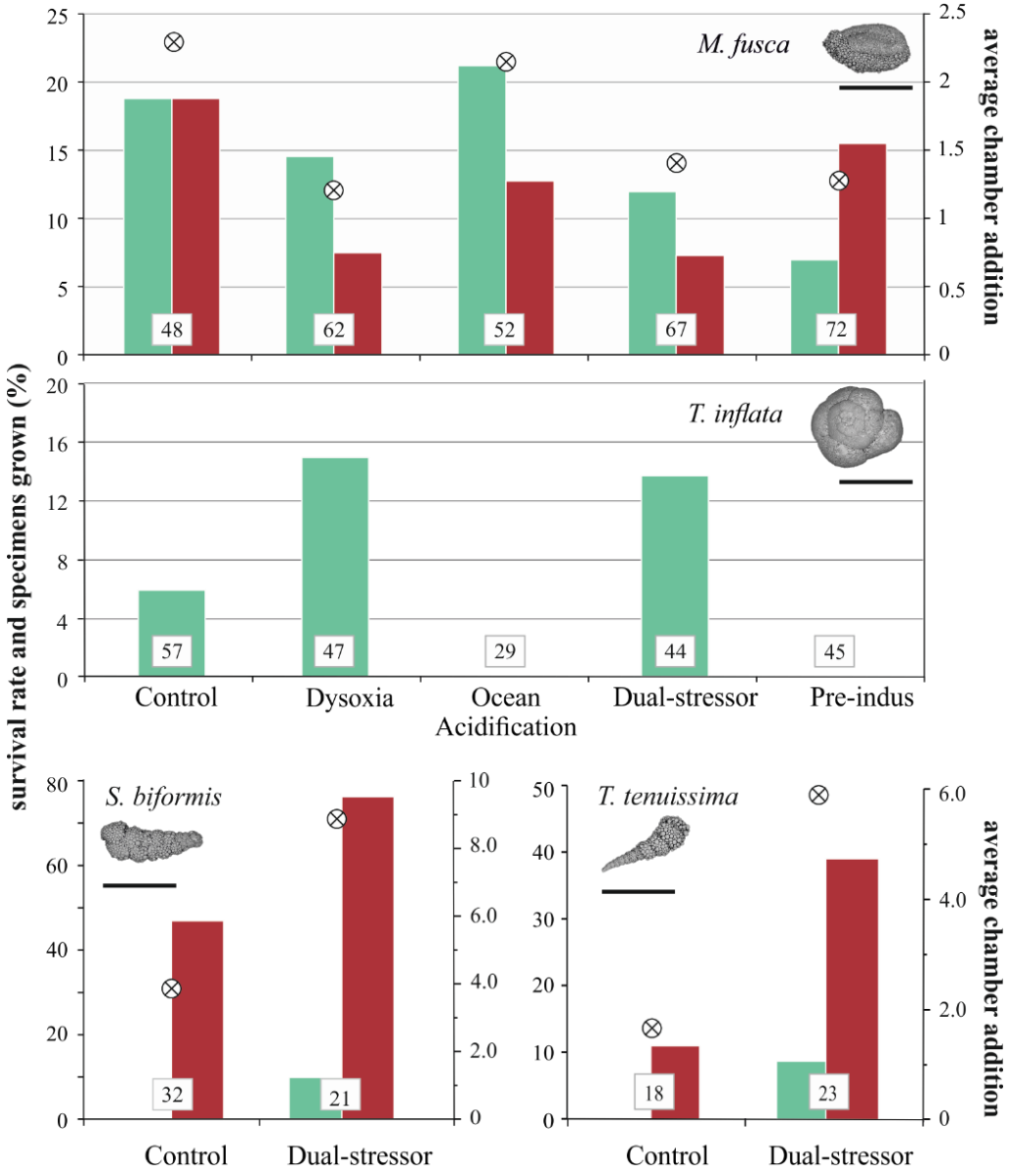

Figure 4. Total number of specimens recovered (n, in white boxes), survival rates (green bars), percentage of specimens that grew any number of chambers during the experiment (specimens grown (%); red bars) and average number of chambers added (open black circles with crosses) of *M. fusca*, *T. inflata*, *T. tenuissima* and *S. biformis*. SEM micrograph; scale bars = 200 µm.

Treatment **Scenario**		**I** **Control**	**II** **Dysoxia**	**III** **OA**	**IV** **Dual-stressor**	**V** **Pre-Indus.**
***p*CO_2 (ppm)**		400	400	2000	2000	275
Oxygen (ml/L)		7.1	0.7	5.9	0.7	4.9
Miliammina fusca.						
Living (%)	**grown**	14.6	1.6	7.7	1.5	2.8
	not grown	4.2	12.9	13.5	10.4	4.2
Dead (%)	**grown**	4.2	6.5	5.8	6.0	12.5
	not grown	77.1	79	73.1	82.1	80.6
Survival rate (%)		18.8	14.5	21.2	11.9	6.9
Specimens grown (%)		18.8	8.1	13.5	7.5	15.3
Avg. chamber addition		2.3	1.2	2.1	1.4	1.3
Trochammina inflata						
Survival rate (%)		5.9	14.9	0.0	13.6	0.0
Spiroplectammina biformis						
Living (%)	**grown**	0.0			9.5	
	not grown	0.0			0.0	
Dead (%)	**grown**	11.1			66.7	
	not grown	88.9			23.8	
Survival rate (%)		0			9.5	
Specimens grown (%)		46.9			76.2	
Avg. chamber addition		3.9			8.9	
Textularia tenuissima						
Living (%)	**grown**	0.0			4.3	
	not grown	0.0			4.3	
Dead (%)	**grown**	11.1			34.8	
	not grown	88.9			56.5	
Survival rate (%)		0			8.7	
Specimens grown (%)		11.11			39.1	
Avg. chamber addition		1.7			5.9	

Table 3. Summary of treatment, survival rates (%), specimens grown (%) and chamber addition per species.

3.1.3 *M. fusca*

This species had lower survival rates in the Pre-industrial, Dysoxia and Dual-stressor treatments compared to the Control and Ocean Acidification treatments (Fig. 5). Also the average chamber addition in the Pre-industrial, Dysoxia and Dual-stressor treatments (1.3, 1.2 and 1.4, respectively) was lower than those of the Control and OA treatments (2.3 and 2.1, respectively). The proportion of growing specimens (specimens grown %) was highest in the Pre-industrial and Control. We found a positive significant correlation (95% confidence, $p<0.001$) between oxygen concentration and % of specimens grown ($R^2 = 0.92$; Fig. 5D). The relation between oxygen content and chamber addition was only slightly significant ($p<0.01$). No clear relationship has been found between either the percentage specimens grown or chamber addition of with pCO_2.

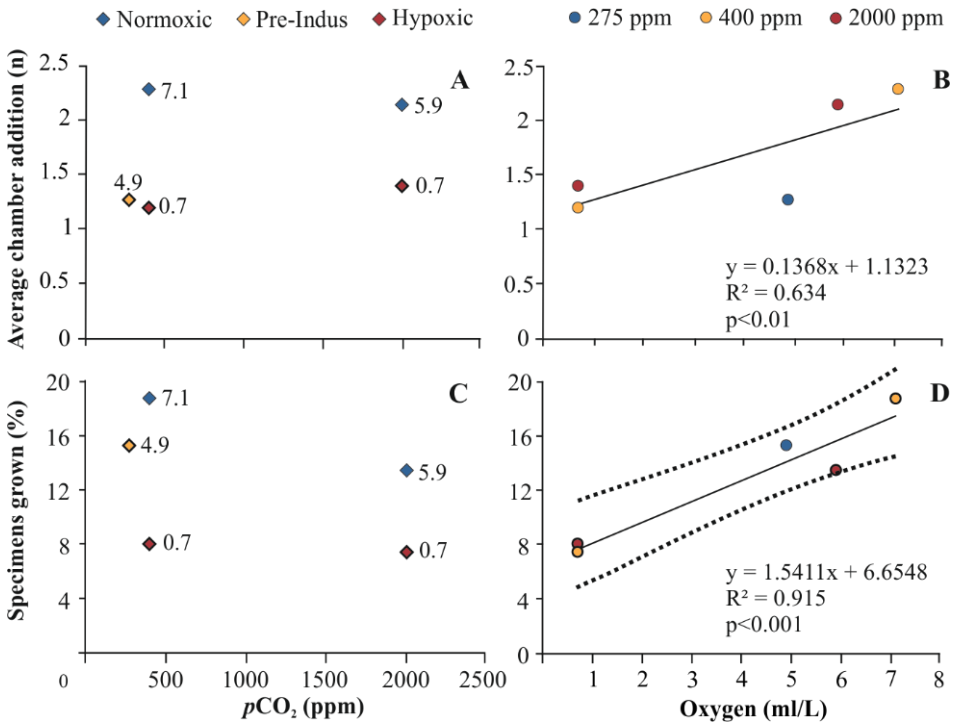

Figure 5. Growth parameters of *M. fusca* versus pCO_2 (A,C) and oxygen content (B,D). Average chamber additions (A and B) and % specimens grown (C and D) with R^2, p-values and 95% confidence interval (dashed lines).

3.2 Cement characteristic

Only tests of *M. fusca* and *T. tenuissima* showed a reaction with HCl, indicating potential presence of carbonate cement and/or incorporation of carbonate-rich particles. Based on published literature, of these two species, only *T. tenuissima* is thought to produce a carbonate cement, as carbonate cement is a main characteristic of the Order Textularia (Sen Gupta, 1999). Raman point measurements were performed on *T. tenuissima* and *M. fusca* as described in Kranz et al. (2010) to measure the adhesive and the aggregated particles separately. The measurement on portions of specimens composed of naturally available sediments identified the particles as typical mineral particles like, e.g., quartz and feldspars, but the adhesive from *M. fusca* and *T. tenuissima* did not show traces of calcium carbonate. Investigating specimens from the experiments in which the foraminifera used glass beads to build their chambers gave the same result concerning the composition of the cement. Measurements on a *T. tenuissima* specimen from the sample collection at the AWI (courtesy Jutta Wollenburg) gave the same result, which was confirmed by additional measurements using an EDX detector coupled to a benchtop electron microscope (Phenom XL), in which the adhesive was identified as being mainly made of carbon (i.e., bioadhesive). Due to this unexpected result, we investigated the cement of all species grown in the experiments. However, none of the investigated specimens contained cement composed of calcium carbonate, and the bubbling caused by HCl was most likely due to aggregated carbonate particles.

4. Discussion

4.1 Effect of (combined) stressors on foraminifera

Foraminiferal cultures are inherently difficult to set up and require considerable attention during the experiment. For investigating the impact of environmental variables there is a tradeoff between duplication of experiments and environmental variables that can be tested. Whereas we do not have enough replication to statistically quantify impact of individual culture conditions, we are able to compare impacts between treatments and also between species. Also by comparing consistency of reactions to different conditions (e.g., survival rate and chamber addition) we slightly add to the robustness of our analyses.

Culturing agglutinating foraminifera under controlled dysoxia and/or ocean acidification scenarios revealed species-specific reactions. *M. fusca* and *T. inflata*

each had different negative reactions towards dysoxia and/or ocean acidification. *M. fusca* was less successful (lowest survival rate, lowest amount of specimens with growth and lowest number of chambers added) when exposed to lower than normoxic conditions compared to aerated conditions regardless of pCO_2. This is confirmed by the relation between oxygen content with both chamber addition and the amount of specimens that added new chambers (Fig. 5B, D). This implies that acidification unlikely impacts this species, at least over this time frame of ~2.5 months, but that the combined effects of oxygen depletion and acidification might surpass a critical threshold. The dual stressor treatment was the sole condition where *M. fusca* lacked growth, indicating that future climate scenarios (i.e., OA + dysoxia; IPCC, 2014) likely will have a negative impact on this species. *T. inflata* seemed to be relatively well adapted to low-oxygen environments. The higher survival rates under both dysoxia and ocean acidification might indicate that *T. inflata* is better able to survive oxygen depletion and OA (at 2000 ppm CO_2). This might also explain previous reports of opportunistic behavior of this genus during the Toarcian Oceanic Anoxic Event (Reolid et al., 2014).

In contrast, both specimens of *T. tenuissima* and *S. biformis* showed on average higher chamber addition rates in dual-stressed conditions, which might be interpreted as an increase in growth rates caused by either stress (e.g. additional chambers; Coccioni, 2000) or favorable conditions. Although difficult to quantify, there appeared to be no clear increase in test deformation, (i.e. change in growth axis; e.g. Geslin et al., 2000) and chambers appeared of normal size and shape. Thus, environmental stress as an explanation for increased growth may be less likely than favorable conditions, suggesting these two species (*T. tenuissima, S. biformis*) might be somewhat adapted to dysoxia and OA. This is consistent with previous studies on *S. biformis* which have shown this opportunistic species is capable of enduring anoxia (Alve, 1995; Asteman et al., 2015).

4.2 Calcification stress versus physiological response

Culturing agglutinating foraminifera in artificial substrate did not only yield information about chamber addition rate during culture experiments, it also allowed analysis of the adhesive of newly formed chambers. We could characterize the adhesive phase (i.e., organic, calcitic or aragonite) while preventing contamination of the signal by presence of particles used in natural test construction. Raman spectrometry indicated no presence of $CaCO_3$ in adhesive of newly formed chambers

of the species that grew new chambers (*M. fusca*, *S. biformis* and *T. tenuissima*) in this study. We, therefore, infer that these three species use an organic compound (bioadhesive) to attach particles. This observation potentially has implications for the classification of *T. tenuissima* in the carbonate-cement producing Order Textularia (Loeblich and Tappan, 1988). Furthermore, the lack of any carbonate cement enables appraisal of solely physiological effect of ocean acidification on foraminifera, without potential side effects from calcification stress, which was previously also tested on thecate foraminifera (Bernhard et al., 2009).

Results from the treatments involving ocean acidification (III and V) showed that the physiological impact on our cultured taxa was not related to a stressed calcification process. We found that for three of our species, pCO_2 (alone) did not impact survival and chamber addition rates negatively. *T. inflata* was the only species with a bioadhesive that appeared negatively impacted by increased pCO_2, but this impact, manifest as total mortality, only occurred in the aerated treatments (III, V). In general, we might say pCO_2 has a secondary or, in some species, no impact on the physiology or metabolism of three agglutinating foraminifera (*M. fusca*, *T. tenuissima* and *S. biformis*), at least over the duration of this experiment. These observations suggest that the negative response of carbonate-producing foraminifera to ocean acidification is potentially solely due to calcification stress (Uthicke et al., 2013).

4.3 Implications for future foraminiferal ecology

Changes in environmental conditions in sediments might result in a shift of the benthic, agglutinating foraminiferal community. We show that species of agglutinating foraminifera had different responses to environmental factors such as ocean acidification and/or dysoxia. In general, pCO_2 did not seem to be the primary stressor for the selected agglutinating foraminifera. In fact, *M. fusca* had increased chamber addition and survival rates in the higher pCO_2 (ocean acidification) compared to the dual stressor treatment, and *T. tenuissima* and *S. biformis* seemed to thrive in combined low oxygen and high pCO_2. Decreases in oxygen concentrations, however, might cause a major shift in species composition. In general, some foraminifera are able to survive low oxygen concentrations by storing nitrate and subsequently respire in the absence of oxygen in a process called denitrification (Risgaard-Petersen et al., 2006). It is not known whether agglutinating foraminifera are also able to respire nitrate, but some species, like *T. tenuissima*, are able to collect and store NO_3^- (Piña-Ochoa et al., 2010), implying that some species of Textularia do

denitrify. This might cause *T. tenuissima* to thrive in future anoxic scenarios. In our study, *T. tenuissima* and *S. biformis* seemed to be well-adapted to, and even more successful (in terms of chamber addition rate and survivorship), in treatments similar to those of future climate scenarios, characterized by a combination of dysoxia and ocean acidification. Average chamber addition rate, and therefore growth, in these species is 2.2-3.4 times higher in the dual stressor treatment, potentially suggesting an accelerated life cycle in future climate scenarios. Although no growth occurred in our experiment, *T. inflata* and *S. biformis* might increase in distribution and abundance in OMZ regions due to its opportunistic behavior (Reolid et al., 2014; Asteman et al., 2015). Conversely, *M. fusca* appeared to be more successful in terms of chamber addition rates in well aerated treatments (Fig. 5), so increasing oxygen depletion (i.e., dysoxia) might decrease growth rates for this species.

5. Conclusions

In general, several carbonate producing foraminifera seem to be less successful (in terms of calcification rate) in future climate scenarios (summarized in Keul et al., 2013a; Doo et al., 2014), compared to some of the agglutinating foraminifera in our study. Such observations may suggest that a future increase in dysoxia and pCO_2 might lead to an increase in the opportunistic agglutinated species and a decrease in the carbonate producing community. However, more dual- or multi-stressor culture studies and longer-term experiments are needed to understand species-specific reactions to projected climate scenarios (Bernhard et al., 2015).

Acknowledgements

We thank the Captain, crew and science party of RV *Endeavor* EN 524 cruise, as well as William Phalen, who supported our salt-marsh sampling. We thank Jutta Wollenburg (AWI) for providing fossil *T. tenuissima* specimens and Jan-Berend Stuut (NIOZ) for a allowing us to work on the SEM (NWO grant 822.01.008 and ERC grant 311152). This research is funded by the NIOZ – Royal Netherlands Institute for Sea Research and the Darwin Centre for Biogeosciences project "*Double Trouble*: Consequences of Ocean Acidification – Past, Present and Future –Evolutionary changes in calcification mechanisms", The Robert W. Morse Senior Scientist Chair (JMB), US NSF grant OCE-1219948 (JMB) and the Netherlands Earth System Science Center (NESSC to GJR).

Chapter 6

Impacts of pH and [CO_3^{2-}] on the incorporation of Zn in foraminiferal calcite

Inge van Dijk, Lennart J. de Nooijer, Mariëtte Wolthers and Gert-Jan Reichart

DOI: 10.1016/j.gca.2016.10.031

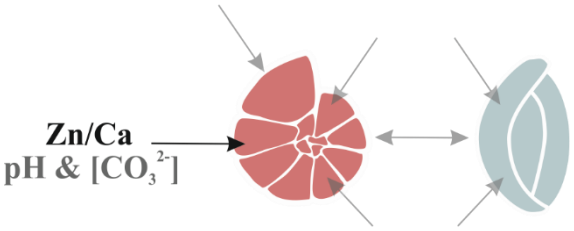

Abstract

The trace elemental composition of foraminiferal shell calcite is known to reflect the environment in which the shell was precipitated. Whereas conservative elements incorporated in foraminiferal shell carbonate reflect factors such as temperature (Mg), carbonate chemistry (B) and salinity (Na), the nutrient type elements (Ba, Cd, and possibly Zn) are useful tools to reconstruct biogeochemical cycling and past ocean circulation. Still also nutrient-type elements will be most likely influenced by factors other than their relative concentrations. Culturing benthic foraminifera under controlled carbonate chemistry conditions allows for disentanglement of impacts of different parameters of the carbon system on the elemental composition of foraminiferal calcite. Here we show that zinc incorporation in cultured specimens of the benthic foraminifer *Ammonia tepida* is correlated to changes in carbonate ion concentration ([CO_3^{2-}]). By modeling activities of different chemical species of Zn in seawater over a range of [CO_3^{2-}], we suggest that Zn^{2+}, rather than other relatively abundant Zn-species (e.g. $ZnCO_3^0$ and $ZnHCO_3^+$) is taken up during biomineralization. Our results suggest that foraminiferal Zn/Ca might be especially useful when combined with other [CO_3^{2-}] proxies, enabling reconstruction of past seawater element concentrations. Conversely, when the nutrient-type element concentrations are known, incorporation of Zn in foraminiferal shells can be used to reconstruct past sea water carbon speciation.

1. Introduction

From the active carbon cycle more than 95% is present in dissolved inorganic form in seawater (Zeebe and Wolf-Gladrow, 2001). Over geological times, changes in carbon speciation determine the amount of CO_2 in the atmosphere and studies of past carbon cycling has provided important insights in the relation between climate and carbon cycling. Past marine inorganic carbon cycling can only be assessed by independently reconstructing at least two individual parameters of the so-called CO_2 system (e.g. pH, ΣCO_2, alkalinity, [CO_3^{2-}]: see Zeebe and Wolf-Gladrow, 2001 for details). The interdependency of these parameters can subsequently be used to reconstruct the complete inorganic carbon system over geological timescales using any combination of the two reconstructed parameters. Combining reconstructed seawater pH and alkalinity (e.g. Hönisch and Hemming, 2005), for example, has resulted in reconstruction of Pleistocene dissolved CO_2 concentrations, thereby allowing estimates of atmospheric CO_2 levels (Hönisch et al., 2009). Accuracy and precision of these reconstructions depend on the quality and the extent to which the applied proxies are truly decoupled. The chemical composition of calcite shells produced by foraminifera is widely used for reconstructing past climate parameters. Besides functioning as a paleothermometer (e.g. using calcitic Mg/Ca; Nürnberg et al., 1996; Nürnberg, 2015; Evans et al., 2016), element concentrations (e.g. B/Ca) and stable isotope ratios (e.g. $\delta^{11}B$) in foraminiferal shells can also reflect different parameters of the inorganic carbon system, including pH and [CO_3^{2-}] (Sanyal et al., 1996; Raitzsch et al., 2011). The co-variation of carbon system parameters in nature often limits field calibrations and core top studies, since this obscures the impact of a single parameter on foraminiferal calcite chemistry. Moreover, such calibrations are often hampered in their application due to additional and/or unknown impacts of other parameters of the inorganic carbon system, environmental parameters (e.g. temperature, salinity) and vital effects (e.g. growth rate). For instance, application of the reported correlation between foraminiferal B/Ca and [CO_3^{2-}] (Yu and Elderfield, 2007; Yu et al., 2010; Rae et al., 2011) may be complicated by additional controls on boron incorporation by changes in seawater pH (Hemming and Hanson, 1992b), DIC and/or [Ca^{2+}] (Uchikawa et al., 2015), temperature and/or salinity (Allen et al., 2011). Experiments that separately assess impacts of different environmental parameters are therefore necessary to improve their application.

To study the isolated impacts of carbon system parameters on foraminiferal calcite chemistry, laboratory experiments where foraminifera are cultured under controlled conditions were designed (Spero et al., 1997; Keul et al., 2013b). In such experiments,

the isolated impact of e.g. pH is studied, when comparing foraminifera grown under conditions with variable versus stable pH. Such an approach was also applied to determine the individual impacts of pH and [CO_3^{2-}] on U incorporation in foraminiferal calcite, which was previously found to correlate with both pH and [CO_3^{2-}] (Russell et al., 2004; Raitzsch et al., 2011). These experiments suggested that carbonate ion concentration rather than other parameters of the inorganic carbon system, controls foraminiferal U/Ca and thereby highlight its potential as an independent [CO_3^{2-}] proxy (Keul et al., 2013a).

Inorganic precipitation experiments previously showed that Zn adsorption onto calcite depends on solution pH (Zachara et al., 1991). However, core top studies (Marchitto et al., 2000; Marchitto et al., 2002) suggested that both Cd/Ca and Zn/Ca in foraminiferal shell carbonate covary with calcite saturation (ΔCO_3^{2-}) and might thus provide a paleoceanographic tracer for deep water masses. At the same time due to their nutrient like behavior, Cd and Zn have the potential to be used in concert to reconstruct small changes in nutrient concentrations in thermocline waters and carbonate saturation state (Bryan and Marchitto, 2010). Since these parameters are difficult to separate in the field we here calibrate incorporation of zinc (Zn) in foraminiferal shell calcite as a function of individually varied seawater pH and [CO_3^{2-}]. We developed an experimental set-up in which these parameters are varied independently, with the newly formed calcite being analyzed for Zn/Ca using LA-ICP-MS. Response to pH and [CO_3^{2-}] were evaluated against inorganic chemical speciation of Zn.

2. Methods

2.1 Foraminifera collection

Between January and April 2013, surface sediment samples were collected during low tide at an intertidal mudflat near Texel, the Netherlands (coordinates: 53°0'21.4"N; 4°45'8.6"E). Samples were sieved over a 1 mm screen to remove the benthic macrofauna. Sediment was stored in small aquaria with seawater collected at the sampling site, thus providing a stock of foraminifera for culture experiments. Prior to the culturing experiments in summer 2013, material from the stock sediment was sieved over a 150 µm screen to concentrate foraminiferal specimens of the species *Ammonia tepida*. From the resulting >150 µm size fraction, living specimens characterized by yellow cytoplasm and pseudopodial activity, were selected for the culturing experiments.

2.2 Seawater preparation

Surface water (salinity = 35.2) from the North Atlantic was filtered (0.2 µm pore-size) and used as a basis for production of approximately 10 L of stock culture media. Since natural Zn/Ca of surface seawater is relatively low (on average 4.4 µmol/mol; Boyle, 1981; Marchitto et al., 2002), Zn concentration of the culture water was increased by adding 2.000 µmol of Zn ICP standard (1000 mg/L, $Zn(NO_3)_2$ in HNO_3 2-3% CentiPUR) to the stock solution. This increases the Zn/Ca of the culture water approximately 15 times compared to average open ocean seawater [Zn]. Increasing the element to calcium ratio of surface seawater [Zn] below 0.1 mg/L does not influence survival and chamber addition rates of the miliolid foraminifera *Pseudotriloculina rotunda (Nardelli et al., 2013)*. For *Ammonia tepida*, increasing the heavy metal element (e.g. Ni) to calcium ratio of surface seawater less than 20 times does not influence growth and morphology (Munsel et al., 2010). The pH of this stock solution was increased to 8.1 by adding a small volume (~5 ml) of 0.1 M NaOH. Subsamples were taken to determine DIC and alkalinity of the stock solution, which was stored in a 10 L Nalgene container at 10°C and placed in the dark. Eight volumes of 750 ml of this stock solution were manipulated with one of two different carbonate system treatments, resulting in four 750 ml bottles per seawater treatment. The advantage of using a single stock solution for all treatments is that they will have identical seawater Zn/Ca.

2.2.1 Carbonate and pH manipulation

In the first treatment, the pH stable treatment, seawater was manipulated to derive media with varying [CO_3^{2-}], while keeping a similar pH. This was accomplished by addition of pre-defined amounts of $NaHCO_3$ (30-265 mg) to four 750 ml bottles filled with seawater from the stock solution. The experimental range included one treatment with [CO_3^{2-}] lower than the stock solution and, therefore, seawater was acidified with HCl and bubbled with nitrogen to lower DIC by CO_2 outgassing. The [DIC] was then increased to the target value by addition of $NaHCO_3$. For all four treatments, added volumes of [DIC] were estimated using CO2SYS software (Pierrot et al., 2006) to relate the inorganic carbon chemistry to target atmospheric CO_2 concentrations (i.e. 180, 760, 1400 and 2000 ppm), representing pre-industrial, predicted concentration for the end of 21st century, and two extreme greenhouse conditions. Pre-mixed gasses with exactly these concentrations were subsequently used during the incubations.

For the second treatment, the acidification experiment, four 750 ml-bottles were filled with seawater from the stock solution and addition of a small volume (~0.5 ml) 0.1M HCl or 0.1M NaOH to obtain media with a range of pH values, whilst keeping a relatively constant [DIC]. Bottles with teflon lining were used to store both sets of treatment solutions without headspace at 7 °C in the dark until start of the culture experiments.

2.3 Culture set-up

Four air tight incubators (each with a volume of approximately 10 L) were installed in a climate chamber with an ambient, constant temperature of 25°C. Incubators were placed in a cabinet, with a day-night cycle of 12 hours:12 hours (300 lux) and connected to four different CO_2 enriched air premixes corresponding with the equilibrium pCO_2 of the treatments (180, 760, 1400 and 2000 ppm CO_2). Prior to entering the 10 L incubators, gas was bubbled through a vessel with deionized water to humidify the gasses flowing into the incubators, minimizing evaporation of the culture media. In each of the four incubators, two 500 ml-bottles containing stock media from both seawater manipulations were stored under these conditions for 4 weeks prior to the start of the experiment to serve as pre-equilibrated stock solutions to be used to replace the foraminiferal culture media. At the start of the culture experiments, Petri dishes containing approximately 20 ml of medium and 5-6 foraminiferal specimens from either one of the stocks were placed (Fig. 1) in each incubator, consequently resulting in 10-17 foraminifera per seawater medium per CO_2 treatment. At the start of the experiment, pictures of individual foraminifera were taken with a DFC420 Leica camera coupled to a M165C Leica microscope to determine amount of chambers per individual at the beginning of the experiment. We were able to identify and recognize our specimens since there were only 5-6 individuals per Petri dish, and every specimen has unique characteristics for recognition (chamber shape, small (coiling) malformations, test diameter, etc.).

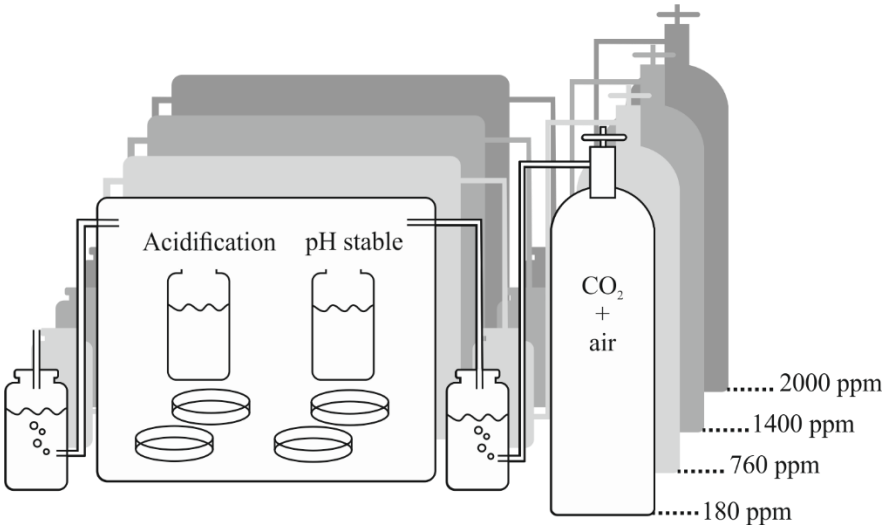

Figure 1. Culture set-up: CO_2 premix connected to an air tight incubator containing two sets of culture samples and both artificial seawater treatments, 'pH stable' and 'Acidification'. The total set-up comprised four incubators, each coupled to one of four different CO_2 premixes.

Twice a week the foraminifera were fed with concentrated *Dunaliella salina* cells. The cultured algal cells were centrifuged three times for 2 minutes at 2000 rpm, after which the solvent was siphoned off and replace with de-ionzed water after every centrifuge step in order to discard the algae culture media. The resulting *Dunaliella* cells were freeze- dried to remove any remaining solvent and diluted in 1 ml of treatment water, resulting in 8 different batches of 1 ml feeding solution. Once a week the culture media were replaced with new equilibrated seawater from the stocks kept in the same incubator. Twice a week, subsamples were taken from the culture water stocks for pH and once every two weeks for DIC and alkalinity analyses. Every time the incubator was opened, the CO_2 premix flow rate was increased from 2L/ hour to 60L/ hour for approximately 60 minutes to quickly replace the air within the incubators, thereby minimizing fluctuations in atmospheric pCO_2 during the culturing experiment. After 6 weeks, all specimens were harvested and photographed again to determine the number of newly grown chambers for each treatment.

2.4 Analytical methods

2.4.1 Carbonate system parameters

pH of the different treatments was measured twice a week using a pH meter (pH110, VWR), to assess the stability of the carbonate system during the experiment. The stock seawater (North Atlantic surface seawater) was subsampled twice for pH, TA and DIC measurements, prior to culture treatment manipulations. Subsamples of the culture media were taken in duplicate to determine DIC concentrations and total alkalinity (TA) twice a week, starting after the pre-incubation period of four weeks. In order to analyze the DIC of the different treatments, subsamples were collected in headspace vials containing a saturated $HgCl_2$ solution (10µl $HgCl_2$/10 ml sample). DIC measurements were performed on an autoanalyzer TRAACS 800 spectrometric system (Stoll et al., 2001). These analyses require only a small amount of sample, while yielding high accuracy (±2 µmol/kg) and precision (±1.5 µmol/kg). Subsamples for TA analysis were collected in 50 ml Falcon tubes and stored after addition of a small volume of saturated $HgCl_2$ solution (10µl $HgCl_2$/10 ml sample). TA was determined using the standard operating procedure for open cell potentiometric titration (Dickson et al., 2007; SOP 3b), using an automatic titrator (Metrohm 888, Titrando), a high accuracy burette (± 0.001 mL), a thermostated reaction vessel (25 ^{0}C) and a combination pH glass electrode (Metrohm 6.0259.100). TA values were calculated by a non-linear least-squares fit to the titration data (Dickson et al., 2007, SOP 3b) in a custom-made script in the open source programming framework R. Quality assurance involved regular analysis of Certified Reference Materials (CRM) obtained from the Scripps Institution of Oceanography (Dickson et al., 2003). The average relative external precision of the TA measurements is 4.64%.

Other carbonate system parameters (including $[CO_3^{2-}]$) were calculated using the average DIC and TA values per treatment and the software CO2SYS v2.1, adapted to Excel by Pierrot et al. (2006). With the equilibrium constants for K1 and K2 of Mehrbach et al. (1973), refitted by Dickson and Millero (1987), we were able to estimate $[CO_3^{2-}]$ and $\Omega_{CALCITE}$ and compare calculated atmospheric CO_2 and pH values to the premix and measured values (Table 1).

Treatment		Measured					Calculated CO2SYS			
		pH	TA µmol/kg		DIC µmol/kg		pCO_2 (ppm)	pH	[CO_3^{2-}] µmol/kg	Ω_{CC}
			AVG ±SD	RSD (%)	AVG ±SD	RSD (%)				
Stock NSW		8.21± 0.02	2397 ±4	2.3	2230 ±11	1.0	300.1	8.15	122.6	2.94
Acidification	**180**	8.28± 0.03	2899 ±19	6.5	2278 ±63	2.8	193.6	8.37	457.9	11.02
	760	8.01± 0.01	2518 ±17	6.6	2295 ±43	1.9	692.2	7.88	172.0	4.14
	1400	7.84± 0.02	2345 ±11	4.8	2252 ±51	2.3	1332.3	7.60	91.1	2.19
	2000	7.61± 0.04	2240 ±19	8.6	2203 ±77	3.5	1896.1	7.44	61.9	1.49
pH stable	**180**	7.94± 0.04	994 ±8	8.1	835 ± 37	4.4	196.3	7.98	77.6	1.87
	760	7.95± 0.02	3886 ±13	3.2	3461 ±55	1.6	728.9	8.02	352.1	8.48
	1400	8.01± 0.02	7341 ±28	3.8	6600 ±62	0.9	1358.8	8.03	684.2	16.47
	2000	8.08± 0.03	11025 ±26	2.4	9898 ±97	1.0	1910.4	8.06	1081.7	26.04

Table 1. Average (Avg) carbon parameters (pH, n=12; TA= Total alkalinity; n=6 DIC=Dissolved Inorganic Carbon, n=6) with (relative) standard deviation of the stock of natural seawater (NSW) and culture water per treatment. CO2SYS was used to calculate carbonate ion concentration ([CO_3^{2-}]) and calcite saturation state (Ω_{CC}) and recalculate pH and atmospheric CO_2 from measured TA and DIC.

2.4.2 Seawater zinc and calcium analysis using SF-ICP-MS

Culture media were subsampled (1 mL), and diluted 300 times with 0.1M HNO_3 before measuring the media's minor and major element compositions in triplicate using an Element-2 sector field double focusing Inductive Coupled Mass spectrometry (SF-ICP-MS; Thermo Scientific, Bremen, Germany) run in medium-resolution mode (m/Δm=3000) to avoid the effect of mass interferences (e.g. $^{40}Ca+^{26}Mg$). The inlet of the mass spectrometer was equipped with a teflon microflow nebulizer and a Peltier cooled spray chamber to maximize stability of the signal. Calcium concentrations were calculated using an external calibration method with seawater matrix-matched standards. External precisions (RSD) are 6% for ^{25}Mg, ^{88}Sr and ^{43}Ca. We obtained an average $[Mg^{2+}]$ of 47±2 mmol/kg, $[Sr^{2+}]$ of 50±6 µmol/kg and $[Ca^{2+}]$ 8.4±0.3 mmol/kg for all treatments (Table 2).

Treatment		$[Zn^{2+}]$ nM	$[Mg^{2+}]$ mM	$[Sr^{2+}]$ µM	$[Ca^{2+}]$ mM	Zn/Ca µmol/mol	Mg/Ca mol/mol	Sr/Ca mmol/mol
Acidification	**180**	563.53 ±12.82	44.54 ±1.78	53.56 ±3.28	8.57 ±0.08	65.79 ±2.15	5.20 ±0.26	6.25 ±0.45
	760	517.59 ±23.65	45.70 ±3.20	49.47 ±1.35	8.51 ±0.44	60.80 ±5.89	5.38 ±0.65	5.82 ±0.46
	1400	570.72 ±31.25	46.87 ±1.41	53.46 ±1.08	8.68 ±0.78	65.73 ±9.51	5.41 ±0.65	6.17 ±0.68
	2000	582.20 ±67.03	47.28 ±2.36	51.41 ±1.15	8.41 ±0.48	69.24 ±11.92	5.63 ±0.60	6.13 ±0.49
pH stable	**180**	537.49 ±5.74	44.62 ±1.34	50.07 ±3.05	7.95 ±0.72	67.60 ±6.81	5.62 ±0.68	6.31 ±0.95
	760	560.96 ±6.42	46.07 ±0.46	54.98 ±2.97	8.52 ±0.62	65.84 ±5.50	5.42 ±0.45	6.47 ±0.82
	1400	542.4 ±22.63	49.79 ±2.49	47.99 ±3.88	8.56 ±0.35	63.43 ±5.04	5.84 ±0.53	5.62 ±0.68
	2000	553.32 ±13.44	48.85 ±0.49	36.22 ±1.58	8.13 ±0.44	68.10 ±4.51	6.02 ±0.39	4.47 ±0.44

Table 2. Element concentrations and element-calcium ratios of the culture media per treatment ± (propagating) SD.

Zn concentrations were determined by pre-concentration over an in-house build ion exchange column (volume approximately 70µl) containing NOBIAS-chelate P1 resin (following Biller and Bruland, 2012). Subsamples of 30 ml were adjusted prior to pre-concentration to a pH of 6.5 ±0.2 using a 3.7M ammonium acetate buffer. Each column was conditioned with 0.05M ammonium acetate buffer for 1 minute after which the seawater was loaded for approximately 20 minutes. After loading the column with the sample it was rinsed with 0.05M ammonium acetate buffer for 2 minutes. The columns were eluted with ~1.5ml 1M HNO_3 and the eluent was analyzed in triplicate on the SF-ICP-MS run in medium-resolution mode. External precision for obtained [Zn^{2+}] was 5.19%, and we obtained an average [Zn^{2+}] of 0.036 mg/L or 554 ± 21 nM (Table 2), which is over 100 times higher than natural deep seawater concentrations, based on global deep water Si:Zn relationship (Marchitto et al., 2000). This concentration of Zn/Ca_{SW} (average of 66 ± 3 µmol/mol) is approximately 15x higher than average surface seawater (4.4 µmol/mol; Boyle, 1981; Marchitto et al., 2000). Still, this concentration is not considered to be toxic to foraminifera (Nardelli et al., 2013).

2.4.3 Elemental concentrations in foraminiferal calcite

After termination of the experiment, foraminiferal shells were cleaned by adding pH buffered sodium hypochloride (15% NaOCl) to microvials with individual foraminifera to remove organic material. After incubation for 20 minutes, samples were rinsed three times with ultrapure water, then dried in a laminar flow cabinet and positioned on a stub. Element concentrations of individual chambers were analyzed by Laser Ablation-ICP-MS (Reichart et al., 2003). To determine foraminiferal Zn/Ca, the laser system (NWR193UC, New Wave Research) at the Royal NIOZ was equipped with a 2-volume cell (New Wave Research), characterized by wash-out time of 1.8 seconds (1% level) and hence allowing to detect variability of obtained Zn/Ca within chamber walls. Single chambers were ablated in a helium environment using a circular laser spot with a diameter of 80 µm. All foraminiferal samples were ablated with an energy density of 1±0.1 J/cm^2 with a repetition rate of 5 Hz. The aerosol was transported with a helium/argon flow into the quadrupole ICP-MS (iCAP-Q, Thermo Scientific). Monitored masses included ^{23}Na, ^{24}Mg, ^{25}Mg, ^{26}Mg, ^{27}Al, ^{43}Ca, ^{44}Ca, ^{55}Mn, ^{66}Zn, and ^{88}Sr. ^{66}Zn is free of interferences when measuring calcium carbonate and SRM NIST glass standards, contrary to ^{67}Zn and ^{68}Zn (Jochum et al., 2012). Zn and Ca intensities over time were integrated with Thermo Qtegra software, avoiding potential contamination or diagenesis of the outer or inner layer of calcite by monitoring the Al- and Mn-signals, resulting in determined Zn/Ca of the experimental

calcite only (Fig. 2). Due to the low Zn incorporation in pre-experimental (field) chambers, we could also distinguish and exclude older chambers by absence of a detectable Zn profile.

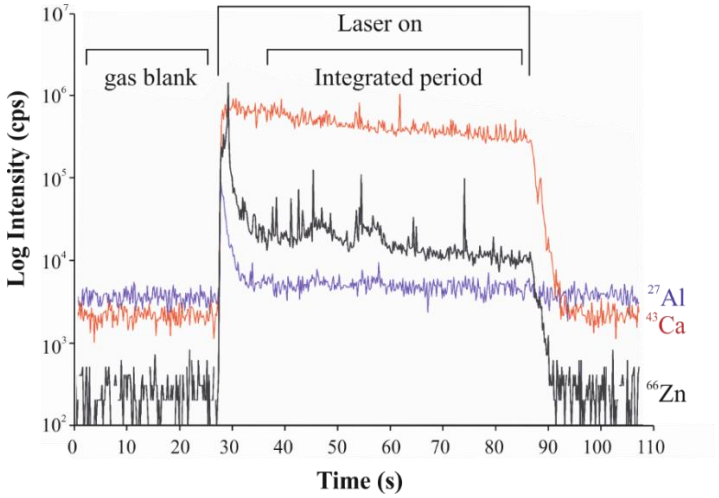

Figure 2. Example of a typical LA-ICP-MS analysis of a single chamber. Gas blanks are deducted from the signal in the integrated period, to obtain elemental concentration of primary calcite.

Calibration was performed against SRM NIST612 glass standard, at an energy density of 5±0.1 J/cm^2, with ^{43}Ca as an internal standard. Using a different energy density between foraminiferal calcite and glass standard has been shown to not affect the analyses (Dueñas-Bohórquez et al., 2009). NIST612 is a suitable calibration standard when measuring Zn/Ca, since Zn concentration of this standard is relatively close (39.1 ppm) to that in the foraminiferal calcite from the experiments used here. To increase precision and accuracy, we applied a linear drift correction over the series of measurements. Relative precision of the analyses (relative standard deviation (RSD) of all NIST612) is 3% for ^{25}Mg, 3% for ^{88}Sr and 2% for ^{66}Zn. In total, 162 chambers were analyzed for eight experimental conditions, resulting in 10-26 single chamber measurements per condition.

We calculated the standard deviation (SD), RSD and standard error (SD/√n; SE) per treatment. The partitioning coefficient of an element (E) between seawater and foraminiferal calcite is expressed as $D_E = (E/Ca_{CALCITE})/(E/Ca_{SW})$. Partion coefficients ($D_{Mg}$, D_{Sr} and D_{Zn}) and element versus calcium ratio ($Zn/Ca_{CALCITE}$) were statistically

compared using a two-sided T-test with 95% confidence levels. This also allows for the calculation of 95% confidence intervals over the average per treatment. F-tests were used to compare the variance in Zn/Ca values of the pH Stable and Acidification treatment (α=0.05).

3. Results

3.1 Calcitic element concentrations

Average elemental ratios in foraminiferal calcite of newly formed chambers (summarized in Table 3) from all treatments were 2.10±0.38 mmol/mol for Mg/Ca, 1.36±0.13 mmol/mol for Sr/Ca and ranges from 45.3-130.7 µmol/mol for Zn/Ca. A summary of the obtained $Zn/Ca_{CALCITE}$, $Mg/Ca_{CALCITE}$ and $Sr/Ca_{CALCITE}$ values are shown in Table 4 and Fig. 3. The relative standard deviations (RSD) of the different elements varies between 15.3-22.2% (Mg/Ca), 6.8-11.9% (Sr/Ca) and 11.5-28% (Zn/Ca). For $Mg/Ca_{CALCITE}$ (ranging from 1.71-2.48 mmol/mol) there was no siginifcant relation with any of the seawater carbonate parameters (pH, [CO_3^{2-}], TA and DIC). $Sr/Ca_{CALCITE}$ of *A. tepida* varies between 1.31-1.40 mmol/mol over both treatments. The partition coefficient D_{Sr} significantly changes over a range of either [CO_3^{2-}], TA and DIC (Fig. 4), while there is no significant relation with pH ($p>0.25$).

Treatment		n	**Foraminifera w/ new chambers**		**Total new chambers (n)**	**Avg. chamber addition (Avg±SD)**	
			n	**(%)**		**42 days**	**Per week**
Acidification	180	12	12	100	22	1.8±0.7	0.26±0.10
	760	15	15	100	22	1.5±0.9	0.21±0.13
	1400	11	8	73	18	1.6±0.7	0.23±0.10
	2000	12	12	100	16	1.3±1.0	0.19±0.15
pH stable	180	11	10	91	18	1.6±0.4	0.23±0.06
	760	11	10	91	16	1.5±0.5	0.21±0.07
	1400	10	9	90	17	1.7±0.7	0.24±0.10
	2000	15	13	87	29	1.9±0.7	0.28±0.10

Table 3: Total number of foraminiferal specimens (n = 10-15) and number of new chambers added per treatment. Average chamber addition (per week) based on linear growth.

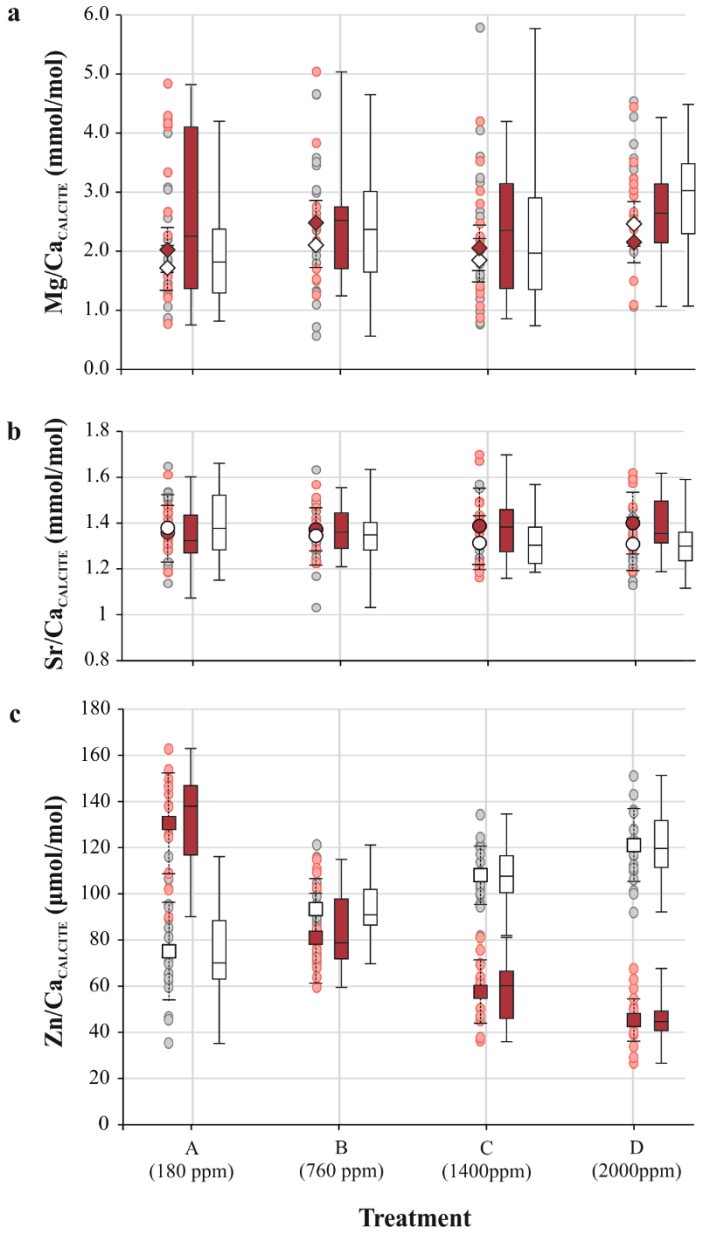

Figure 3. Mg/Ca$_{CALCITE}$ (a; diamonds), Sr/Ca$_{CALCITE}$ (b; circles) and Zn/Ca$_{CALCITE}$ (c; squares) average±SD element to calcium ratios and LA-ICP-MS single measurements of both Acidification (white symbols and grey dots respectively) and pH Stable (red symbols and pink dots resp.) with related boxplots for all treatments (A-D).

Treatment		N	Zn/$Ca_{CALCITE}$ µmol/mol				D_{Zn}	Mg/$Ca_{CALCITE}$ mmol/mol				D_{Mg} *10^{-3}	Sr/$Ca_{CALCITE}$ mmol/mol				D_{Sr}
			Avg	SD	RSD	SE		Avg	SD	RSD	SE		Avg	SD	RSD	SE	
Acidification	**180**	22	75.1	21.0	28.0	4.5	**1.1**	1.71	0.38	22.2	0.12	**0.33**	**1.38**	0.14	10.5	0.05	**0.22**
	760	28	93.4	12.9	13.8	2.4	**1.5**	2.10	0.38	18.1	0.08	**0.39**	**1.35**	0.12	9.2	0.03	**0.23**
	1400	18	108.2	12.5	11.5	2.9	**1.6**	1.84	0.37	20.1	0.09	**0.34**	**1.31**	0.12	8.8	0.04	**0.21**
	2000	23	121.2	15.8	13.0	3.3	**1.8**	2.46	0.38	15.4	0.08	**0.44**	**1.31**	0.11	8.7	0.03	**0.21**
pH stable	**180**	15	130.7	21.7	16.6	5.6	**1.9**	2.02	0.38	18.8	0.09	**0.36**	**1.36**	0.12	8.8	0.04	**0.22**
	760	15	81.0	19.4	24.0	5.0	**1.3**	2.48	0.38	15.3	0.10	**0.46**	**1.37**	0.09	6.8	0.04	**0.21**
	1400	15	57.5	13.6	23.6	3.5	**0.9**	2.05	0.39	19.0	0.10	**0.35**	**1.39**	0.17	11.9	0.04	**0.25**
	2000	26	45.3	9.1	20.0	1.8	**0.7**	2.15	0.35	16.3	0.07	**0.36**	**1.40**	0.13	9.6	0.03	**0.31**

Table 4. Overview of Zn/Ca, Mg/Ca, and Sr/Ca ratios in foraminiferal calcite (Avg=average; SD=standard deviation; RSD=relative standard deviation; SE=standard error) results from LA-ICP-MS, and partitioning coefficients D_E in bold.

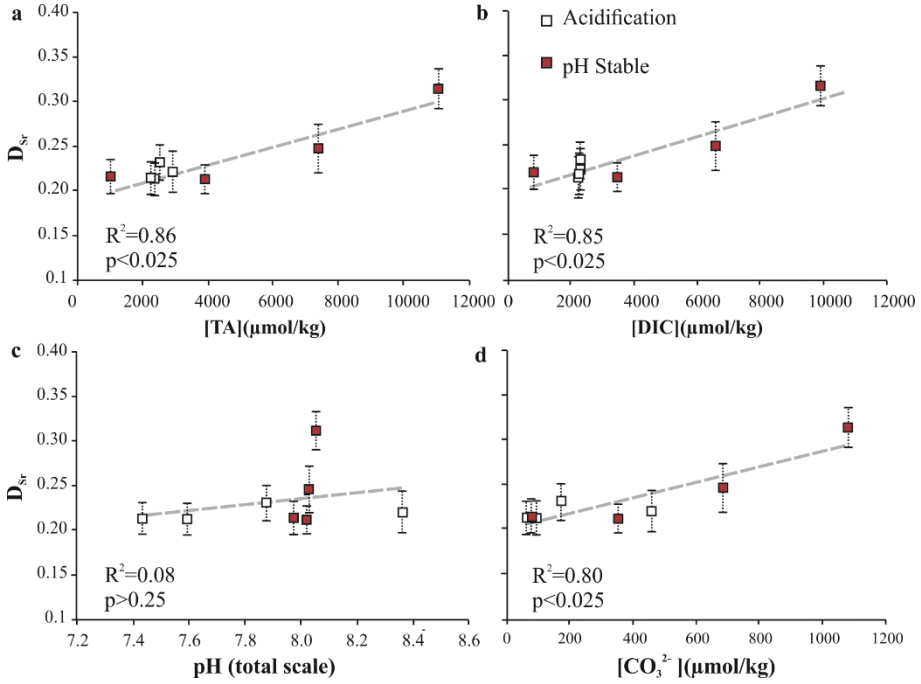

Figure 4. D_{Sr}±SD of the pH stable (red) and Acidification (white) treatment. Top panel: D_{Sr} versus a) Total Alkalinity (TA) and b) Dissolved Inorganic Carbon (DIC). Lower panel: D_{Sr} versus c) pH and d) $[CO_3^{2-}]$. Grey dashed lines are linear regressions, R^2 and p-vales (95% confidence) are reported in the graph.

3.2 Zn/Ca variability

The precision of Zn/Ca for the calibration standard (2%) was much smaller than the observed variability between measurements on chambers from the same treatment, which show a relative standard deviation of 11.5-28.0%. Foraminiferal Zn/Ca values from the variable pH treatments vary between 75.1 and 121.2 µmol/mol, and Zn/Ca of foraminifera cultivated at stable pH lies between 45.3 and 130.7 µmol/mol (Fig. 5). When plotting Zn incorporation as a function of either TA or DIC (Fig. 5a, b), $Zn/Ca_{CALCITE}$ decreases with both increasing TA and DIC in the pH stable treatment, resulting in an overall correlation with both these parameters ($p<0.05$). However, average $Zn/Ca_{CALCITE}$ varies strongly within the Acidification experiment, over a narrow range in TA and DIC. When plotting $Zn/Ca_{CALCITE}$ versus pH (Fig. 5c), we observe a large range in Zn/Ca values (45.3-130.7 µmol/mol) when pH remains relatively stable (7.9-8.08).

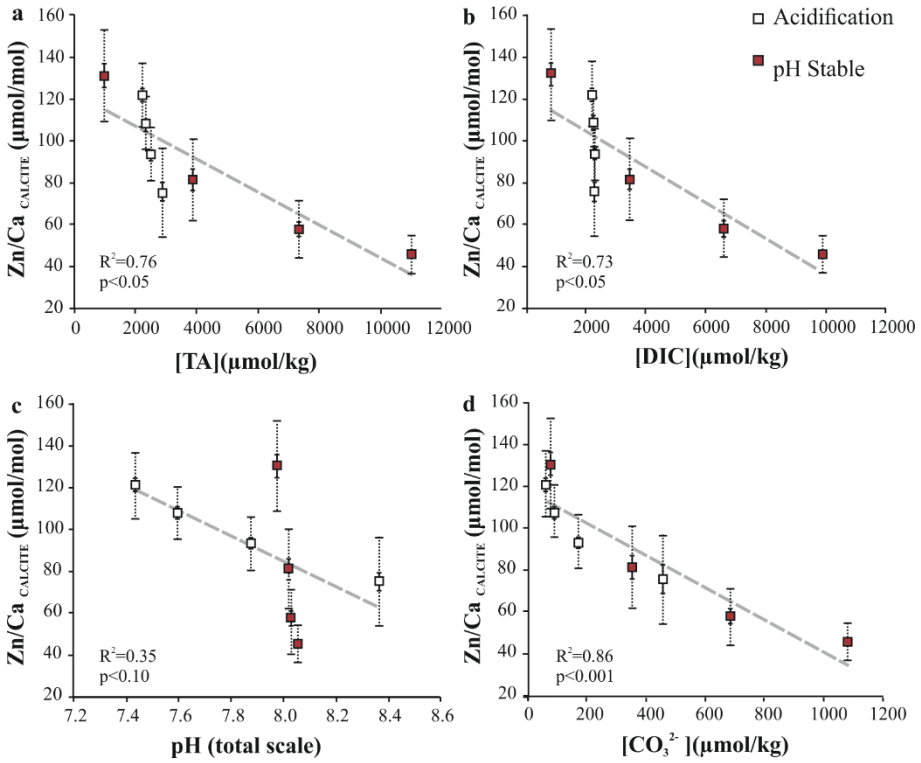

Figure 5. Zn/Ca$_{CALCITE}$ of the pH stable (red) and Acidification (white) treatment. Top panel: Zn/Ca$_{CALCITE}$ versus a) Total Alkalinity (TA) and b) Dissolved Inorganic Carbon (DIC). Lower panel: Zn/Ca$_{CALCITE}$ versus c) pH and d) [CO_3^{2-}]. Standard errors (solid line) and -deviations (dotted line), caused by intra and inter specimen variablity are plotted for every treatment. Grey dashed lines are linear regressions, R^2 and p-vales are noted in the graph.

When comparing the variance in Zn/Ca values for the pH Stable group with the Acidification group using a F-test, we observe that the variance of the Acidification group is significantly smaller than the pH Stable group (left-sided F-test, α=0.05). This implies that the observed variation in Zn incorporation is not controlled by pH, but rather by another parameter of the inorganic carbon system that somewhat covaries with pH in the Acidification treatment (e.g. [CO_3^{2-}]). The best overall fit is shown when Zn incorporation is plotted as a function of [CO_3^{2-}] (Fig. 5d; p<0.001). We obtain a highly significant relation (p<0.0005) when D_{Zn} ranges from 1.9 to 0.7 and [CO_3^{2-}] changes from 61.9 to 1081.7 µmol/kg (Fig. 6).

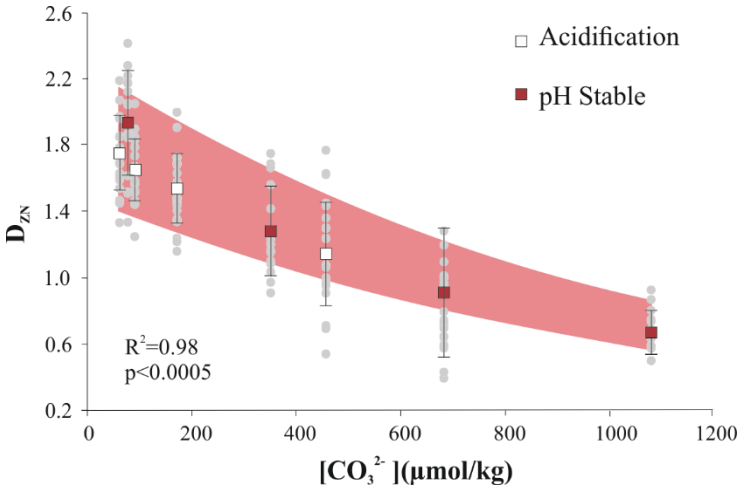

Figure 6. Partitioning coefficient, D_{Zn} ± SD of individual ablations (grey circles) and the average per treatment (pH stable = red, Acidification = white). The relationship between D_{Zn} (Y) and $[CO_3^{2-}]$ (X) can be expressed as $Y = ae^{bx}$, where a= 1.86±0.38 and b= -0.001±0.0001 (solid line). Dashed lines indicate 95% confidence interval.

4. Discussion

4.1 Chamber addition rates

When comparing the average chamber addition of the foraminifera in this study (Table 3) with a foraminiferal culture study with enriched heavy metals (Munsel et al., 2010), we find almost 10-fold higher chamber addition rates per week (0.23 versus 0.03-0.04 chambers per week in the 10- and 20-fold enrichment treatment). This could be due to additional stress in the study by Munsel et al. (2010), by increasing the concentration of three heavy metals (Cu, Ni and Mn) instead of one, or due to the introduction of fluorescent label calcein. Long-term exposure to calcein has an adverse effect on benthic foraminifera, even when using low concentration of 5mg/L (Kurtarkar et al., 2015), which may explain the overall lower new chamber yield in the culture study of Munsel et al. (2010).

4.2 Element incorporation as a function of seawater carbonate chemistry

Culturing foraminifera under a range of inorganic carbonate conditions shows that incorporation of Zn in shell calcite correlated particularly to [CO_3^{2-}] (Fig. 5d), since the range in foraminiferal Zn/Ca is relatively large when either of the other components (i.e. pH, TA and DIC) are stable or vary over a limited range. Although co-variation is observed with pH, TA and DIC of the culture media (Fig. 6a-c) this seems an artefact from the inherent coupling of these parameters in the seawater carbonate system. This suggests that $Zn/Ca_{CALCITE}$ provides a robust proxy for carbonate ion concentration. No impact of seawater pH, TA and/or DIC is necessary to explain the observed trends. In contrast to $Zn/Ca_{CALCITE}$, foraminiferal Sr/Ca decreases when [CO_3^{2-}], TA and/or DIC increases (Fig. 4 and Table 4). Sr incorporation in foraminiferal calcite has been suggested to change with pH (Lea et al., 1999), and later-on has been proposed to react to changes in [CO_3^{2-}] (Dissard et al., 2010). We show that D_{Sr} is not significantly impacted by pH (Fig. 4), but by either [CO_3^{2-}], DIC or TA. Foraminiferal Mg/Ca (2.10±0.38 mmol/mol) are in good agreement with the expected Mg/Ca (2.17 mmol/mol) based on existing temperature calibrations for this species (Toyofuku et al., 2011). Moreover, Mg/Ca does not vary systematically with seawater carbonate chemistry, confirming results from earlier studies (e.g. Dueñas-Bohórquez et al., 2011), but are in contrast with others (Kısakürek et al., 2008; Evans et al., 2016).

4.3 Intra- and inter-specimen Zn/Ca variability

In our study we observed appreciable intra- and/or inter-specimen variability in $Zn/Ca_{CALCITE}$. The relative standard deviation (RSD) of measured $Zn/Ca_{CALCITE}$ between specimens ranged from 11.5 to 28.0%, depending on the treatment (Table 4). This variability is considerably higher than the external precision (RSD = 2%), based on multiple analyses of the calibration standard (NIST612). One of the causes for this relative high variability in the Zn/Ca of foraminifera might be laboratory contamination. $Zn/Ca_{CALCITE}$ has been proven challenging to measure (Bruland et al., 1978), due to the combination of generally low concentrations in calcium carbonate and potential contamination when handling samples in the laboratory. Therefore, to optimize our $Zn/Ca_{CALCITE}$ measurements, we did not apply an acid leach during cleaning of the foraminiferal samples since this may increase $Zn/Ca_{CALCITE}$ values (Marr et al., 2013). We also increased the initial Zn concentrations in the culture water and cultured foraminifera without natural sediment to avoid contamination by

presence of Zn-containing clay particles. Therefore, contamination is an unlikely cause for the observed inter- and/or intraspecimen variability in Zn/Ca. Zn can also be introduced in the culture vessels by the addition of food, since the growth media for algae contains measurable concentrations of Zn. However, since we separated this culture media from the *Dunaliella* cells by centrifuging and freeze-drying, we assume this amount of additional Zn is either absent or negligible.

Another source for the variability in $Zn/Ca_{CALCITE}$ within treatments might be the stability of the experimental set-up over time. Due to the slope of the relationship between D_{Zn} and $[CO_3^{2-}]$ (Fig. 6), small deviations of pCO_2 during the culture experiment may have caused variability in $[CO_3^{2-}]$ and thereby, minor variation in intra- and/or inter-variability of $Zn/Ca_{CALCITE}$. Relative stability of TA (RSD <8.6%) and [DIC] (RSD <4.4 %) during the course of the experiments (Table 1), however, suggest that variability in $[CO_3^{2-}]$ was minor. Nevertheless, changes in seawater carbonate chemistry on time scales shorter than that required to build a shell and/or single chamber could result in a heterogeneous Zn distribution between foraminiferal shell chambers. Even though short-term variability might not have been detected due to the frequency of the sampling, it unlikely accounts for the range in measured $Zn/Ca_{CALCITE}$, as this would have averaged out in the time needed for a foraminifera to add chambers.

Variability in Zn/Ca, like other proxies based on foraminiferal carbonate, may be explained by differences in e.g. ontogeny, growth rates and biological activity (Zeebe et al., 2008; Raitzsch et al., 2010; Wit et al., 2012), which all might affect element fractionation during biomineralization (Erez, 2003; De Nooijer et al., 2014b). In a number of studies (Erez, 2003; Eggins et al., 2004; Sadekov et al., 2005; Kunioka et al., 2006; Hathorne et al., 2009; De Nooijer et al., 2014a; Branson et al., 2015) it has been shown that other elements like Mg, Ba and B can be heterogeneously distributed within chamber. In our study, besides a relatively high variability in $Zn/Ca_{CALCITE}$, we also observed similar high RSD values for $Mg/Ca_{CALCITE}$ (15.3-22.2%), which might indicate that Zn is also incorporated heterogeneously. This high variability, caused by heterogeneity in Zn distribution within a foraminifera might limit the precision of this potential proxy. However, it has been shown for foraminiferal $Mg/Ca_{CALCITE}$ that the trend between the margin of error and sample size ($1/\sqrt{n}$; Sadekov et al., 2008; De Nooijer et al., 2014a) is in line with a more or less random distribution. Hence oversampling and statistical treatment of the data should cancel out such effects. Like $Mg/Ca_{CALCITE}$, the uncertainty in estimated average $Zn/Ca_{CALCITE}$ would then also decrease exponentially with increasing sample size. Such an averaging corresponds

with the within chamber-wall variability in Zn being primarily related to a lamellar mode of calcification (Reiss, 1960). The minimum number of specimens required for an accurate estimate of average population Zn/Ca depends on the constraints needed for the [CO_3^{2-}] concentration, following similar models as previously published for Mg/Ca and temperature (Wit et al., 2012).

4.4. Zinc is incorporated as Zn^{2+}

To explore the mechanisms underlying incorporation of Zn in foraminiferal calcite, activities of different species of Zn were modeled as a function of changing [CO_3^{2-}] using the software package PHREEQC (Parkhurst and Appelo, 1999) and the standard PHREEQC llnl database. For all experimental treatments, free Zn (Zn^{2+}) increases with increasing carbonate ion concentration. Simultaneously, activity of aqueous Zn-carbonate complexes ($ZnCO_3^0$ and $ZnHCO_3^+$) decreased or remained similar over the range of [CO_3^{2-}] studied here. These modeled activities were plotted against the average $Zn/Ca_{CALCITE}$ corresponding the [CO_3^{2-}] from our treatments (Fig. 7). The incorporation of Zn in foraminiferal shell calcite increased with Zn^{2+} activity for both the pH stable and the Acidification treatments. When running the model with normal (15 times lower) [Zn], we find similar profiles for the activity of different Zn species. This suggests that the incorporation of Zn is mainly determined by the (bio-) availability of Zn as free Zn^{2+} ion, which is in turn affected by changes in [CO_3^{2-}], and are not impacted by the total [Zn]. However, the slope of the relationship between $Zn/Ca_{CALCITE}$ and Zn^{2+} activity is slightly different for the two seawater manipulations, hinting at an additional control on the incorporation of Zn. This might indicate either that [CO_3^{2-}] influences other mechanisms that control Zn incorporation, e.g. growth rates (both chamber addition and calcification rate), metabolism, ontogeny, or that a second (carbon) parameter secondarily affects Zn-incorporation. The second possibility is less likely, due to the observed strong correlation between [CO_3^{2-}] and D_{Zn} ($p<0.0005$). Nevertheless, we cannot exclude TA or DIC as a potential secondary, minor control on Zn in foraminiferal shell calcite. Of all parameters investigated here, pH might be the least likely to have an effect on Zn-incorporation, since the observed change in incorporated Zn is largest when pH remains stable.

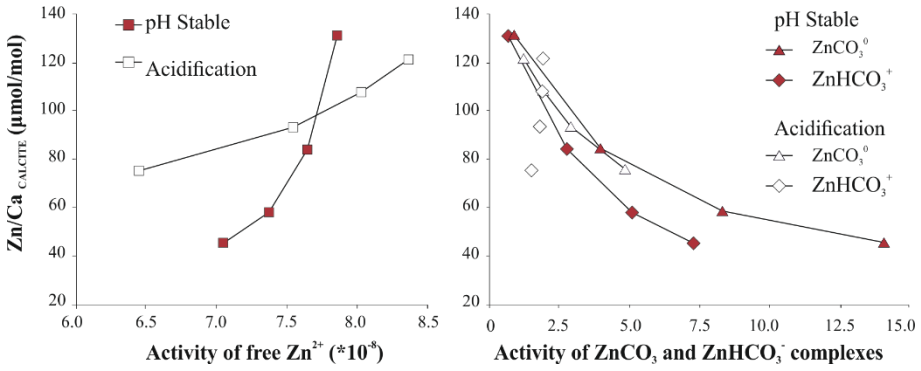

Figure 7. Zn/Ca in foraminiferal calcite at different activities of free Zn^{2+} (left panel) and Zn-carbonate complexes (right panel; triangles= $ZnCO_3^0$; diamonds= $ZnHCO_3^+$) corresponding with the [CO_3^{2-}] of the different treatments and seawater manipulations (pH stable = red; Acidification = white)

4.5 Inorganic precipitation versus biomineralization

Even though inorganic calcite precipitation is not directly comparable to foraminiferal calcification (Elderfield et al., 1996), comparing results of these two types of experiments may increase our understanding of some of the controls on element incorporation during biomineralization (De Nooijer et al., 2014b). Results from inorganic adsorption experiments (Zachara et al., 1991) show that the relation between calcite Zn/Ca and [CO_3^{2-}] is similar to that found here for the benthic foraminifer *Ammonia tepida*. Inorganically precipitated calcite crystal surfaces have a higher affinity for Zn as pH of the growth medium increases. In a study by Zachara et al. (1991) pH of different treatments was changed by manipulating DIC (although not explicitly stated in the paper), which implies that e.g. $NaHCO_3$ was added to achieve the desired solution composition and pH, resulting a similar anti-correlation of pH and [CO_3^{2-}] created in the experiments presented here. However, in the experiments of Zachara et al. (1991), where the solution was in equilibrium with calcite, the calcite surface characteristics will vary with pH. With progressively higher pH, the surface becomes more negatively charged, enhancing the adsorption of positively charged ions such as Zn^{2+} (Wolthers et al., 2008). In our culturing study, with solutions that are supersaturated with respect to calcite, there is an opposite trend: a decrease in Zn association with pH (Fig. 5c). Clearly, the local control of the foraminifera on the calcifying fluid (De Nooijer et al., 2009; Glas et al., 2012), combined with the impact

of free Zn^{2+} activity overrule any potential surface charge effects on Zn uptake. During calcification in perforate species, Ca^{2+} is actively taken up in the cytoplasm via transmembrane transporters, and is probably not stored in intravesuclar reservoirs (De Nooijer et al., 2014b). Our results suggest that uptake of Zn^{2+} follows the same pathways as Ca^{2+}, with more Zn^{2+} being incorporated with increasing availability of free Zn^{2+}. In our culture study, foraminiferal D_{Zn} varies between 1.9 and 0.7, while inorganically precipitated calcite has a D_{Zn} of approximately 6 at similar temperature and pressure, but higher seawater [Zn] (2120 nM; Crocket and Winchester, 1966). This suggests that foraminifera incorporate less Zn than expected from an a-biological perspective. Such an apparent discrimination against Zn is in line with uptake over a membrane as suggested above.

4.6 The effect of calcite saturation state on D_{Zn}

Marchitto et al. (2005) found a positive relation between calcite saturation state, expressed as ΔCO_3^{2-} ($[CO_3^{2-}]_{in\ situ}$ - $[CO_3^{2-}]_{saturation}$) and D_{Zn}. A similar effect has been reported for other elements, like D_{Cd} and D_{Ba} by McCorkle et al. (1995), who showed reduced incorporation of trace metals in undersaturated waters. Apparently, the mechanics behind the relation between [CO_3^{2-}] and Zn incorporation found in our study and the studies of Marchitto et al. (2000, 2002 and 2005) stem from two different controls. These last studies analyzed foraminiferal Zn in deep-sea foraminifera of core-tops in near-undersaturated seawater and argues Rayleigh fractionation causes the internal calcification reservoir to be flushed rapidly, resulting in lower D_{Zn} due to lower calcite saturation state. In our case, the culture media were always well above calcite saturation state (lowest Ω = 1.49; Table 1). This might indicate that the influence of near-undersaturation with respect to calcite does not affect our data, in which the incorporation of Zn is mainly governed by the amount of bioavailability of Zn^{2+}.

There is a distinct offset observed between estimates of *Cibicidoides wuellerstorfi* (D_{Zn}=9; Marchitto et al., 2000), *Cibicidoides pachyderma* (D_{Zn}=22; Bryan and Marchitto, 2010), the miliolid *Pseudotriloculina rotunda* (D_{Zn}=0.2-4.0; Nardelli et al., 2016) and our culture calibration for *Ammonia tepida* (D_{Zn}=1.9-0.7). This offset could be caused by the different seawater [Zn], due to difference in fractionation in natural conditions. Nardelli et al. (2016) show that lower seawater [Zn] results in higher D_{Zn}, which could explain why Zn partitioning is higher in the *Cibicidoides* species, which probably calcified at lower (deep sea) seawater [Zn]. Furthermore, observed

differences might stem from species-specific vital effects due to calcification strategy, contamination, study type (culturing versus field-calibration) and/or accuracy in determination of $Zn/Ca_{SEAWATER}$, but might also reflect an additional environmental control on Zn incorporation. Temperature, for instance, influences crystal growth rates (Morse et al., 2007), which consequently might have an effect on the sorption and subsequent incorporation of metals on the crystal structure. Also other environmental factors, e.g. salinity, not constrained here, might affect these partitioning coefficients.

4.7 Paleoceanographic implications

The relationship between $[CO_3^{2-}]$ and foraminiferal Zn/Ca could be applied for reconstructing two types of parameters. Firstly, our results show that foraminiferal Zn/Ca might indeed be used as a proxy for $[CO_3^{2-}]$, and furthermore, that it also is not biased by changes in pH. However, when aiming to reconstruct $[CO_3^{2-}]$ using $Zn/Ca_{CALCITE}$ one must take into account the difference in behavior of D_{Zn} versus $[CO_3^{2-}]$ due to undersaturation effect discussed in section 4.6. Furthermore, as Zn in ocean water follows a nutrient-like behavior, an independent estimate of past seawater [Zn] is necessary. For instance, Bryan and Marchitto (2010) show that in thermocline waters, $Zn/Ca_{CALCITE}$ of *Cibicidoides pachyderma* increases with increasing $[CO_3^{2-}]$, however, [Zn] is not constrained in these samples. This would allow for unravelling of past seawater composition and reconstruction of past nutrient profiles. For instance, if U/Ca (Keul et al, 2013b) and Cd/Ca (Marchitto et al., 2002) are primarily controlled by changes in $[CO_3^{2-}]$ and the element to calcium ratio (E/Ca) of the seawater, simultaneous measurement of these elements on a single foraminifera by LA-ICP-MS would results in several independent reconstructions of $[CO_3^{2-}]$. Differences between these reconstructions reflect changes in the concentrations of these elements relative to each other. When the errors of the different $E/Ca_{CALCITE}$ measurements are sufficiently low, it might be possible to reconstruct the concentrations of these elements in seawater. Future research must focus on confirming these proxies (e.g. Zn/Ca, Cd/Ca and U/Ca) as being mainly controlled by $[CO_3^{2-}]$, and decreasing the error in their relationship to $[CO_3^{2-}]$. When past seawater Zn concentration is known, the global deep water Zn:Si relationship [Zn] = 0.052[Si] + 0.79 with [Zn] in nmol/kg and [Si] in µmol/kg (Marchitto et al., 2000) can be used to estimate past [Si] (profiles) of the ocean. Moreover, since the ratio between [Zn] and [Cd] varies between water masses, relative changes in these elements may reflect changes in oceanic circulation, as has been shown by Marchitto et al. (2002). So reconstructing seawater E/Ca by

using an independent [CO_3^{2-}] proxy, in theory, one will be able to reconstruct past seawater element composition and even ocean circulation.

Secondly, when past seawater Zn/Ca is constrained, the relationship between carbonate ion concentration and Zn incorporation in *Ammonia tepida* can be used to reconstruct a change in [CO_3^{2-}] from e.g. 200 to 300 µmol/kg, which would result in an increase in foraminiferal Zn/Ca of 9.5% (Fig. 5). In combination with a proxy for other inorganic carbonate system parameters (e.g. $\delta^{11}B$ from foraminiferal calcite for seawater pH; Hönisch et al., 2009; Sanyal et al., 1996), Zn/Ca can enable reconstruction of the complete carbon system and thereby, past atmospheric CO_2. However, currently, the sensitivity of the relationship between $Zn/Ca_{CALCITE}$ and [CO_3^{2-}], in combination with the relative large variability in $Zn/Ca_{CALCITE}$, is too large to reconstruct meaningful changes in [CO_3^{2-}] smaller than interglacial-glacial cycles. Including multiple elements with a similar type of mixed nutrient/carbonate system behavior could help to improve such reconstructions.

5. Conclusions

We decoupled pH and carbonate ion concentration in a controlled growth experiment, culturing the benthic foraminifer *Ammonia tepida*. Impact of individual inorganic carbonate parameters on Zn incorporation in the shell calcite was determined using laser ablation ICP-MS measurements of individual shell chambers. This showed that foraminiferal Zn/Ca decreases with increasing [CO_3^{2-}], with only minor impacts of pH, DIC and TA. Modelling Zn speciation in seawater showed that the amount of bioavailable zinc in seawater decreases with increasing [CO_3^{2-}], in line with the observed Zn/Ca values in the foraminiferal shells. This results confirm an earlier field calibration of Zn/Ca values to changes in [CO_3^{2-}] (Marchitto et al., 2000), and shows Zn incorporation to be independent from pH. Therefore, we argue that foraminifera Zn/Ca values, combined with an independent other [CO_3^{2-}] proxy, potentially allow reconstructing past nutrient profiles. Conversely, combining foraminiferal Zn/Ca with an other independent carbonate system proxy (for e.g. pH), enables reconstruction of the complete carbon system and thereby, past atmospheric CO_2.

Acknowledgments

This research is funded by the NIOZ – Royal Netherlands Institute for Sea Research and the Darwin Centre for Biogeosciences project ‘‘Double Trouble: Consequences of Ocean Acidification – Past, Present and Future –Evolutionary changes in calcification mechanisms” and the Netherlands Earth System Science Center (NESSC to GJR). MW acknowledges the U.K.’s Natural Environment Research Council [fellowship #NE/J018856/1] and funding from the Foundation for Fundamental Research on Matter (FOM), which is part of the Netherlands Organization for Scientific Research (NWO). We would like to thank Kirsten Kooijman for supplying Dunaliella cultures, Patrick Laan and Wim Boer for analyzing seawater elemental composition, Wim Boer for support with LA-ICP-MS analyses, Karel Bakker for DIC measurements and Marco Houtekamer for measuring TA of the culture media. We would like to thanks two anonymous reviewers for their constructive comments.

Chapter 7

Sulfur in foraminiferal calcite as a potential proxy for seawater carbonate ion concentration

Inge van Dijk, Lennart J. de Nooijer, Wim Boer and Gert-Jan Reichart

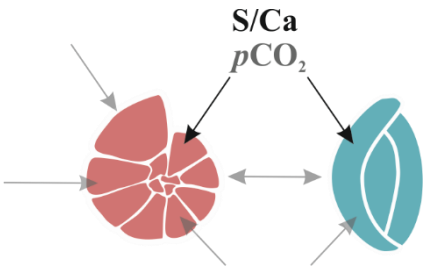

Abstract

Sulfur (S) incorporation in foraminiferal shells is hypothesized to change with carbonate ion concentration [CO_3^{2-}], due to substitution of sulfate for carbonate ions in the calcite crystal lattice. Hence S/Ca values of foraminiferal carbonate shells are expected to reflect sea water carbonate chemistry. To calibrate incorporation of S in foraminiferal calcite as a function of carbonate chemistry, we cultured juvenile clones of the larger benthic species *Amphistegina gibbosa* and *Marginopora vertebralis* over a 350-1200 ppm range of pCO_2 values, corresponding to a range in [CO_3^{2-}] of 93 to 211 µmol/kg. We also investigated the potential effect of salinity on S incorporation by culturing juvenile *Amphistegina lessonii* over a large salinity gradient (25-45). Results show $S/Ca_{CALCITE}$ is not impacted by salinity, but increases with increasing pCO_2 (and thus decreasing [CO_3^{2-}] and pH), indicating S incorporation may be used as a proxy for [CO_3^{2-}] and/or pH. Higher S incorporation in high-Mg species *M. vertebralis* suggests a superimposed biomineralization effect on the incorporation of S. Microprobe imaging reveals co-occurring banding of Mg and S in *Amphistegina lessonii*, which is in line with a strong biological control and might explain higher S incorporation in high Mg species. Provided a species-specific calibration is available, foraminiferal S/Ca values might add a valuable new tool for reconstructing past ocean carbonate chemistry.

1. Introduction

The interaction between the atmosphere and the ocean is a crucial component of the global climate system as the ocean and atmosphere exchange e.g. heat and gases. Due to the large size of the ocean it thereby acts as a reservoir and buffer for the atmosphere on geological timescales. Since the industrial revolution in the mid-eighteen century, ongoing anthropogenic burning of fossil fuels has resulted in a rapid increase of atmospheric CO_2 (Feely et al., 2009). Exchange of CO_2 between ocean and atmosphere has resulted in an uptake of approximately 25% of the anthropogenic carbon emissions by oceans over the last decades (Doney et al., 2009). When CO_2 enters the ocean, a suite of chemical reactions occur that lead to a decreased carbonate saturation state and the release of protons, a process called 'ocean acidification' (OA; Gattuso and Hansson, 2011). Carbonate precipitating organisms, including pteropods and coccolithophores, might be negatively impacted by these changes (e.g., Riebesell et al., 2000; Orr et al., 2005). Past ocean acidification events could provide valuable insight in the impact of ocean acidification on a global scale (Hönisch et al., 2012), but rely on our ability to accurately reconstruct carbon chemistry of the ocean. Different parameters of the ocean inorganic carbonate system are highly dependent on each other, allowing reconstruction of all parameters (e.g. pCO_2, total alkalinity, dissolved inorganic carbon [DIC] and pH) from the reconstruction of only two parameters (Zeebe and Wolf-Gladrow, 2001). Currently proxies permit reconstruction of some of these parameters (Hönisch and Hemming, 2005; Beerling and Royer, 2011), whereas others are more difficult to assess. Therefore, development of new, and improvement of existing proxies is necessary to increase the accuracy and precision of such reconstructions.

Uptake of minor and trace metals in the shells of calcareous foraminifera provide a widely used toolbox to reconstruct past ocean conditions. For example, the relation between temperature and Mg incorporation in foraminiferal carbonate is reasonably well constrained (e.g. Nürnberg et al., 1996; Nürnberg, 2015) and is frequently used as a paleothermometer (e.g. Elderfield and Ganssen, 2000; Lear et al., 2000; Barker et al., 2005). In comparison to temperature reconstructions, estimates of the inorganic carbon system in the past (seawater pH, alkalinity, saturation state, etc.) are less well constrained. The boron isotopic composition of foraminiferal shells is used as a proxy for pH (Sanyal et al., 1996; Hönisch and Hemming, 2005), while the concentrations of trace elements including U (Russell et al., 2004; Keul et al., 2013b), B (Yu and Elderfield, 2007) and Zn (Marchitto et al., 2000, Chapter 6) in calcite correlate to carbonate ion concentration ([CO_3^{2-}]). However, partitioning of these elements is

often not controlled by a single parameter (e.g., Allen and Hönisch, 2012), which is why (new) independent proxies are still needed to accurately reconstruct past ocean chemistry.

After chloride, sulfate (SO_4^{2-}) is the most abundant anion in the ocean and over geological time scales its concentration is largely controlled by the sulfur cycle (Walker, 1986). It is hypothesized that SO_4^{2-} in seawater is the only source of sulfur (S) in biogenic carbonate (Pingitore et al., 1995) and that S/Ca values change with carbonate ion concentration (Berry, 1998). Since the molar ratio of Ca:CO_3 in calcite is close to 1, SO_4/CO_3 can be approximated by S/Ca, which can be determined from foraminiferal shells. Over longer times scales, sulfate concentrations in the ocean have not been stable, ranging between ~10 and 30 mM during the Phanerozoic (Demicco et al., 2005), due to the balance between pyrite and shale formation/oxidation and the release of sulfur gasses (SO_2 and H_2S) by volcanic activity (Walker, 1986). The most important pathway for mineralization of marine sedimentary organic matter is the reduction of sulfate (Jørgensen, 1982; Kasten and Jørgensen, 2000). Residence time of sulphate in the ocean is currently estimated at 13-20 Ma (Claypool et al., 1980; Bottrell and Newton, 2006), which implies that on longer timescales foraminiferal S/Ca likely primarily reflects seawater [SO_4^{2-}] (Paris et al., 2014). On shorter time scales, however, foraminiferal S/Ca values are most likely linked to seawater carbon speciation due to substitution of SO_4^{2-} for CO_3^{2-} .

Here we present and compare foraminiferal shell S/Ca data obtained from different species of benthic foraminifera cultured over either a range of pCO_2 (350-1200 ppm CO_2) or salinity (25-45), while keeping seawater S/Ca constant. Our culture set up allows us to independently quantify the impacts of these two environmental parameters on foraminiferal S/Ca, whereas in the field, these parameters are usually coupled (i.e. alkalinity and salinity). Furthermore, we investigate the micro-distribution of S within foraminiferal chamber walls to assess the potential biological imprint on S incorporation.

2. Methods

2.1 Foraminifera collection

Macro-algae (*Dictyota* sp.) were hand collected in November 2015 at a depth of 2-3 meters in Gallows Bay, St. Eustatius (N 17°28’31.6”, W 62°59’9.4”). Local salinity and temperature were ~34 and ~29°C, respectively. Macro-algae samples were

transported to the laboratory at the Caribbean Netherlands Science Institute (CNSI, St. Eustatius) and placed in a 5 liter aquarium filled with unfiltered and aerated seawater. Algae debris was sieved over a 600 and 90 µm mesh to dislodge larger benthic foraminifera and the resulting 90-600 µm fraction was used as a stock to select specimens. Approximately 100-200 individuals of the rotaliid *Amphistegina gibbosa* and milliolid *Marginopora vertebralis*, characterized by yellow cytoplasm and pseudopodial activity, were isolated for the culturing experiments. To obtain juveniles, groups of 10-15 adults were transferred in 20 mL Petri dishes containing sand-filtered in-situ seawater and concentrated freeze-dried algae (*Dunaliella salina*) and stored at a constant temperature of 25 °C and a 12hr/12hr day/night cycle at a light intensity of approximately 300 par. After a reproduction event, juvenile clones were allowed to grow ~2 chambers before they were transferred to the culture vessel and incubated at experimental conditions.

2.2 Experimental set-up

Seawater (5µm filtered) was transferred in one of four 100L barrels. The pCO_2 in the headspace of these barrels was measured by a Li-Cor CO_2/H_2O analyzer (LI-7000), that was used to regulate addition of CO_2 and/ or CO_2-scrubbed air to keep the pCO_2 of each barrel at pre-set levels. Set-points for pCO_2 were 350 (A), 450 (B), 760 (C) and 1200 (D) ppm. This resulted in four batches of seawater with a range of pH, [CO_3^{2-}] and saturation states, but with constant elemental composition, alkalinity and salinity. Salinity (34.0±0.2) was measured with a salinometer (VWR CO310). Per condition, 2 liters of culture water was stored bubble-free in eight 250 ml Nalgene bottles with teflon lined Nalgene caps at 4°C until further use. Nalgene was used because of its low gas permeability. At the start of the experiment, and for every water exchange, one of the 250 ml bottles for every of the four conditions was opened and used. This ensured that at the end of the experiment, media in the culture vessel were still in equilibrium with the pCO_2 set at the start of the experiment (see below for analytical checks).

Around eighty clones of juvenile and one-hundred adult specimen of *A. gibbosa* and three generations (I-III) of clones and eighty adult specimen of *M. vertebralis* were divided in duplicates over the four pCO_2 treatments and placed in 70 ml tissue bottles with gas-tight caps (Falcon ®) in a thermostat set at 25°C (Figure 1). This resulted in 8 tissue bottles with juvenile foraminifera and 8 tissue bottles with adult specimens (see Table 1 for specifications).

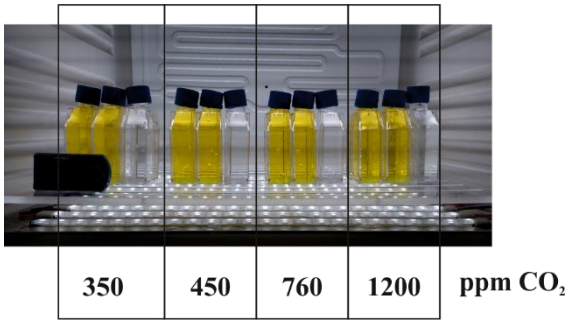

Figure 1. Set-up of the culture experiment at 25°C with LED shelves (300 par). Tissue bottles containing natural seawater pre-equilibrated to 350, 450, 760 or 1200 ppm CO_2 with either adult (yellow media due to added calcein) or juvenile (clear media) foraminifera.

Species	Stage	A	B	C	D
		350 ppm	**440 ppm**	**760 ppm**	**1200 ppm**
A. gibbosa	Juvenile	~20 (I)	~20 (I)	~20 (I)	~20 (I)
	Adults	27	22	25	19
M. vertebralis	Juvenile	~35 (I)	~35 (II)	~35 (III)	n.m.
	Adults	16	21	19	21

Table 1. Number of foraminifera in treatment A-D, incubated as either juvenile or adults. Roman numbers indicate generation of juveniles. N.m indicates not measured.

The fluorescent compound calcein (Bis[N,N-bis(carboxymethyl)aminomethyl]-fluorescein) was added to the culture vessels (5 mg/L seawater) containing adult specimen, to determine which chambers were formed during the culture experiment (Bernhard et al., 2004). Short-term exposure (<three weeks) to calcein has no detectable impact on the physiology of benthic foraminifera (Kurtarkar et al., 2015) and the presence of calcein has no noticeable effect on the incorporation of Mg and Sr in foraminiferal calcite (Dissard et al., 2009). Temperature within the thermostat was monitored by a temperature logger (Traceable Logger Trac, Maxi Thermal), measuring air temperature every minute. The average temperature over the whole experiment was 25±0.2°C.

The shelves within the thermostat were equipped with customized LED shelves to ensure that all foraminifera were cultured at similar light intensities. These shelves were designed to give similar amount of light (par) over a certain distance. The LED lights were controlled by a time controller and set to 30% for 12hr/12hr, which equals to 300 par (high-light condition). Light intensities were checked with an Odyssey logger (Dataflow Systems). Culture media was replaced every four days, to avoid build-up of organic waste and to obtain stable seawater element concentrations and carbon chemistry. Foraminifera were fed after every water change with 0.5 ml of freeze-dried cells of the algae *Dunaliella salina* cells, dissolved in seawater from the associated treatment. Foraminifera were allowed to produce new calcite for 21 days, after which they were rinsed with ultrapure water (>17MΩ) three times, dried at 40°C and stored in micropaleontology slides until further geochemical analysis at the Royal NIOZ (The Netherlands).

A parallel experiment was run to investigate potential impact of salinity (25-45) on S incorporation. The setup of this experiment (Geerken et al., in prep) (duration, light regime, feeding frequency, etc.) was similar to the experiment described above, in which the inorganic carbon chemistry was controlled. Salinity was modified by mixing high salinity sub-boiled water with di-ionized water.

2.3 Analytical methods

2.3.1 Seawater carbon parameters

At the start and termination of the experiment, 125 ml samples of the different experimental conditions were collected to analyze the DIC and total alkalinity (TA) on a Versatile INstrument for the Determination of Titration Alkalinity (VINDTA), which was installed at the CNSI for the duration of the experiments. In addition, smaller subsamples of all treatments were collected every four days in headspace-free vials containing a saturated $HgCl_2$ solution (10µl $HgCl_2$/10 ml sample) and transported to the Royal NIOZ) in order to re-analyze DIC on an autoanalyzer TRAACS 800 spectrometric system (Stoll et al., 2001). Using the DIC and TA values measured on the VINDTA in the software CO2SYS v2.1, adapted to Excel by Pierrot et al. (2006), the other carbon parameters (including [CO_3^{2-}] and $\Omega_{CALCITE}$) were calculated. Using the equilibrium constants for K1 and K2 of Mehrbach et al. (1973), refitted by Dickson and Millero (1987), allows us to reconstruct [CO_3^{2-}] and $\Omega_{CALCITE}$ and compare calculated pCO_2 to the set-point of the pCO_2 controller (Table 2).

Treatment	Set-point	Measured			Calculated (CO2SYS)			
	pCO_2 ppm	TA µmol/kg	DIC µmol/kg		pCO_2 ppm	$[CO_3^{2-}]$ µmol/kg	pH (total scale)	Ω
			VINDTA	TRAACS				
A	350	2302.8± 8.2	2007.5± 10.7	2009.1±7.1	401.1	211.2	8.04	5.1
B	450	2305.2± 5.8	2021.3± 12.5	2004.0±14.9	424.7	204.1	8.02	4.9
C	760	2304.4± 0.9	2100.8± 13.4	2100.2±5.0	645.7	153.3	7.86	3.7
D	1200	2300.3± 0.7	2201.4± 4.1	2203.7±2.6	1233.7	92.7	7.61	2.2

Table 2. Carbon parameters (TA= Total Alkalinity, n=2, DIC=Dissolved Inorganic Carbon, n=2) with (relative) standard deviation of the culture water per treatment of the pCO_2 experiment. DIC was measured with both a VINDTA and TRAACS system. CO2SYS was used to calculate carbonate ion concentration and calcite saturation state (Ω) and recalculate pH and atmospheric CO_2 from measured TA and DIC (VINDTA).

2.3.2 Seawater analysis using SF-ICP-MS

Duplicate subsamples were collected in 50 ml LDPE Nalgene bottles at the start and end of the experiment and during replacement of the culture media, and immediately frozen at -80^{0}C. After transportation to the Royal NIOZ, the melted samples were acidified with QD HCl to pH ~1.8. Seawater composition of the samples, as well as the seawater standard IAPSO, was analyzed on an Element-2 (Thermo Scientific) sector field double focusing inductively coupled plasma mass spectrometer (SF-ICP-MS) run in medium resolution mode. Analytical precision (relative standard deviation) was 3% for Ca, 4% for Mg, 3% for S and 1% for Sr. We obtained average seawater values of 5.25±0.06 mol/mol for Mg/Ca, 2.57±0.09 mol/mol for S/Ca and 8.63±0.05 mmol/mol for Sr/Ca. For the salinity experiment, average S/Ca is 2.90±0.12 mol/mol and [S] of the culture water ranges from 13.9 mM to 45.0 mM over a salinity range of 25-45.

2.3.3 Elemental concentrations in foraminiferal calcite

2.3.3.1 Cleaning methods

For cleaning we followed an adapted version of the protocol by Barker et al. (2003). *Amphistegina lessonii* cultured over a salinity range of 25-45 were transferred from a laser ablation stub to 0.5ml TreffLab PCR-tubes. A few specimens were set apart for electron microprobe analysis. Since these foraminifera had been fixed on laser ablation stub with double sided tape, we performed an additional cleaning step. First, ultrapure water (>18.2 MΩ) was added and all vials were transferred to an ultrasonic bath (ELMA) for 1 minute using moderate sound settings to keep tests intact (80kHz, 50% power, degas function). After removal of the supernatant, this step was repeated twice. To all vials, 250µl of supra pure methanol (Aristar) was added and again transferred to the ultrasonic bath for 1 minute (same settings), after which the solvent was removed and this cleaning step repeated. In order to remove all methanol, the foraminifera were rinsed three times with ultrapure water and after the last rinse, all the water was removed. Foraminifera (*A. gibbosa* and *M. vertebralis*) from the inorganic carbon chemistry manipulations (2.2), as well as specimens from the salinity experiment were transferred to another acid-cleaned 0.5 ml PCR-tubes (TreffLab). To each vial, 250µl of fresh prepared 1% H_2O_2 (buffered with 0.5M NH_4OH) was added to remove organic matter. The vials were heated for 10 minutes in a water bath at 95 °C, and placed in an ultrasonic bath for 30 seconds after which the oxidizing reagent was removed. These steps (organic removal procedure) were repeated twice. Foraminiferal samples were subsequently rinsed five times with ultrapure water.

The foraminifera that were incubated as adult specimens in the pCO_2-controlled experiment were dried in a laminar flow cabinet and placed on a stub and individual foraminifera were photographed with a fluorescence microscope (Axioplan 2, Zeiss), equipped with a flexible LED light source (Colibri, Zeiss) and a camera (Axiocam MRc5, Zeiss) to assess the number of chambers added during the experiment.

2.3.3.2 Foraminiferal Mg/Ca and Sr/Ca analysis using LA-Q-ICP-MS

Element concentrations of individual fluorescent chambers were analyzed by Laser Ablation-ICP-MS (Reichart et al., 2003; Chapter 4). To determine foraminiferal element concentrations, the laser system (NWR193UC, New Wave Research) at the Royal NIOZ was equipped with a 2-volume 2 cell (New Wave Research), characterized by wash-out time of <1.5 seconds (based on Na at 1% level).

Foraminiferal chambers were ablated in a helium environment using a circular laser spot with a diameter of 60 µm. All foraminiferal samples were ablated with an energy density of 1±0.1 J/cm^2 and a repetition rate of 6 Hz. The resulting aerosol was transported on a helium flow through an in-house designed smoother, where it was mixed with a nitrogen flow (5 mL/min), into the quadrupole ICP-Q-MS (iCAP-Q, Thermo Scientific). Monitored masses included ^{23}Na, ^{24}Mg, ^{25}Mg, ^{43}Ca, ^{44}Ca, and ^{88}Sr. To monitor drift over time we also measured two carbonate standards, namely the certified coral JCp-1 (*Porites* sp.) and MACS-3 (synthetic calcium carbonate) after every ten samples. In addition, we analyzed several standards at the start of every series of measurements, specifically, JCt-1 (giant clam), and two in-house standards; NIOZ Foraminifera House Standard (NFHS-1) and the NIOZ Calcite House Standard (NCHS-1) together with SRM NIST 610 and 612, which were analyzed using a deviating energy density of 5±0.1 J/cm^{-2}. Elemental intensities over time were integrated using an adapted version of the LA-ICP-MS reduction program SILLS (for details see Chapter 4; Guillong et al., 2008). Calibration was performed against MACS-3 carbonate standard, with ^{43}Ca as an internal standard. To increase accuracy, we applied a linear drift correction over the series of measurements using the MACS-3 analysis. Analytical precision (relative standard deviation (RSD) of all MACS-3 measurements) is 3% for ^{24}Mg, ^{25}Mg and ^{88}Sr. In total, 366 chambers of 93 foraminifera were analyzed, resulting in 59-126 single chamber measurements per seawater treatement. We calculated the standard deviation (SD), RSD and standard error (SD/√n; SE) for all element/Ca ratios per treatment. The partitioning coefficient (D) of an element (E) between seawater and foraminiferal calcite is expressed as $D_E = (E/Ca_{CALCITE})/(E/Ca_{SW})$.

2.3.3.3 Foraminiferal S/Ca solution analysis using SF-ICP-MS

The juveniles from the clone groups from the OA experiment and foraminifera from the salinity experiment were transferred to 0.5ml acid-cleaned vials and placed in a laminar flow cabin to dry. The lowest possible molarity of HNO_3^- was chosen to decrease the S blank values. To every vial, 150 µl of ultrapure 0.05 M HNO_3^- (PlasmaPURE) was added to dissolve all foraminiferal calcite. To ensure proper dissolution, vials were placed in an ultrasonic bath for 15 minutes (37 kHz, 100% power). Dissolution was visually checked. To determine the amount of Ca (ppm) in the HNO_3^- solutions with dissolved foraminiferal calcite, a five second pre-scan for ^{43}Ca in medium resolution on chromatography mode with self-aspiration (110 µL/min) was performed on the SF-ICP-MS. Accordingly to these results, samples

were diluted to obtain 100 ppm Ca solutions. We used 5x higher concentrations than our standard method (20 ppm Ca) to increase the S-signal of our samples and thus to increase the signal/noise ratio. These final solutions were measured again for ~120 seconds per sample. Masses ^{32}S, ^{34}S and ^{43}Ca were analyzed in medium resolution. This way the $^{16}O^{16}O$ and ^{32}S peaks could be fully separated. In addition to the foraminiferal samples we measured the pure carbonate standard NIST915a and the biogenic carbonate standards NFHS-1 and JCp-1 were used as drift monitors. To determine foraminiferal S/Ca (mmol/mol), we used a ratio calibration method (De Villiers et al., 2002). Both $^{32}S/Ca$ and $^{34}S/Ca$ gave similar results. Of the two sulfur isotopes ^{32}S is more abundant leading to a higher signal to noise ratio and better counting statistics. Therefore, the S/Ca presented are based on the $^{32}S/Ca$ results.

2.3.3.4 Microprobe analysis

To determine the distribution of Ca, S, Mg and Sr within foraminiferal chamber walls, we analyzed cross-sections of chambers of embedded foraminifera on a Field emission Electron Probe Micro Analyzer (JEOL JXA-8530F). First, post-ablated foraminifera were fixed in a Petri dish with double sided tape. Aluminum rings were placed in a way that one foraminifer was centered per ring. The foraminifera were placed in a house-made vacuum chamber coupled to a peristaltic pump. The rings were filled under vacuum with 2020 Araldite® resin (Huntsman International LLC) using an injector needle. After filling, the rings with resin were placed in an oven set at 45 ^{0}C for 5 days, to harden the resin and degas the sample. The embedded foraminifera were then polished with increasingly finer grained sanding paper until a cross-section of the foraminifera was visible. After a final polishing step (0.3 µm grains) foraminifera were carbon-coated and secured in the microprobe sample holder. After selection of target areas, several small high resolution maps (130x130 points) were analyzes at 7.0kV in beam scan mode for different elements (Ca, Mg, S, Sr and Na) with a dwell time of 350 ms. The resulting concentration (level) maps were converted to qualitative Mg/Ca and S/Ca maps in MatLab by dividing the matrices. Pores and resin were avoided by excluding areas where Ca levels were < 200 (Ca level in foraminiferal carbonate was always higher than 300 in our samples). For two maps we created Mg and S profiles by selecting rectangular areas (50*100 pixels), perpendicular to the chamber wall. The smoothed average intensities were plotted together with the organic linings (obtained from SEM photographs) to compare the spatial relation between S and Mg bands with organic linings.

3. Results

3.1 Calcitic element concentrations

Average elemental ratios for the pCO_2 experiment (*A. gibbosa*) were 27.6 mmol/mol for $Mg/Ca_{CALCITE}$, 1.7 mmol/mol for $Sr/Ca_{CALCITE}$, while $S/Ca_{CALCITE}$ ranged from 0.95-1.30 mmol/mol. For the salinity experiment (*A. lessonii*), we obtained average value of 1.32 for $S/Ca_{CALCITE}$ (Table 3).

Treatment		**Species**	**SF-ICP-MS Juvenile specimen**			**LA-ICP-MS Adult specimen (w/ calcein)**					
			$S/Ca_{CALCITE}$ mmol/mol			**$Mg/Ca_{CALCITE}$ mmol/mol**			**$Sr/Ca_{CALCITE}$ mmol/mol**		
			AVG	**SD**	**D_S $*10^{-3}$**	**AVG**	**SE**	**D_{Mg} $*10^{-3}$**	**AVG**	**SE**	**D_{Sr}**
pCO_2 experiment (ppm pCO_2)	350	*A. gibbosa*	0.95	0.03	**0.37**	27.8	0.5	**5.3**	1.69	0.01	**0.20**
	450		1.02	0.01	**0.40**	25.9	0.6	**4.9**	1.70	0.02	**0.21**
	760		1.10	0.03	**0.43**	28.2	0.7	**5.4**	1.73	0.02	**0.22**
	1200		1.30	0.01	**0.51**	28.7	0.6	**5.5**	1.73	0.02	**0.21**
	350	*M. vertebralis*	8.95	0.09	**3.48**	147.7	0.6	**28.2**	2.0	0.01	**0.23**
	450		9.60	0.10	**3.73**	144.2	0.8	**27.5**	2.0	0.01	**0.23**
	760		10.40	0.10	**4.05**	143.0	0.6	**27.3**	2.0	0.01	**0.23**
	1200		n.m.	n.m.	**n.m.**	148.3	0.5	**28.3**	2.0	0.01	**0.23**
Salinity experiment	25	*A. lessonii*	1.32	0.01	**0.46**						
	30		1.27	0.01	**0.44**						
	35		1.34	0.01	**0.46**						
	40		n.m.	n.m	**n.m.**						
	45		1.35	0.01	**0.47**						

Table 3. Overview of $S/Ca_{CALCITE}$ (SF-ICP-MS), $Mg/Ca_{CALCITE}$ and $Sr/Ca_{CALCITE}$ (LA-Q-ICP-MS) in foraminiferal calcite (AVG=average; SD = standard deviation, SE=standard error) and partitioning coefficients D_E in bold. $S/Ca_{CALCITE}$ are based on SF-ICP-MS results, $Mg/Ca_{CALCITE}$ and $Sr/Ca_{CALCITE}$ are from LA-ICP-MS analysis. N.m. indicates not measured

No significant correlation is observed between $S/Ca_{CALCITE}$ and salinity. We observed no significant correlation (95% confidence interval) between either $Mg/Ca_{CALCITE}$ or $Sr/Ca_{CALCITE}$ with pCO_2 for both *A.gibbosa* and *M. vertebralis*. However, $S/Ca_{CALCITE}$ and pCO_2 are significantly (resp. $p<0.005$ and $p<0.05$) positively correlated (Fig. 2).

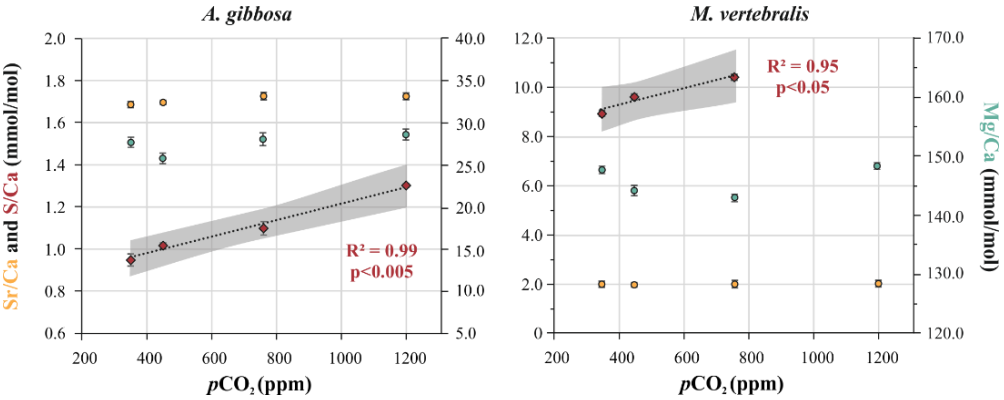

Figure 2. Average foraminiferal S/Ca (±SD) by SF-ICP-MS, Mg/Ca (±SE) and Sr/Ca (±SE) by LA-ICP-MS of *A. gibbosa* (left) and *M. vertebralis* (right) for the four inorganic carbon treatments. Linear trendline with R^2, p-value and the 95% confidence interval (shaded area) are plotted only for $S/Ca_{CALCITE}$.

For *M. vertebralis* we measured an average ratio of 147.4 ($Mg/Ca_{CALCITE}$) and 2.0 ($Sr/Ca_{CALCITE}$) mmol/mol, whereas $S/Ca_{CALCITE}$ ranged from 8.95-10.4 mmol/mol, when pCO_2 was manipulated from 350 to 760 ppm. The average $S/Ca_{CALCITE}$ is 9.5 times higher and $Mg/Ca_{CALCITE}$ is 4.3 times higher for *M. vertebralis* compared to *A. gibbosa* over the same pCO_2 range. When plotting $S/Ca_{CALCITE}$ of *A. gibbosa* and *M. vertebralis* cultured in the pCO_2-controlled experiments, we observe a linear decrease of sulfur content with increasing [CO_3^{2-}] for both species, albeit with an appreciable offset (Fig. 3).

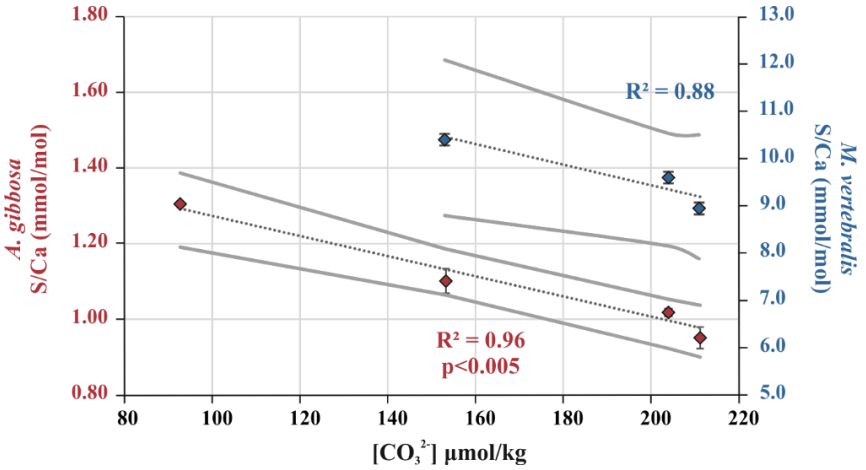

Figure 3. Average S/Ca$_{CALCITE}$ (±SD) per treatment of *A. gibbosa* (red; p<0.005) and *M. vertebralis* (blue) versus [CO_3^{2-}]. For both species, the linear regression line (dotted lines) with R^2 and the 95% confidence interval (grey lines) are indicated.

3.2 Micro-distribution of S/Ca

To investigate micro-distribution of Mg, S and Sr within a foraminiferal chamber wall we analyzed two areas in a cross-section of *A. lessonii* (Fig. 4). Magnesium levels were in general ~15 times higher than S levels, and maxima occurred every ~5-7 µm (profile 1) or ~2-5 µm (profile 2). Analyzing two profiles in the target areas also revealed banding of S in the chamber wall, which on the scale studied coincides with bands high in Mg (Fig. 5). In profile 1, we observed four Mg and S bands with five organic linings. We observed seven to eight Mg and S bands and organic linings in profile 2. Comparing the position of high S- and Mg bands shows that they mostly occur at or close to the organic linings, although they do not systematically overlap, as also observed for the POS by Paris et al. (2014). Both S and Mg bands show similar decreasing trends in intensity from the inner (higher ratios) to the outer (lower ratios) surface of the foraminiferal chamber wall.

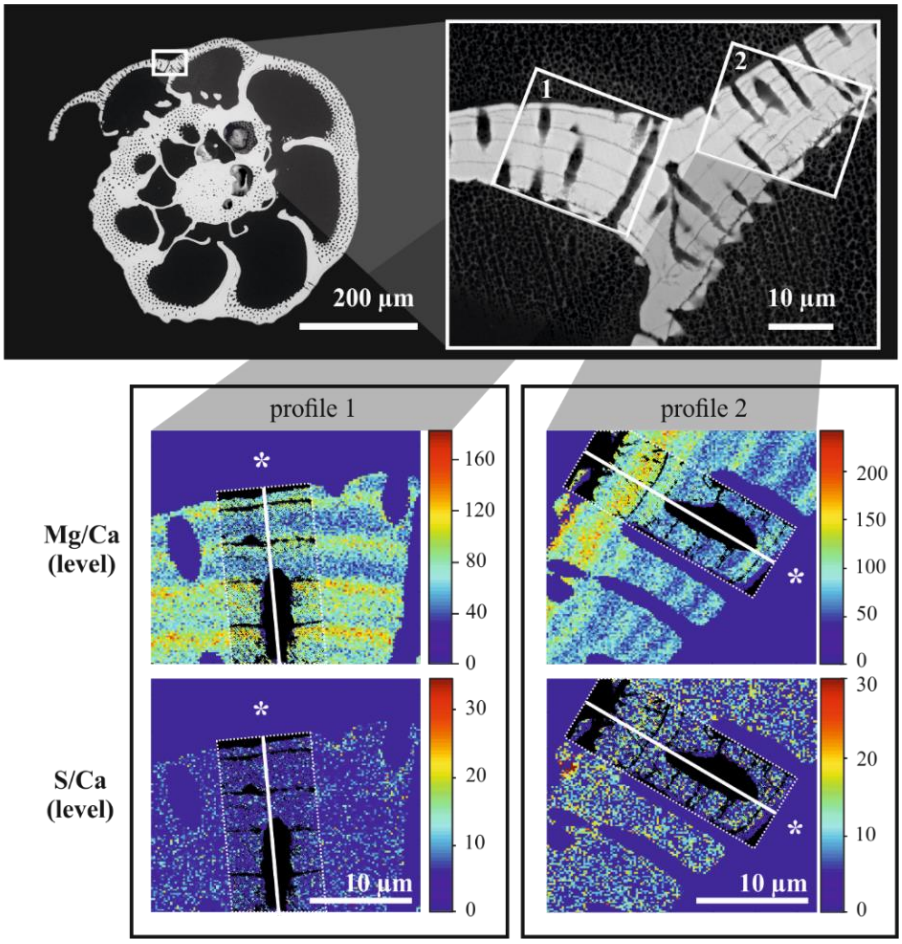

Figure 4. Microprobe imaging of *Amphistegina lessonii*, cultured at salinity of 25. Top panels: SEM overview and close-up photograph with target areas (1 and 2). Lower panels: Microprobe areas (1 and 2) with Mg/Ca (top) and S/Ca (bottom) with organic sheet overlay of areas of interest (dotted layer) and profile lines (white). Asterisk indicate the outside surface of the foraminiferal shell wall.

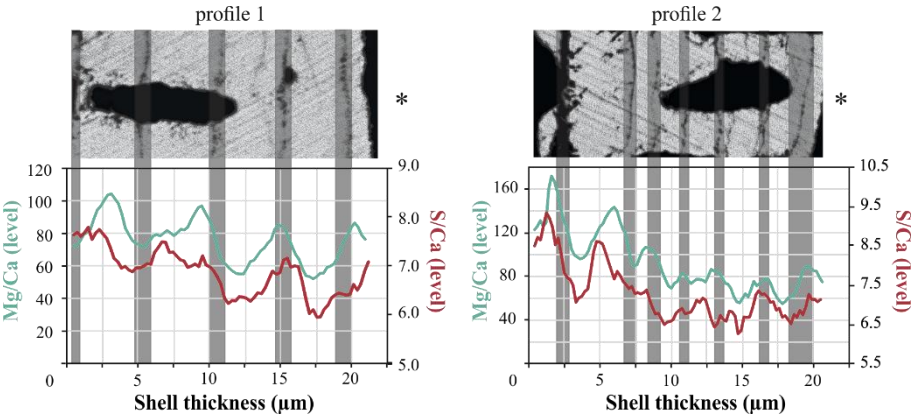

Figure 5. SEM photographs of profile areas 1 and 2 (Fig. 4) with average Mg (green) and S (red) levels across profile area 1 (left) and 2 (right). Dark grey panels are areas associated with organic linings, identified on the SEM pictures (Fig. 4). Asterisk indicate the outside of the foraminifera.

4. Discussion

4.1 Sulfur in foraminifera carbonate

In biogenic carbonate, sulfur is present as SO_4 that substituted for carbonate ions during calcium carbonate precipitation (Staudt et al., 1994; Pingitore et al., 1995). Besides the sulfate ions bound in the crystal lattice, sulfur-containing components (e.g. certain amino acids) may also be present in the organic matter within the shell wall (Bé and Ericson, 1963; Robbins and Brew, 1990). Even though the foraminifer's cytoplasm is removed from the shell during the oxidation step in the cleaning protocol (2.3.3.1), it is possible that organic matter from e.g. the primary organic sheet (POS) and other organic linings remain trapped in-between laminar calcite layers. Potentially, part of the total S measured by SF-ICP-MS could originate from these organic components. The total amount of organic material found in the shells of *Heterostegina depressa* is 0.1-0.2 wt% of the total shell and is mainly composed of two fractions: one consisting of potentially heavily sulfated polysaccharides (glycosaminoglycans) and one with mainly proteins (Weiner and Erez, 1984). The former fraction contains approximately 16% sulfur by wt (e.g. chondroitin sulfate), whereas the protein fraction contains very little sulfur (like aspartate, glutamate, serine). The amount of sulfur-containing amino acids in this fraction contributes less than 5% to the total amino acids, and of this 5% at most 30% in weight is sulfur

(Robbins and Brew, 1990). The relative contributions of the protein and polysaccharide fractions within foraminiferal shells differs between species and is poorly quantified (Ní Fhlaithearta et al., 2013). However, assuming that both fractions contribute equally to the total organic weight, 0.009-0.018 wt% of the shell would be organic sulfur, which is in line with pyrolises GC-MS analyses of isolated organic linings from foraminiferal shells (Ní Fhlaithearta et al., 2013). Still, since S content in our foraminifera was between ~2000 and 3000 ppm, potentially up to 5 % of our S signal could be derived from organic-bound S. This value is higher than the 1.1% organic sulfur calculated by Paris et al. (2014), since the contribution from sulfated polysaccharides was not taken into account in their calculations. Since the peaks in the sulfur intensity do not fully correspond to the position of the organic linings (our study; Paris et al., 2014), and sulfurized polysaccharides were not isolated in foraminiferal organic linings (Ni Fhlaithearta et al., 2013), it is likely that in our study, the contribution of organic-bound S was most likely considerably smaller than 5%."

4.2 Controls on S/Ca in foraminiferal calcite

We observed no systematic impact of salinity on $S/Ca_{CALCITE}$ (Table 3), but S incorporation does vary with pCO_2 in both the intermediate-Mg foraminifer *A. gibbosa* ($p<0.005$) and the high-Mg foraminifer *M. vertebralis* (Fig. 3). When assuming a linear relation between S incorporation and [CO_3^{2-}], $S/Ca_{CALCITE}$ decreases with 21% per 100 µmol/kg [CO_3^{2-}] increase for *A. gibbosa*, and 19% for *M. vertebralis*, suggesting S incorporation in both species is governed by the same underlying process. Assuming all Sulfur being related to lattice substitution of SO_4 for CO_3 we expect foraminiferal S/Ca to linearly decrease with increasing [CO_3^{2-}]. However, based on the experiment as such, also several other parameters of the carbonate system could be responsible for the observed trend in S/Ca as in the pCO_2 experiment several parameters changed in concert. Still, as sulfate speciation in seawater does not change over the pH interval studied here, S/Ca most likely varies directly as a function of SO_4/CO_3.

In the salinity experiments also [CO_3^{2-}] changed, as alkalinity and salinity correlated linearly. Still, seawater [SO_4^{2-}] had no detectable impact on S/Ca when seawater [S] was varied between 22.86 and 38.09 mM in the experiment with varying salinity. Because the SO_4/CO_3 of the media was constant, also foraminiferal S/Ca remained relatively constant despite varying [CO_3^{2-}]. In contrast in the pCO_2 controlled experiment (Fig. 2), S/Ca increased with increasing SO_4/CO_3 and hence decreasing

$[CO_3^{2-}]$ and pH. This suggests that $S/Ca_{CALCITE}$ may be a useful tool to reconstruct changes in seawater $[CO_3^{2-}]$ over timescales of several millions of years, or when seawater $[SO_4^{2-}]$ is known, also over longer time scales. However, superimposed on the impact of $[CO_3^{2-}]$ on S incorporation, biomineralization also impacts foraminiferal S/Ca, and species-specific differences therein are likely responsible for the observed offset in S/Ca between the hyaline *A. gibbosa* and miliolid *M. vertebralis.* Also the observed banding (Fig. 4 and 5) and co-occurrence of S banding with Mg banding suggests a biomineralization related control on S incorporation .

4.3 Banding in foraminiferal carbonate

Certain elements have a heterogeneous distribution in foraminiferal chamber walls, often expressed as banding of these elements. Such banding has been reported for a variety of species, including large benthic foraminifera (Evans and Müller, 2013), planktonic species with symbionts (Eggins et al., 2004; Kunioka et al., 2006; Hathorne et al., 2009; Paris et al., 2014) and without symbionts (Sadekov et al., 2005). Our results show that such banding is also present in *A. lessonii* and that bands with elevated concentrations of Mg and S co-occur within the chamber wall. This implies that phases of high Mg and high S formed simultaneously during calcification and hence potentially that their incorporation may be mechanistically linked. Bands are located close to the organic layers, but in all cases considerably wider than could be explained by the organic linings themselves (Fig. 5). This is in line with the very minimal contribution of the organic layers to the measured S/Ca. Intensity of the concentrations in these bands seem to decrease from the inside, where they are the highest around the POS, towards the outer surface of the chamber wall (also observed by Sadekov et al., 2005; Paris et al., 2014).

The bilamellar calcification model suggests that chamber formation in hyaline foraminifera (Reiss, 1957) starts with the formation of the primary organic sheet (POS), after which the first stages of calcification commence by precipitation of carbonate on either side of the POS (Hemleben et al., 1977; Bé et al., 1979; Erez, 2003). This model combined with our observations suggests that the initial carbonate is enriched in several elements, with the bands high in Mg and S close to the POS (Fig. 5). Banding observed in the outer part of the chamber wall are linked to organic sheets that are formed during calcification of successive chambers (known as outer organic layers or OOL; Hemleben et al., 1977), enveloping the rest of the test. The banding in S and Mg (Fig. 4 and 5) and their relation with organic layers suggests that

the processes responsible for delivery of ions to the site of calcification (SOC) are not constant over time. The recently proposed balance between ions (e.g. Ca^{2+}) transported across the membrane separating the SOC from the surrounding medium (Nehrke et al., 2013) and proton pumping (Glas et al., 2012) mechanistically links Mg and S incorporation. When during ongoing chamber wall formation Ca^{2+} is actively pumped, with only small amounts of Mg leaking in through passive transport (Nehrke et al., 2013), internal pH and hence carbonate speciation also changes (De Nooijer et al., 2009). Hence, both Mg/Ca and SO_4/CO_3 decrease at the SOC with ongoing calcification, albeit not necessarily at the same rate, as observed in the cross sections of these elements incorporated. The large role of biomineralization at the same time also explains the overall differences in elemental composition observed in high- and low-Mg producing foraminifera.

Element incorporation in the calcite of the miliolid *M. vertebralis*, however, may not be caused by the mechanisms proposed in existing calcification models (Erez, 2003; Nehrke et al., 2013; De Nooijer et al., 2014b), since miliolid foraminifera produce their calcite in a fundamentally different way as hyaline foraminifera do (Berthold, 1976; Hemleben et al., 1986; Debenay et al., 1998; De Nooijer et al., 2009). The overall high Mg/Ca ratios in miliolid foraminifera (Blackmon and Todd, 1959; Toyofuku and Kitazato, 2005; Bentov and Erez, 2006) are comparable to (or even somewhat higher than) what is expected based on inorganic partition coefficients (Mucci, 1987; Morse et al., 2007). In the terminology of the passive transport model of Nehrke et al. (2013) this corresponds to a very large contribution of the seawater vacuoles. Hence, major, minor and trace element composition in the seawater-derived vacuoles is only slightly modified and the calcite needles precipitate in the presence of relatively high [Mg^{2+}] and high SO_4/CO_3 values.

4.4 Internal pH

Even though hyaline and miliolid species have a fundamentally different way of precipitating their shells, it has been shown that both groups increase their internal pH to promote precipitation of calcite (De Nooijer et al., 2008; De Nooijer et al., 2009). Increasing the pH at the site of calcification would shift the most dominant form of DIC from HCO_3^- to CO_3^{2-} and hence increase the saturation state in the SOC. However, it is not known whether foraminifera increase their internal pH up to a set value (e.g. pH = 9) or that they elevate their internal pH by a fixed value compared to ambient pH (Ries, 2011). Which of these two alternatives characterizes foraminiferal

proton pumping, however, is important for the incorporation of ions other than Ca^{2+} and carbonate.

When internal pH increases to a certain set value, incorporation of elements of which the chemical speciation depends strongly on pH is not expected to vary as a function of ambient pH/ saturation state/ $[CO_3^{2-}]$. Instead, incorporation of these elements would always be determined by the same, internal pH at the site of calcification. Since e.g. foraminiferal Zn/Ca and U/Ca changes with $[CO_3^{2-}]$ (Russell et al., 2004; Keul et al., 2013b; van Dijk et al., 2017), and the boron isotopic signature of foraminiferal calcite changes as a function of pH (Sanyal et al., 1996), it is more likely that foraminifera increase their internal pH by a set difference compared to the external seawater pH. This implies that a 0.4 pH unit change in seawater pH (lowest-highest pCO_2 treatments), also results in a 0.4 pH unit change in the internal pH. Assuming a 1 unit offset during calcification, this would translate to an increase in pH at the SOC between the experiments from 8.6 to 9.0. The consequence for the internal $[CO_3^{2-}]$ is an increase of 37.1%, which matches well with the observed decrease in $S/Ca_{CALCITE}$ (36.8%). Therefore, the observed decrease in S/Ca hints to maintenance of a high internal pH with a fixed difference compared to the surrounding seawater pH.

5. Conclusions

Sulfur incorporation in foraminiferal calcite does not significantly change over a large salinity gradient (25-45), but changes linearly with inorganic carbon speciation. We propose that seawater $[CO_3^{2-}]$ is the main parameter affecting S/Ca in foraminiferal calcite, due to lattice substitution of sulfate for carbonate ions. Microprobe imaging reveals S banding within the chamber wall, which more or less co-occurs with Mg banding. The miliolid foraminifer *Marginopora vertebralis* incorporates more S than hyaline *Amphistegina gibbosa*, hinting at an underlying biomineralization signal. Foraminiferal S/Ca provides the potential to reconstruct past seawater carbonate chemistry when taking into account species-specific differences in incorporated sulfur.

Acknowledgments

This research is funded by the NIOZ – Royal Netherlands Institute for Sea Research and the Darwin Centre for Biogeosciences project "Double Trouble: Consequences of Ocean Acidification – Past, Present and Future –Evolutionary changes in calcification mechanisms" and the program of the Netherlands Earth System Science Center (NESSC). Great thanks to all participants of the 2015 foraminifera culture expedition at the CNSI, St. Eustatia: Jelle Bijma and Gernot Nehrke from the AWI, Brett Metcalfe (VU), Alice Webb (NIOZ) and Didier de Bakker (NIOZ/IMARES). Bob Koster and Steven van Heuven are thanked for designing and constructing the controlled pCO_2 set-up. Esmee Geerken is thanked for support with the salinity culture experiment at the NIOZ. Furthermore, we would like to thank Patrick Laan and Karel Bakker for seawater analysis, Leonard Bik and Michiel Kienhuis for their help with polishing, Sergei Matveev and Tilly Bouten for providing technical support with the microprobe at University of Utrecht, Esmee Geerken for microprobe image processing.

Concluding remarks

Within the project "Double Trouble: Consequences of Ocean Acidification – Past, Present and Future –Evolutionary changes in calcification mechanisms", I tried to illuminate mechanisms determining element incorporation in foraminifera with different calcification strategies. In particular, I aimed to assess the interplay between ocean acidification and biomineralization processes. Insight in processes in calcification likely improves foraminifera as reconstruction tools for past environmental changes, as well as it increases the accuracy of predictions regarding future carbonate production by these organisms. Constraining the mechanisms involved in foraminiferal (trace) elements uptake is pivotal for improving existing proxies and potentially discovering new proxies to reconstruct past ocean chemistry.

Trends in element incorporation

One of the important findings of this thesis, is that different species display large differences in element uptake and incorporation (Chapter 4 and 7). These differences coincide with the distinction between porcelaneous and hyaline calcification, although there are also striking similarities in response to changes in pCO_2 (Chapter 4, Fig 4). While miliolid species have very comparable element partition coefficients between species, hyaline foraminifera show a large inter-species range in elemental incorporation (Chapter 4; Fig 4). In hyaline species, incorporation of certain elements, like Mg, Na and Sr, seems to be co-dependent, resulting in relatively high Element/Ca ratios in some species and low ratios of all these elements in other species. The different responses of hyaline and porcelaneous foraminifera clearly show the underlying impact of calcification strategies results in different element uptake. The strong correlation between element incorporation in hyaline foraminifera may considerably improve species-specific proxy-calibrations. To account for inter-species differences in element incorporation and to allow proxy-application to extinct species, it is necessary to understand trends in element incorporation between species and how this potentially affects environmental sensitivities of this incorporation across taxa.

Foraminiferal calcification

Calcification in foraminifera is often simplified by comparing seawater chemistry with calcite chemistry, which is then expressed as the partition coefficient (D). This partitioning of elements often differs from inorganic partition coefficients, which is in

most cases explained as so-called ‘vital effects’ or ‘biological control’. However, notice has to be taken that the chemical composition of seawater likely changes before calcification, due to speciation in the foraminiferal microenvironment, and subsequently also due to transport of ions to or out of the site of calcification (Fig. 1). Finally, not all elements precipitate at the same rate, causing an offset between the site of calcification and the formed calcite, which changes over time. The latter might be underlying the banding observed in most hyaline foraminifera. Actual precipitation at the site of calcification might be rather similar to inorganic partitioning.

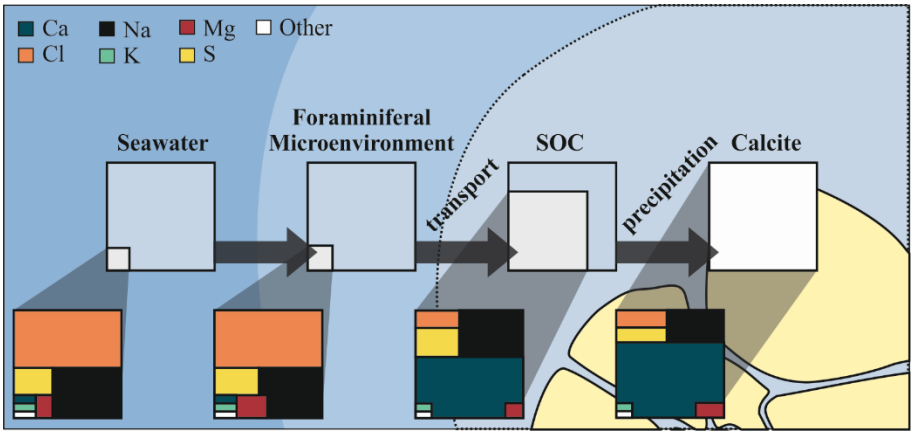

Figure 1. Hypothetical modification of ambient seawater (left) by changes in the foraminiferal microenvironment (second panel), the fractionation caused by selective uptake of ions to the site of calcification (SOC; third panel) and during calcium carbonate precipitation (right). Elements in (relative ppm). Modified after de Nooijer et al., 2014.

So far, there is no consensus on the processes controlling element uptake during foraminiferal calcification. Resolving these issues might increase our understanding of proxy functioning (or the limits of certain proxies) and explain observed species-specific reactions. In terms of calcification, I mainly focus on ‘transport’ between the microenvironment and site of calcification. Combining the observations from different experimental studies (Chapter 4, 6 and 7), allows for the construction of a schematic overview of how seawater carbonate chemistry and trace element speciation might influence trace element transport to the site of calcification of a representative miliolid and hyaline species (Fig. 2).

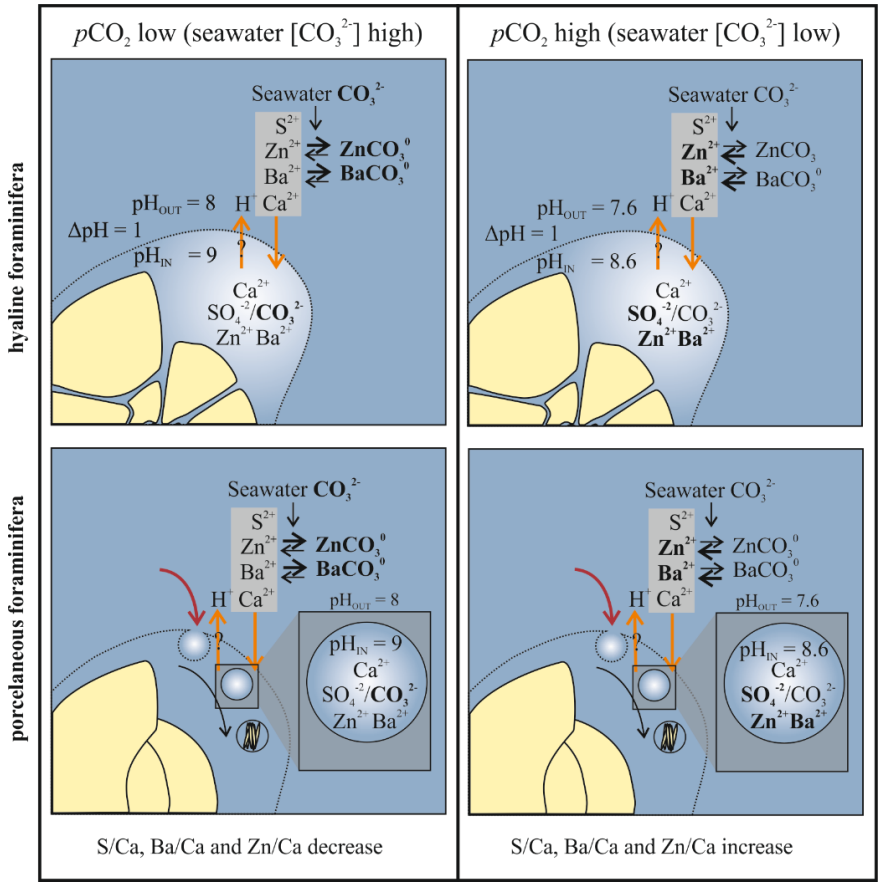

Fig. 2. Schematic overview of the impact of changing seawater [CO_3^{2-}] on foraminiferal calcification in perforate/hyaline (top panels) and imperforate/porcelaneous (lower panels) species. Two scenarios are explored, low pCO_2 (left panels) and high pCO_2 (right panels). Increases in availability of elements, e.g. due to a shift in chemical speciation, are indicated in bold. Orange arrows indicate Ca^{2+} channels, red arrow indicate possible seawater transport (by e.g. passive transport or seawater endocytosis). Question mark indicates possible exchange of Ca^{2+} for protons.

This overview is based on an earlier model (Nehrke et al. (2013), in which calcium is transported to the site of calcification by Ca^{2+} channels. These channels are capable of transferring other ions, like e.g. Mg, Sr and Na (Hess and Tsien, 1984; Allen and Sanders, 1994; Sather, 2005), perhaps in exchange for protons, which decreases the pH in the foraminiferal microenvironment (Glas et al., 2012). However, it is

hypothesized that only free ions are transferred by these channels, explaining why Zn and Ba in foraminiferal carbonate is still dependent on the amount of free ions (Chapter 4 and 6). For example, high seawater [CO_3^{2-}] will cause a large fraction of these elements to be present in stable complexes with carbonate, which are unlikely to cross the cell membrane separating the microenvironments and the calcifying fluid, therefore altering the ratio between Ca^{2+} and e.g. Ba^{2+} and Zn^{2+} at the site of calcification and hence in the shell carbonate.

Calcification of porcelaneous foraminifera is suggested to take place in small vacuoles. In chapter 4 we argue that these calcification vessicles likely contain high concentrations of Mg^{2+}, SO_4^{2-}, Ba^{2+}, etc. as a result of seawater endocytosis. This would imply a relatively reduced need for additional transport of ions by Ca^{2+} channels compared to perforate species, since imperforate species already obtain calcium from the secluded seawater. The presence of seawater vacuoles in foraminifera has been observed by Bentov et al. (2009) and future research should focus on comparing the presence of these vacuoles in species with contrasting calcification strategies.

Internal pH

Since both hyaline and miliolid foraminifera increase their internal pH (De Nooijer et al., 2009), while acidifying their microenvironment (Glas et al., 2012), the uptake of Ca^{2+} might be directly coupled to proton pumping. By increasing their internal pH, most inorganic carbon will be present in the form of CO_3^{2-}. It is not known if foraminifera change their internal pH by a fixed value (e.g. a certain amount of units) compared to the surrounding seawater, and not to a set-value (e.g. to a pH of 9.5). In the latter case, the internal pH of a foraminifer would remain constant for different pCO_2 scenarios. In this case it is still possible to get different Zn/Ca values of the foraminifers shell, since the amount of Zn at the site of calcification is determined by the Zn complexation due to the inorganic carbonate parameters of the surrounding seawater. However, the first case is more logical, since it would also explain why changes in shell S/Ca are observed as a function of pCO_2 and hence carbonate ion concentration (Chapter 7). Since sulfur does not easily form complexes with carbonate, the amount of sulfate at the site of calcification is thus the same as outside the foraminifera. If internal pH would always be increased to the same value, the SO_4^{2-}/CO_3^{2-} at the site of calcification, and therefore the shell S/Ca would remain the same. Processes influencing the pH at the site of calcification need further investigation, especially under different pCO_2 scenarios, as this is crucial for all foraminiferal proxies related to the inorganic carbonate system of seawater (^{11}B, B/Ca, U/Ca, etc).

Precipitation

In this thesis I did not specifically discuss the final step in calcification, namely precipitation at the site of calcification. The question whether elements are incorporated as free ions or as carbonate complexes (as is the case for inorganically precipitated carbonates) remains to be answered. Although the transport to (and thus availability of ions at, the site of calcification) might be determined by element and carbonate complexation outside the foraminifera, high internal pH (and thus $[CO_3^{2-}]$) causes elements like Ba^{2+} and Zn^{2+} to be present at the SOC as stable carbonate complexes. This is in line with foraminifera using carbonate-complexes of elements that speciate as a function $[CO_3^{2-}]$, like Ba^{2+} and Zn^{2+} as building blocks for their shell, but does not provide conclusive proof.

Symbionts

A potential important factor in foraminiferal calcification, especially in larger benthic and planktonic foraminifera, is the activity of symbionts. Although this was not directly investigated in my thesis, preliminary data from night and day calcein labelling experiments conducted at the Caribbean Netherlands Science Institute (CNSI), show increased chamber addition for several symbiont bearing species (*Marginopora vertebralis, Amphistegina gibbosa* and *Astergerina carinata*) during daytime. Also observations where symbionts seem to be actively transported to the SOC might indicate they enhance (the initial phase of) calcification. The role of symbionts might explain why different larger benthic foraminifera show different (ecological) responses to ocean acidification scenarios (Doo et al., 2014). Since reef foraminifera produce ~5% of the global carbonate reef budget (Langer et al., 1997) and might be important for reef island resilience (Dawson et al., 2012), it is crucial to quantify and understand their response to ocean acidification.

In conclusion, this study aimed at increasing our understanding of foraminiferal calcification and element take up as a function of ocean acidification. For specific processes and (trace) elements this approach has succeeded. Furthermore, in this study we propose two proxies for reconstructing ocean inorganic carbonate chemistry, namely Zn/Ca (Chapter 6) and S/Ca (Chapter 7) of foraminiferal shells. These proxies have to be further explored, especially the impact of other environmental factors on element uptake is of vital importance for the robustness of these proxies. Also several new questions have arisen, like the role of symbionts and which elemental species foraminifera utilize for chamber formation.

References

Allen, G.J. and Sanders, D. (1994) Two Voltage-Gated, Calcium Release Channels Coreside in the Vacuolar Membrane of Broad Bean Guard Cells. *The Plant Cell* 6, 685-694.

Allen, K.A. and Hönisch, B. (2012) The planktic foraminiferal B/Ca proxy for seawater carbonate chemistry: A critical evaluation. *Earth and Planetary Science Letters* 345-348, 203-211.

Allen, K.A., Hönisch, B., Eggins, S.M., Haynes, L.L., Rosenthal, Y. and Yu, J. (2016) Trace element proxies for surface ocean conditions: A synthesis of culture calibrations with planktic foraminifera. *Geochimica et Cosmochimica Acta* 193, 197-221.

Allen, K.A., Hönisch, B., Eggins, S.M., Yu, J., Spero, H.J. and Elderfield, H. (2011) Controls on boron incorporation in cultured tests of the planktic foraminifer *Orbulina universa*. *Earth and Planetary Science Letters* 309, 291-301.

Allison, N., Austin, H., Austin, W. and Paterson, D.M. (2011) Effects of seawater pH and calcification rate on test Mg/Ca and Sr/Ca in cultured individuals of the benthic, calcitic foraminifera *Elphidium williamsoni*. *Chemical Geology* 289, 171-178.

Allison, N., Austin, W., Paterson, D. and Austin, H. (2010) Culture studies of the benthic foraminifera *Elphidium williamsoni*: Evaluating pH, $\Delta[CO_3^{2-}]$ and inter-individual effects on test Mg/Ca. *Chemical Geology* 274, 87-93.

Alve, E. (1995) Benthic foraminiferal distribution and recolonization of formerly anoxic environments in Drammensfjord, southern Norway. *Marine Micropaleontology* 25, 169-186.

Alve, E. and Bernhard, J. (1995) Vertical migratory response of benthic foraminifera to controlled oxygen concentrations in an experimental mesocosm. *Marien Ecology Progress Series*.

Anand, P., Elderfield, H. and Conte, M.H. (2003) Calibration of Mg/Ca thermometry in planktonic foraminifera from a sediment trap time series. *Paleoceanography* 18.

Angell, R.W. (1980) Test morphogenesis (chamber formation) in the foraminifer *Spiroloculina hyalina* Schulze. *Journal of Foraminiferal Research* 10, 89-101.

Arvidson, R.S., Guidry, M.W. and Mackenzie, F.T. (2011) Dolomite controls on Phanerozoic seawater chemistry. *Aquatic Geochemistry* 17, 735-747.

Arvidson, R.S., Mackenzie, F.T. and Guidry, M. (2006) MAGic: A Phanerozoic model for the geochemical cycling of major rock-forming components. *American Journal of Science* 306, 135-190.

Asteman, I., Hanslik, D. and Nordberg, K. (2015) An almost completed pollution-recovery cycle reflected by sediment geochemistry and benthic foraminiferal assemblages in a Swedish–Norwegian Skagerrak fjord. *Marine Pollution Bulletin* 95, 126-140.

Barker, S., Cacho, I., Benway, H. and Tachikawa, K. (2005) Planktonic foraminiferal Mg/Ca as a proxy for past oceanic temperatures: a methodological overview and data compilation for the Last Glacial Maximum. *Quaternary Science Reviews* 24, 821-834.

Barker, S., Higgins, J.A. and Elderfield, H. (2003) The future of the carbon cycle: review, calcification response, ballast and feedback on atmospheric CO_2. *Philos Trans A Math Phys Eng Sci* 361, 1977-1998; discussion 1998-1979.

Bé, A.W.H. and Ericson, D.B. (1963) Aspects of calcification in planktonic foraminifera (*Sarcodina*). *Annals of the New York Academy of Sciences* 109, 65-81.

Bé, A.W.H., Hemleben, C., Anderson, O.R. and Spindler, M. (1979) Chamber formation in planktonic foraminifera. *Micropaleontology* 25, 294-307.

Beer, C.J., Schiebel, R. and Wilson, P.A. (2010) Testing planktic foraminiferal shell weight as a surface water [CO_3^{2-}] proxy using plankton net samples. *Geology* 38, 103-106.

Beerling, D.J. and Royer, D.L. (2011) Convergent cenozoic CO_2 history. *Nature Geoscience* 4, 418-420.

Bender, H. and Hemleben, C. (1988) Constructional aspects in test formation of some agglutinated Foraminifera., in: F.M., G., Rögl, F. (Eds.), Second Workshop on Agglutinating Foraminifera. Abh. Geol. Bundesanstalt, pp. 13-21.

Bengtson, P. (1988) Open nomenclature. *Palaeontology* 31, 223-227.

Bentov, S., Brownlee, C. and Erez, J. (2009) The role of seawater endocytosis in the biomineralization process in calcareous foraminifera. *Proceedings of the National Academy of Sciences of the United States of America* 106, 21500-21504.

Bentov, S. and Erez, J. (2006) Impact of biomineralization processes on the Mg content of foraminiferal shells: A biological perspective. *Geochemistry, Geophysics, Geosystems* 7.

Berner, R. (1975) The role of magnesium in the crystal growth of calcite and aragonite from sea water. *Geochimica et Cosmochimica Acta* 39, 489-504.

Berner, R.A. (2004) A model for calcium, magnesium and sulfate in seawater over Phanerozoic time. *American Journal of Science* 304, 438-453.

Bernhard, J.M., Blanks, J.K., Hintz, C.J. and Chandler, G.T. (2004) Use of the fluorescent calcite marker calcein to label foraminiferal tests. *Journal of Foraminiferal Research* 34, 96-101.

Bernhard, J.M., Mollo-Christensen, E., Eisenkolb, N. and Starczak, V.R. (2009) Tolerance of allogromiid Foraminifera to severely elevated carbon dioxide concentrations: Implications to future ecosystem functioning and paleoceanographic interpretations. *Global and Planetary Change* 65, 107-114.

Bernhard, J.M. and Reimers, C.E. (1991) Benthic foraminiferal population fluctuations related to anoxia: Santa Barbara Basin. *Biogeochemistry* 15, 127-149.

Bernhard, J.M., Sen Gupta, B.K. and Borne, P.F. (1997) Benthic foraminiferal proxy to estimate dysoxic bottom-water oxygen concentrations; Santa Barbara Basin, U.S. Pacific continental margin. *Journal of Foraminiferal Research* 27, 301-310.

Bernhard, J.M., Wit, J.C. and McCorkle, D.C. (2015) Triple stress: Results of a long-term experiment to assess impact of ocean acidification, deoxygenation, and warming on benthic foraminiferal community composition and growth. *Geological Society of America Abstracts with Programs* 47, 702.

Berry, J.N. (1998) Sulfate in foraminiferal calcium carbonate: Investigating a potential proxy for sea water carbonate ion concentration. Massachusetts Institute of Technology, Cambridge, p. 88.

Berthold, W.-U. (1976) Biomineralisation bei milioliden Foraminiferen und die Matritzen-Hypothese. *Naturwissenschaften* 63, 196-197.

Bijma, J., Hönisch, B. and Zeebe, R.E. (2002) Impact of the ocean carbonate chemistry on living foraminiferal shell weight: Comment on "Carbonate ion concentration in glacial-age deep waters of the Caribbean Sea" by WS Broecker and E. Clark. *Geochemistry, Geophysics, Geosystems* 3, 1-7.

Billups, K. and Schrag, D. (2002) Paleotemperatures and ice volume of the past 27 Myr revisited with paired Mg/Ca and $^{18}O/^{16}O$ measurements on benthic foraminifera. *Paleoceanography* 17.

Blackmon, P.D. and Todd, R. (1959) Mineralogy of some foraminifera as related to their classification and ecology *J. Paleontol.* 33, 1-15.

Bothner, M.H., Spiker, E., Johnson, P., Rendigs, R. and Aruscavage, P. (1981) Geochemical evidence for modern sediment accumulation on the continental shelf off southern New England. *Journal of Sedimentary Research* 51.

Bots, P., Benning, L., Rickaby, R. and Shaw, S. (2011) The role of SO_4 in the switch from calcite to aragonite seas. *Geology* 39, 331-334.

Bottrell, S.H. and Newton, R.J. (2006) Reconstruction of changes in global sulfur cycling from marine sulfate isotopes. *Earth-Science Reviews* 75, 59-83.

BouDagher-Fadel, M.K., Banner, F.T. and Whittaker, J.E. (1997) Early evolutionary history of planktonic foraminifera. Chapman & Hall, London.

Boyle, E.A. (1981) Cadmium, zinc, copper, and barium in foraminifera tests. *Earth and Planetary Science Letters* 53, 11-35.

Branson, O., Kaczmarek, K., Redfern, S.A.T., Misra, S., Langer, G., Tyliszczak, T., Bijma, J. and Elderfield, H. (2015) The coordination and distribution of B in foraminiferal calcite. *Earth and Planetary Science Letters* 416, 67-72.

Broecker, W.S., Peng, T.-H. and Beng, Z. (1982) Tracers in the Sea. Lamont-Doherty Geological Observatory, Columbia University.

Bruland, K.W., Knauer, G.A. and Martin, J.H. (1978) Zinc in north-east Pacific water. *Nature* 271, 741-743.

Bryan, S.P. and Marchitto, T.M. (2010) Testing the utility of paleonutrient proxies Cd/Ca and Zn/Ca in benthic foraminifera from thermocline waters. *Geochemistry, Geophysics, Geosystems* 11, n/a-n/a.

Claypool, G.E., Holser, W.T., Kaplan, I.R., Sakai, H. and Zak, I. (1980) The age curves of sulfur and oxygen isotopes in marine sulfate and their mutual interpretation. *Chemical Geology* 28, 199-260.

Clémence, M.-E. and Hart, M.B. (2013) Proliferation of *Oberhauserellidae* during the recovery following the Late Triassic extinction: paleoecological implications. *J. Paleontol.* 87, 1004-1015.

Coccioni, R. (2000) Benthic Foraminifera as Bioindicators of Heavy Metal Pollution, in: Martin, R.E. (Ed.), Environmental Micropaleontology: The Application of Microfossils to Environmental Geology. Springer US, Boston, MA, pp. 71-103.

Comeau, S., Gorsky, G., Jeffree, R., Teyssié, J.-L. and Gattuso, J.-P. (2009) Impact of ocean acidification on a key Arctic pelagic mollusc (*Limacina helicina*). *Biogeosciences* 6, 1877-1882.

Copestake, P. and Johnson, B. (2014) Lower Jurassic Foraminifera from the Llanbedr (Mochras Farm) Borehole, North Wales, UK. Monograph of the Palaeontological Society, London.

Crocket, J.H. and Winchester, J.W. (1966) Coprecipitation of zinc with calcium carbonate. *Geochimica et Cosmochimica Acta* 30, 1093-1109.

Dawson, J.L., Hua, Q. and Smithers, S.G. (2012) Benthic foraminifera: their importance to future reef island resilience.

De Choudens-Sánchez, V. and Gonzalez, L.A. (2009) Calcite and aragonite precipitation under controlled instantaneous supersaturation: elucidating the role of $CaCO_3$ saturation state and Mg/Ca ratio on calcium carbonate polymorphism. *Journal of Sedimentary Research* 79, 363-376.

De Moel, H., Ganssen, G.M., Peeters, F.J.C., Jung, S.J.A., Kroon, D., Brummer, G.J.A. and Zeebe, R.E. (2009) Planktic foraminiferal shell thinning in the Arabian Sea due to anthropogenic ocean acidification? *Biogeosciences* 6, 1917-1925.

De Nooijer, L.J., Hathorne, E.C., Reichart, G.J., Langer, G. and Bijma, J. (2014a) Variability in calcitic Mg/Ca and Sr/Ca ratios in clones of the benthic foraminifer *Ammonia tepida*. *Marine Micropaleontology* 107, 32-43.

De Nooijer, L.J., Spero, H.J., Erez, J., Bijma, J. and Reichart, G.J. (2014b) Biomineralization in perforate foraminifera. *Earth-Science Reviews* 135, 48-58.

De Nooijer, L.J., Toyofuku, T. and Kitazato, H. (2009) Foraminifera promote calcification by elevating their intracellular pH. *Proceedings of the National Academy of Sciences* 106, 15374-15378.

De Nooijer, L.J., Toyofuku, T., Oguri, K., Nomaki, H. and Kitazato, H. (2008) Intracellular pH distribution in foraminifera determined by the fluorescent probe HPTS. *Limnol Oceanogr Methods* 6, 610-618.

De Villiers, S., Greaves, M. and Elderfield, H. (2002) An intensity ratio calibration method for the accurate determination of Mg/Ca and Sr/Ca of marine carbonates by ICP-AES. *Geochemistry, Geophysics, Geosystems* 3.

Debenay, J.-P., Guillou, J.-J., Geslin, E., Lesourd, M. and Redois, F. (1998) Processus de cristallisation de plaquettes rhomboédriques à la surface d'un test porcelané de foraminifère actuel. *Geobios* 31, 295-302.

Delaney, M.L., Bé, A.W. and Boyle, E.A. (1985) Li, Sr, Mg, and Na in foraminiferal calcite shells from laboratory culture, sediment traps, and sediment cores. *Geochimica et Cosmochimica Acta* 49, 1327-1341.

Demicco, R.V., Lowenstein, T.K., Hardie, L.A. and Spencer, R.J. (2005) Model of seawater composition for the Phanerozoic. *Geology* 33, 877.

Dickson, A.G., Afghan, J.D. and Anderson, G.C. (2003) Reference materials for oceanic CO_2 analysis: a method for the certification of total alkalinity. *Marine Chemistry* 80, 185-197.

Dickson, A.G. and Millero, F.J. (1987) A comparison of the equilibrium constants for the dissociation of carbonic acid in seawater media. *Deep Sea Research Part A. Oceanographic Research Papers* 34, 1733-1743.

Dickson, J. (2002) Fossil echinoderms as monitor of the Mg/Ca ratio of Phanerozoic oceans. *Science* 298, 1222-1224.

Dickson, J. (2004) Echinoderm skeletal preservation: calcite-aragonite seas and the Mg/Ca ratio of Phanerozoic oceans. *Journal of Sedimentary Research* 74, 355-365.

Dissard, D., Nehrke, G., Reichart, G.J. and Bijma, J. (2010) Impact of seawater pCO_2 on calcification and Mg/Ca and Sr/Ca ratios in benthic foraminifera calcite: results from culturing experiments with *Ammonia tepida*. *Biogeosciences* 7, 81-93.

Dissard, D., Nehrke, G., Reichart, G.J., Nouet, J. and Bijma, J. (2009) Effect of the fluorescent indicator calcein on Mg and Sr incorporation into foraminiferal calcite. *Geochemistry, Geophysics, Geosystems* 10, n/a-n/a.

Doney, S.C., Fabry, V.J., Feely, R.A. and Kleypas, J.A. (2009) Ocean acidification: the other CO_2 problem. *Ann Rev Mar Sci* 1, 169-192.

Doo, S.S., Fujita, K., Byrne, M. and Uthicke, S. (2014) Fate of Calcifying Tropical Symbiont-Bearing Large Benthic Foraminifera: Living Sands in a Changing Ocean. *Biological Bulletin* 226, 169-186.

Dueñas-Bohórquez, A., da Rocha, R.E., Kuroyanagi, A., Bijma, J. and Reichart, G.-J. (2009) Effect of salinity and seawater calcite saturation state on Mg and Sr incorporation in cultured planktonic foraminifera. *Marine Micropaleontology* 73, 178-189.

Dueñas-Bohórquez, A., Raitzsch, M., De Nooijer, L.J. and Reichart, G.-J. (2011) Independent impacts of calcium and carbonate ion concentration on Mg and Sr incorporation in cultured benthic foraminifera. *Marine Micropaleontology* 81, 122-130.

Eggins, S., Sadekov, A. and Dedeckker, P. (2004) Modulation and daily banding of Mg/Ca in tests by symbiont photosynthesis and respiration: a complication for seawater thermometry? *Earth and Planetary Science Letters* 225, 411-419.

Elderfield, H., Bertram, C.J. and Erez, J. (1996) A biomineralization model for the incorporation of trace elements into foraminiferal calcium carbonate. *Earth and Planetary Science Letters* 142, 409-423.

Elderfield, H. and Ganssen, G. (2000) Past temperature and $\delta^{18}O$ of surface ocean waters inferred from foraminiferal Mg/Ca ratios. *Nature* 405, 442-445.

Elderfield, H., Vautravers, M. and Cooper, M. (2002) The relationship between shell size and Mg/Ca, Sr/Ca, $\delta^{18}O$, and $\delta^{13}C$ of species of planktonic foraminifera. *Geochemistry, Geophysics, Geosystems* 3, 1-13.

Erez, J. (2003) The source of ions for biomineralization in foraminifera and their implications for paleoceanographic proxies. *Reviews in Mineralogy and Geochemistry* 54, 115-149.

Evans, D., Erez, J., Oron, S. and Müller, W. (2015) Mg/Ca-temperature and seawater-test chemistry relationships in the shallow-dwelling large benthic foraminifera *Operculina ammonoides*. *Geochimica et Cosmochimica Acta* 148, 325-342.

Evans, D. and Müller, W. (2012) Deep time foraminifera Mg/Ca paleothermometry: Nonlinear correction for secular change in seawater Mg/Ca. *Paleoceanography* 27, n/a-n/a.

Evans, D. and Müller, W. (2013) LA-ICP-MS elemental imaging of complex discontinuous carbonates: An example using large benthic foraminifera. *Journal of Analytical Atomic Spectrometry* 28, 1039-1044.

Evans, D., Wade, B.S., Henehan, M., Erez, J. and Müller, W. (2016) Revisiting carbonate chemistry controls on planktic foraminifera Mg/Ca: implications for sea surface temperature and hydrology shifts over the Paleocene–Eocene Thermal Maximum and Eocene–Oligocene transition. *Clim. Past* 12, 819-835.

Falini, G., Gazzano, M. and Ripamonti, A. (1994) Crystallization of calcium carbonate in presence of magnesium and polyelectrolytes. *Journal of Crystal Growth* 137, 577-584.

Farkaš, J., Böhm, F., Wallmann, K., Blenkinsop, J., Eisenhauer, A., van Geldern, R., Munnecke, A., Voigt, S. and Veizer, J. (2007) Calcium isotope record of Phanerozoic oceans: Implications for chemical evolution of seawater and its causative mechanisms. *Geochimica et Cosmochimica Acta* 71, 5117-5134.

Feely, R.A., Doney, S.C. and Cooley, S.R. (2009) Ocean acidification: present conditions and future changes in a high-CO_2 world. *Oceanography* 22, 36-47.

Fernandez-Diaz, L., Putnis, A., Prieto, M. and Putnis, C.V. (1996) The role of magnesium in the crystallization of calcite and aragonite in a porous medium. *Journal of sedimentary research* 66.

Filipson, H., Bernhard, J., Lincoln, S. and McCorkle, D. (2010) A culture-based calibration of benthic foraminiferal paleotemperature proxies: Delta O-18 and Mg/Ca results. *Biogeosciences* 7, 1335-1347.

Friedrich, O., Schiebel, R., Wilson, P.A., Weldeab, S., Beer, C.J., Cooper, M.J. and Fiebig, J. (2012) Influence of test size, water depth, and ecology on Mg/Ca, Sr/Ca, $\delta^{18}O$ and $\delta^{13}C$ in nine modern species of planktic foraminifers. *Earth and Planetary Science Letters* 319, 133-145.

Fuchs, W. (1967) Über Ursprung und Phylogenie der Trias- "*Globigerinen*" und die Bedeutung dieses Formenkreises für das echte Plankton. *Verhandlungen der Geologischen Bundesanstalt, Wien* 1967, 135-176.

Fuchs, W. (1970) Eine alpine, tiefliassische Foraminiferenfauna von Hernstein in Niederösterreich. *Verhandlungen der Geologischen Bundesanstalt, Wien* 1970, 66-145.

Fujita, K., Hikami, M., Suzuki, A., Kuroyanagi, A., Sakai, K., Kawahata, H. and Nojiri, Y. (2011) Effects of ocean acidification on calcification of symbiont-bearing reef foraminifers. *Biogeosciences* 8, 2089-2098.

Gattuso, J.-P. and Hansson, L. (2011) Ocean acidification. OUP Oxford.

Geslin, E., Heinz, P., Jorissen, F. and Hemleben, C. (2004) Migratory responses of deep-sea benthic foraminifera to variable oxygen conditions: laboratory investigations. *Marine Micropaleontology* 53, 227-243.

Geslin, E., Stouff, V., Debenay, J.-P. and Lesourd, M. (2000) Environmental Variation and Foraminiferal Test Abnormalities, in: Martin, R.E. (Ed.), Environmental Micropaleontology: The Application of Microfossils to Environmental Geology. Springer US, Boston, MA, pp. 191-215.

Glas, M.S., Langer, G. and Keul, N. (2012) Calcification acidifies the microenvironment of a benthic foraminifer (*Ammonia sp.*). *Journal of Experimental Marine Biology and Ecology* 424–425, 53-58.

Gobler, C.J., DePasquale, E.L., Griffith, A.W. and Baumann, H. (2014) Hypoxia and Acidification Have Additive and Synergistic Negative Effects on the

Growth, Survival, and Metamorphosis of Early Life Stage Bivalves. *PLoS ONE* 9, e83648.

Gooday, A.J., Bernhard, J.M., Levin, L.A. and Suhr, S.B. (2000) Foraminifera in the Arabian Sea oxygen minimum zone and other oxygen-deficient settings: taxonomic composition, diversity, and relation to metazoan faunas. *Deep Sea Research Part II: Topical Studies in Oceanography* 47, 25-54.

Gooday, A.J., Bowser, S.S. and Bernhard, J.M. (1996) Benthic foraminiferal assemblages in Explorers Cove, Antarctica: A shallow-water site with deep-sea characteristics. *Progress in Oceanography* 37, 117-166.

Guillong, M., Meier, D.L., Allan, M.M., Heinrich, C.A. and Yardley, B.W. (2008) SILLS: A MATLAB-based program for the reduction of laser ablation ICP-MS data of homogeneous materials and inclusions. *Mineralogical Association of Canada Short Course Series* 40, 328-333.

Gussone, N., Langer, G., Thoms, S., Nehrke, G., Eisenhauer, A., Riebesell, U. and Wefer, G. (2006) Cellular calcium pathways and isotope fractionation in *Emiliania huxleyi*. *Geology* 34, 625-628.

Hansen, K.W. and Wallmann, K. (2003) Cretaceous and Cenozoic evolution of seawater composition, atmospheric O_2 and CO_2: a model perspective. *American Journal of Science* 303, 94-148.

Hardie, L.A. (1996) Secular variation in seawater chemistry: An explanation for the coupled secular variation in the mineralogies of marine limestones and potash evaporites over the past 600 my. *Geology* 24, 279-283.

Hart, M., Hylton, M., Oxford, M., Price, G., Hudson, W. and Smart, C. (2003) The search for the origin of the planktic Foraminifera. *Journal of the Geological Society* 160, 341-343.

Hart, M.B. (1984) Benthos ’83; 2nd International Symposium on Benthic Foraminifera, Pau, April 1983, in: Oertli, H.J. (Ed.). Elf Aquitaine, Esso REP and Total CFP, Pau and Bordeaux, pp. 289-298.

Hart, M.B. (1999) The evolution and biodiversity of Cretaceous planktonic Foraminiferida. *Geobios* 32, 247-255.

Hart, M.B., Hudson, W., Smart, C.W. and Tyszka, J. (2012) A reassessment of ‘*Globigerina bathoniana*’ Pazdrowa, 1969 and the palaeoceanographic significance of Jurassic planktic foraminifera from southern Poland. *Journal of Micropalaeontology* 31, 97-109.

Hart, M.B., Leighton, A.D., Smart, C.W., Pettit, L.R., Medina-Sánchez, I.N., Harries, P.J., Cárdenas, A.L., Hall-Spencer, J.M. and Prol-Ledesma, R.M. (2014) Ocean acidification in modern seas and its recognition in the geological record: The Cretaceous/Paleogene boundary in Texas and Alabama. *Gulf Coast Association of Geological Societies Transactions* 64, 193-213.

Hart, M.B., M. J. Oxford and Hudson, W. (2002) The early evolution and palaeobiogeography of Mesozoic planktonic foraminifera, in: Crame, J.A., Owen, A.W. (Eds.), Palaeobiogeography and biodiversity change: the Ordovician and Mesozoic-Cenozoic radiations. Geological Society of London.

Hart, M.B., Price, G.D. and Smart, C.W. (2008) Foraminifera and sequence stratigraphy of the lower part of the Speeton Clay Formation (Lower Cretaceous) in NE England. *Annalen des Naturhistorischen Museums in Wien. Serie A für*

Mineralogie und Petrographie, Geologie und Paläontologie, Anthropologie und Prähistorie, 423-442.

Hasiuk, F.J. and Lohmann, K.C. (2010) Application of calcite Mg partitioning functions to the reconstruction of paleocean Mg/Ca. *Geochimica et Cosmochimica Acta* 74, 6751-6763.

Hastings, D.W., Russell, A.D. and Emerson, S.R. (1998) Foraminiferal magnesium in *Globeriginoides sacculifer* as a paleotemperature proxy. *Paleoceanography* 13, 161-169.

Hathorne, E.C., James, R.H. and Lampitt, R.S. (2009) Environmental versus biomineralization controls on the intratest variation in the trace element composition of the planktonic foraminifera *G. inflata* and *G. scitula*. *Paleoceanography* 24, n/a-n/a.

Hemleben, C., Be, A.W.H., Anderson, O.R. and Tuntivate, S. (1977) Test morphology, organic layers and chamber formation of the planktonic foraminifer *Globorotalia menardii* (d'Orbigny). *Journal of Foraminiferal Research* 7, 1-25.

Hemleben, C.H., Anderson, O.R., Berthold, W. and Spindler, M. (1986) Calcification and chamber formation in Foraminifera-a brief overview, in: Leadbeater, B.S., Riding, R. (Eds.), Biomineralization in lower plants and animals. Clarendon Press,, Oxford, pp. 237-249.

Hemming, N. and Hanson, G. (1992a) Boron isotopic composition and concentration in modern marine carbonates. *Geochimica et Cosmochimica Acta* 56, 537-543.

Hemming, N.G. and Hanson, G.N. (1992b) Boron isotopic composition and concentration in modern marine carbonates. *Geochimica et Cosmochimica Acta* 56, 537-543.

Hernroth, B., Krång, A.-S. and Baden, S. (2015) Bacteriostatic suppression in Norway lobster (*Nephrops norvegicus*) exposed to manganese or hypoxia under pressure of ocean acidification. *Aquatic Toxicology* 159, 217-224.

Hershey, J.P., Fernandez, M., Milne, P.J. and Millero, F.J. (1986) The ionization of boric acid in NaCl, Na-Ca-Cl and Na-Mg-Cl solutions at 25° C. *Geochimica et cosmochimica acta* 50, 143-148.

Hess, P. and Tsien, R.W. (1984) Mechanism of ion permeation through calcium channels. *Nature* 309, 453-456.

Heuser, A., Eisenhauer, A., Böhm, F., Wallmann, K., Gussone, N., Pearson, P.N., Nägler, T.F. and Dullo, W.C. (2005) Calcium isotope ($\delta^{44/40}$Ca) variations of Neogene planktonic foraminifera. *Paleoceanography* 20.

Hoegh-Guldberg, O., Mumby, P.J., Hooten, A.J., Steneck, R.S., Greenfield, P., Gomez, E., Harvell, C.D., Sale, P.F., Edwards, A.J., Caldeira, K., Knowlton, N., Eakin, C.M., Iglesias-Prieto, R., Muthiga, N., Bradbury, R.H., Dubi, A. and Hatziolos, M.E. (2007) Coral Reefs Under Rapid Climate Change and Ocean Acidification. *Science* 318, 1737-1742.

Holland, H.D. (2005) Sea level, sediments and the composition of seawater. *American Journal of Science* 305, 220-239.

Holland, H.D., Horita, J. and Seyfried, W.E. (1996) On the secular variations in the composition of Phanerozoic marine potash evaporites. *Geology* 24, 993-996.

Holland, H.D. and Zimmermann, H. (2000) The Dolomite Problem Revisited. *International Geology Review* 42, 481-490.

Hönisch, B., Allen, K.A., Lea, D.W., Spero, H.J., Eggins, S.M., Arbuszewski, J., Rosenthal, Y., Russell, A.D. and Elderfield, H. (2013) The influence of salinity on Mg/Ca in planktic foraminifers – Evidence from cultures, core-top sediments and complementary $\delta^{18}O$. *Geochimica et Cosmochimica Acta* 121, 196-213.

Hönisch, B., Allen, K.A., Russell, A.D., Eggins, S.M., Bijma, J., Spero, H.J., Lea, D.W. and Yu, J. (2011) Planktic foraminifers as recorders of seawater Ba/Ca. *Marine Micropaleontology* 79, 52-57.

Hönisch, B. and Hemming, N.G. (2005) Surface ocean pH response to variations in pCO_2 through two full glacial cycles. *Earth and Planetary Science Letters* 236, 305-314.

Hönisch, B., Hemming, N.G., Archer, D., Siddall, M. and McManus, J.F. (2009) Atmospheric carbon dioxide concentration across the Mid-Pleistocene Transition. *Science* 324, 1551-1554.

Hönisch, B., Ridgwell, A., Schmidt, D.N., Thomas, E., Gibbs, S.J., Sluijs, A., Zeebe, R., Kump, L., Martindale, R.C., Greene, S.E., Kiessling, W., Ries, J., Zachos, J.C., Royer, D.L., Barker, S., Marchitto, T.M., Moyer, R., Pelejero, C., Ziveri, P., Foster, G.L. and Williams, B. (2012) The Geological Record of Ocean Acidification. *Science* 335, 1058-1063.

Hoogakker, B.A., Klinkhammer, G.P., Elderfield, H., Rohling, E.J. and Hayward, C. (2009) Mg/Ca paleothermometry in high salinity environments. *Earth and Planetary Science Letters* 284, 583-589.

Horita, J., Zimmermann, H. and Holland, H.D. (2002) Chemical evolution of seawater during the Phanerozoic: Implications from the record of marine evaporites. *Geochimica et Cosmochimica Acta* 66, 3733-3756.

Houghton, J.T., Ding, Y., Griggs, D.J., Noguer, M., van der Linden, P.J., Dai, X., Maskell, K. and Johnson, C. (2001) Climate change 2001: the scientific basis. Cambridge University Press, Cambridge, Uk and New York, N.Y., USA.

Ilyina, T. and Zeebe, R.E. (2012) Detection and projection of carbonate dissolution in the water column and deep-sea sediments due to ocean acidification. *Geophysical Research Letters* 39, n/a-n/a.

IPCC (2007) Climate Change 2007: The AR4 Synthesis Report, Geneva.

IPCC (2014) Climate Change 2014: Impacts, Adaptation, and Vulnerability. Part A: Global and Sectoral Aspects. Contribution of Working Group II to the Fifth Assessment Report of the Intergovernmental Panel on Climate Change. Cambridge University Press, Cambridge, United Kingdom and New York, NY, USA.

Ishikawa, M. and Ichikuni, M. (1984) Uptake of sodium and potassium by calcite. *Chemical geology* 42, 137-146.

Jakubowska, M. and Normant, M. (2015) Metabolic rate and activity of blue mussel *Mytilus edulis trossulus* under short-term exposure to carbon dioxide-induced water acidification and oxygen deficiency. *Marine and Freshwater Behaviour and Physiology* 48, 25-39.

Jochum, K.P., Scholz, D., Stoll, B., Weis, U., Wilson, S.A., Yang, Q., Schwalb, A., Börner, N., Jacob, D.E. and Andreae, M.O. (2012) Accurate trace element

analysis of speleothems and biogenic calcium carbonates by LA-ICP-MS. *Chemical Geology* 318–319, 31-44.

Jørgensen, B.B. (1982) Mineralization of organic matter in the sea bed - the role of sulphate reduction. *Nature* 296, 643-645.

Jørgensen, N.O. (1977) Wall structure of some arenaceous foraminifera from the Maastrichtian White Chalk (Denmark). *Journal of Foraminiferal Research* 7, 313-321.

Kasten, S. and Jørgensen, B.B. (2000) Sulfate Reduction in Marine Sediments, in: Schulz, H.D., Zabel, M. (Eds.), Marine Geochemistry. Springer Berlin Heidelberg, Berlin, Heidelberg, pp. 263-281.

Kester, D.R., Duedall, I.W., Connors, D.N. and Pytkowicz, R.M. (1967) Preparation of artificial seawater. *Limnology and oceanography* 12, 176-179.

Keul, N., Langer, G., De Nooijer, L.J. and Bijma, J. (2013a) Effect of ocean acidification on the benthic foraminifera *Ammonia* sp. is caused by a decrease in carbonate ion concentration. *Biogeosciences* 10, 6185-6198.

Keul, N., Langer, G., De Nooijer, L.J., Nehrke, G., Reichart, G.-J. and Bijma, J. (2013b) Incorporation of uranium in benthic foraminiferal calcite reflects seawater carbonate ion concentration. *Geochemistry, Geophysics, Geosystems* 14, 102-111.

Kiessling, W., Aberhan, M. and Villier, L. (2008) Phanerozoic trends in skeletal mineralogy driven by mass extinctions. *Nature Geoscience* 1, 527-530.

Kiessling, W., M. E. Clapham, A. J. W. Hendy, F. T. Fursich, L. Villier, Alroy, J. and Miller, A.I. (2015) Taxonomic occurrences of to 600 Foraminferea, Foraminiferida, and Foraminifera recorded in, Fossilworks: The evolution of terrestrial ecosystems database, and the paleobiology database, Fossilworks. http://fossilworks.org.

Kısakürek, B., Eisenhauer, A., Böhm, F., Garbe-Schönberg, D. and Erez, J. (2008) Controls on shell Mg/Ca and Sr/Ca in cultured planktonic foraminifera, *Globigerinoides ruber* (white). *Earth and Planetary Science Letters* 273, 260-269.

Kleypas, J.A., Buddemeier, R.W., Archer, D., Gattuso, J.-P., Langdon, C. and Opdyke, B.N. (1999) Geochemical Consequences of Increased Atmospheric Carbon Dioxide on Coral Reefs. *Science* 284, 118-120.

Kranz, S.A., Gladrow, D.W., Nehrke, G., Langer, G. and Rosta, B. (2010) Calcium carbonate precipitation induced by the growth of the marine cyanobacteria *Trichodesmium*. *Limnology and Oceanography* 55, 2563-2569.

Kunioka, D., Shirai, K., Takahata, N., Sano, Y., Toyofuku, T. and Ujiie, Y. (2006) Microdistribution of Mg/Ca, Sr/Ca, and Ba/Ca ratios in *Pulleniatina obliquiloculata* test by using a NanoSIMS: Implication for the vital effect mechanism. *Geochemistry, Geophysics, Geosystems* 7, n/a-n/a.

Kuroyanagi, A., Kawahata, H., Suzuki, A., Fujita, K. and Irie, T. (2009) Impacts of ocean acidification on large benthic foraminifers: Results from laboratory experiments. *Marine Micropaleontology* 73, 190-195.

Kurtarkar, S.R., Saraswat, R., Nigam, R., Banerjee, B., Mallick, R., Naik, D.K. and Singh, D.P. (2015) Assessing the effect of calcein incorporation on physiological processes of benthic foraminifera. *Marine Micropaleontology* 114, 36-45.

Langer, M.R. (2008) Assessing the Contribution of Foraminiferan Protists to Global Ocean Carbonate Production. *Journal of Eukaryotic Microbiology* 55, 163-169.

Langer, M.R., Silk, M.T. and Lipps, J.H. (1997) Global ocean carbonate and carbon dioxide production; the role of reef Foraminifera. *Journal of Foraminiferal Research* 27, 271-277.

Langlet, D., Baal, C., Geslin, E., Metzger, E., Zuschin, M., Riedel, B., Risgaard-Petersen, N., Stachowitsch, M. and Jorissen, F.J. (2014) Foraminiferal species responses to in situ, experimentally induced anoxia in the Adriatic Sea. *Biogeosciences* 11, 1775-1797.

Lea, D.W., Mashiotta, T.A. and Spero, H.J. (1999) Controls on magnesium and strontium uptake in planktonic foraminifera determined by live culturing. *Geochimica et Cosmochimica Acta* 63, 2369-2379.

Lear, C.H., Elderfield, H. and Wilson, P.A. (2000) Cenozoic deep-Sea temperatures and global ice volumes from Mg/Ca in benthic foraminiferal calcite. *Science* 287, 269-272.

Loeblich, A.R. and Tappan, H. (1984) Suprageneric classification of the Foraminiferida (Protozoa). *Micropaleontology*, 1-70.

Loeblich, A.R. and Tappan, H. (1988) Foraminiferal Genera and their Classification. Van Nostrant Reinhold, New York.

Lowenstein, T.K., Timofeeff, M.N., Brennan, S.T., Hardie, L.A. and Demicco, R.V. (2001) Oscillations in Phanerozoic seawater chemistry: Evidence from fluid inclusions. *Science* 294, 1086-1088.

Manno, C., Morata, N. and Bellerby, R. (2012) Effect of ocean acidification and temperature increase on the planktonic foraminifer *Neogloboquadrina pachyderma* (sinistral). *Polar Biology* 35, 1311-1319.

Marchitto, T.M., Curry, W.B. and Oppo, D.W. (2000) Zinc concentrations in benthic foraminifera reflect seawater chemistry. *Paleoceanography* 15, 299-306.

Marchitto, T.M., Lynch-Stieglitz, J. and Hemming, S.R. (2005) Deep Pacific $CaCO_3$ compensation and glacial–interglacial atmospheric CO_2. *Earth and Planetary Science Letters* 231, 317-336.

Marchitto, T.M., Oppo, D.W. and Curry, W.B. (2002) Paired benthic foraminiferal Cd/Ca and Zn/Ca evidence for a greatly increased presence of Southern Ocean Water in the glacial North Atlantic. *Paleoceanography* 17, 10-11-10-18.

Marr, J.P., Bostock, H.C., Carter, L., Bolton, A. and Smith, E. (2013) Differential effects of cleaning procedures on the trace element chemistry of planktonic foraminifera. *Chemical Geology* 351, 310-323.

Martin, R.E. (1995) Cyclic and secular variation in microfossil biomineralization: clues to the biogeochemical evolution of Phanerozoic oceans. *Global and Planetary Change* 11, 1-23.

McCorkle, D.C., Martin, P.A., Lea, D.W. and Klinkhammer, G.P. (1995) Evidence of a dissolution effect on benthic foraminiferal shell chemistry: $\delta^{13}C$, Cd/Ca, Ba/Ca, and Sr/Ca results from the Ontong Java Plateau. *Paleoceanography* 10, 699-714.

McIntyre-Wressnig, A., Bernhard, J.M., McCorkle, D.C. and Hallock, P. (2013) Non-lethal effects of ocean acidification on the symbiont-bearing benthic foraminifer *Amphistegina gibbosa*. *Marine Ecology Progress Series* 472, 45-60.

Mehrbach, C., Culberson, C.H., Hawley, J.E. and Pytkowicx, R.M. (1973) Measurement of the apparent dissociation constants of carbonic acid in seawater at atmospheric pressure. *Limnology and Oceanography* 18, 897-907.

Mewes, A., Langer, G., De Nooijer, L.J., Bijma, J. and Reichart, G.-J. (2014) Effect of different seawater Mg^{2+} concentrations on calcification in two benthic foraminifers. *Marine micropaleontology* 113, 56-64.

Mewes, A., Langer, G., Reichart, G.-J., De Nooijer, L.J., Nehrke, G. and Bijma, J. (2015) The impact of Mg contents on Sr partitioning in benthic foraminifers. *Chemical Geology* 412, 92-98.

Mezger, E.M., de Nooijer, L.J., Boer, W., Brummer, G.J.A. and Reichart, G.J. (2016) Salinity controls on Na incorporation in Red Sea planktonic foraminifera. *Paleoceanography*, n/a-n/a.

Morse, J.W., Arvidson, R.S. and Lüttge, A. (2007) Calcium carbonate formation and dissolution. *Chemical Reviews* 107, 342-381.

Moy, A.D., Howard, W.R., Bray, S.G. and Trull, T.W. (2009) Reduced calcification in modern Southern Ocean planktonic foraminifera. *Nature Geosci* 2, 276-280.

Mucci, A. (1987) Inlfuence of temperature on the composition of magnesian calcite overgrowths preciptated from seawater. *Geochimica et Cosmochimica Acta* 51, 1977-1984.

Mucci, A. and Morse, J.W. (1983) The incorporation of Mg^{2+} and Sr^{2+} into calcite overgrowths: influences of growth rate and solution composition. *Geochimica et Cosmochimica Acta* 47, 217-233.

Mucci, A. and Morse, J.W. (1985) Auger spectroscopy determination of the surface-most adsorbed layer composition on aragonite, calcite, dolomite, and magnesite in synthetic seawater. *American Journal of Science* 285, 306-317.

Munsel, D., Kramar, U., Dissard, D., Nehrke, G., Berner, Z., Bijma, J., Reichart, G.J. and Neumann, T. (2010) Heavy metal incorporation in foraminiferal calcite: results from multi-element enrichment culture experiments with *Ammonia tepida*. *Biogeosciences* 7, 2339-2350.

Murray, J.W. (1973) Wall structure of some agglutinating Foraminiferida. *Palaeontology* 16, 777-786.

Nancollas, G.H. and Sawada, K. (1982) Formation of scales of calcium carbonate polymorphs: The influence of magnesium ion and inhibitors. *Journal of Petroleum Technology* 34, 645-652.

Nardelli, M.P., Malferrari, D., Ferretti, A., Bartolini, A., Sabbatini, A. and Negri, A. (2016) Zinc incorporation in the miliolid foraminifer Pseudotriloculina rotunda under laboratory conditions. *Marine Micropaleontology* 126, 42-49.

Nardelli, M.P., Sabbatini, A. and Negri, A. (2013) Experimental chronic exposure of the foraminifer *Pseudotriloculina rotunda* to zinc. *Acta Protozoologica* 52, 193.

Nehrke, G., Keul, N., Langer, G., De Nooijer, L.J., Bijma, J. and Meibom, A. (2013) A new model for biomineralization and trace - element signatures of Foraminifera tests. *Biogeosciences* 10, 6759-6767.

Nehrke, G. and Nouet, J. (2011) Confocal Raman microscope mapping as a tool to describe different mineral and organic phases at high spatial resolution within marine biogenic carbonates: case study on *Nerita undata* (Gastropoda, Neritopsina). *Biogeosciences* 8, 3761-3769.

Ní Fhlaithearta, S., Ernst, S.R., Nierop, K.G., de Lange, G.J. and Reichart, G.-J. (2013) Molecular and isotopic composition of foraminiferal organic linings. *Marine Micropaleontology* 102, 69-78.

Nürnberg, D. (2015) Mg/Ca Paleothermometry, in: Harff, J., Meschede, M., Petersen, S., Thiede, J. (Eds.), Encyclopedia of Marine Geosciences. Springer Netherlands, pp. 1-3.

Nürnberg, D., Bijma, J. and Hemleben, C. (1996) Assessing the reliability of magnesium in foraminiferal calcite as a proxy for water mass temperatures. *Geochimica et Cosmochimica Acta* 60, 803-814.

Orr, J.C., Fabry, V.J., Aumont, O., Bopp, L., Doney, S.C., Feely, R.A., Gnanadesikan, A., Gruber, N., Ishida, A., Joos, F., Key, R.M., Lindsay, K., Maier-Reimer, E., Matear, R., Monfray, P., Mouchet, A., Najjar, R.G., Plattner, G.K., Rodgers, K.B., Sabine, C.L., Sarmiento, J.L., Schlitzer, R., Slater, R.D., Totterdell, I.J., Weirig, M.F., Yamanaka, Y. and Yool, A. (2005) Anthropogenic ocean acidification over the twenty-first century and its impact on calcifying organisms. *Nature* 437, 681-686.

Oxford, M.J., Hart, M.B. and Watkinson, M.P. (2004) Foraminiferal characterisation of mid-upper Jurassic sequences in the Wessex Basin (United Kingdom). *Rivista Italiana di Paleontologia e Stratigrafia (Research In Paleontology and Stratigraphy)* 110.

Paris, G., Fehrenbacher, J.S., Sessions, A.L., Spero, H.J. and Adkins, J.F. (2014) Experimental determination of carbonate-associated sulfate $\delta^{34}S$ in planktonic foraminifera shells. *Geochemistry, Geophysics, Geosystems* 15, 1452-1461.

Parkhurst, D.L. and Appelo, C. (1999) User's guide to PHREEQC (Version 2): A computer program for speciation, batch-reaction, one-dimensional transport, and inverse geochemical calculations. US Geol. Surv, Denver, Colorado.

Pawlowski, J., Holzmann, M., Berney, C., Fahrni, J., Gooday, A.J., Cedhagen, T., Habura, A. and Bowser, S.S. (2003) The evolution of early Foraminifera. *Proc Natl Acad Sci U S A* 100, 11494-11498.

Pierrot, D., Lewis, E. and Wallace, D.W.R. (2006) MS Excel Program Developed for CO_2 System Calculations, ORNL/CDIAC-105a. Carbon Dioxide Information Analysis Center, Oak Ridge National Laboratory, U.S.

Piña-Ochoa, E., Høgslund, S., Geslin, E., Cedhagen, T., Revsbech, N.P., Nielsen, L.P., Schweizer, M., Jorissen, F., Rysgaard, S. and Risgaard-Petersen, N. (2010) Widespread occurrence of nitrate storage and denitrification among Foraminifera and *Gromiida*. *Proceedings of the National Academy of Sciences* 107, 1148-1153.

Pingitore, N.E., Meitzner, G. and Love, K.M. (1995) Identification of sulfate in natural carbonates by x-ray absorption spectroscopy. *Geochimica et Cosmochimica Acta* 59, 2477-2483.

Porter, S.M. (2007) Seawater chemistry and early carbonate biomineralization. *Science* 316, 1302-1302.

Porter, S.M. (2010) Calcite and aragonite seas and the de novo acquisition of carbonate skeletons. *Geobiology* 8, 256-277.

Prazeres, M., Uthicke, S. and Pandolfi, J.M. (2016) Influence of local habitat on the physiological responses of large benthic foraminifera to temperature and nutrient stress. *Scientific Reports* 6, 21936.

Premoli Silva, I. and Slite, W.V. (1999) Cretaceous paleoceanography: Evidence from planktonic foraminiferal evolution, in: Barrera, E., Johnson, C.C. (Eds.), Evolution of the Cretaceous ocean-climate system. Geological Society of America.

Rabalais, N., Cai, W.-J., Carstensen, J., Conley, D., Fry, B., Hu, X., Quiñones-Rivera, Z., Rosenberg, R., Slomp, C., Turner, E., Voss, M., Wissel, B. and Zhang, J. (2014) Eutrophication-Driven Deoxygenation in the Coastal Ocean. *Oceanography* 27, 172-183.

Rabalais, N.N., Díaz, R.J., Levin, L.A., Turner, R.E., Gilbert, D. and Zhang, J. (2010) Dynamics and distribution of natural and human-caused hypoxia. *Biogeosciences* 7, 585-619.

Rae, J.W.B., Foster, G.L., Schmidt, D.N. and Elliott, T. (2011) Boron isotopes and B/Ca in benthic foraminifera: Proxies for the deep ocean carbonate system. *Earth and Planetary Science Letters* 302, 403-413.

Raitzsch, M., Dueñas-Bohórquez, A., Reichart, G.J., De Nooijer, L.J. and Bickert, T. (2010) Incorporation of Mg and Sr in calcite of cultured benthic foraminifera: impact of calcium concentration and associated calcite saturation state. *Biogeosciences* 7, 869-881.

Raitzsch, M., Hathorne, E.C., Kuhnert, H., Groeneveld, J. and Bickert, T. (2011) Modern and late Pleistocene B/Ca ratios of the benthic foraminifer *Planulina wuellerstorfi* determined with laser ablation ICP-MS. *Geology* 39, 1039-1042.

Raja, R., Saraswati, P.K., Rogers, K. and Iwao, K. (2005) Magnesium and strontium compositions of recent symbiont-bearing benthic foraminifera. *Marine Micropaleontology* 58, 31-44.

Raup, D.M. and Sepkoski Jr, J.J. (1982) Mass extinctions in the marine fossil record. *Science* 215, 1501-1503.

Reddy, M.M. and Wang, K.K. (1980) Crystallization of calcium carbonate in the presence of metal ions: I. Inhibition by magnesium ion at pH 8.8 and 25°C. *Journal of Crystal Growth* 50, 470-480.

Reichart, G.-J., Jorissen, F., Anschutz, P. and Mason, P.R. (2003) Single foraminiferal test chemistry records the marine environment. *Geology* 31, 355-358.

Reiss, Z. (1957) The *Bilamellidea*, nov. superfam., and remarks on cretaceous *Globorotaliids*.

Reolid, M., Nikitenko, B.L. and Glinskikh, L. (2014) Trochammina as opportunist foraminifera in the Lower Jurassic from north Siberia. *Polar Research* 33.

Riding, R. and Liang, L. (2005) Seawater chemistry control of marine limestone accumulation over the past 550 million years. *Revista Española de Micropaleontología* 37, 1-11.

Riebesell, U., Zondervan, I., Rost, B., Tortell, P.D., Zeebe, R.E. and Morel, F.M.M. (2000) Reduced calcification of marine plankton in response to increased atmospheric CO_2. *Nature* 407, 364-367.

Ries, J. (2010) Geological and experimental evidence for secular variation in seawater Mg/Ca (calcite-aragonite seas) and its effects on marine biological calcification. *Biogeosciences* 7, 2795-2849.

Ries, J.B. (2004) Effect of ambient Mg/Ca ratio on Mg fractionation in calcareous marine invertebrates: A record of the oceanic Mg/Ca ratio over the Phanerozoic. *Geology* 32, 981-984.

Ries, J.B. (2011) A physicochemical framework for interpreting the biological calcification response to CO_2-induced ocean acidification. *Geochimica et Cosmochimica Acta* 75, 4053-4064.

Ries, J.B., Cohen, A.L. and McCorkle, D.C. (2009) Marine calcifiers exhibit mixed responses to CO_2-induced ocean acidification. *Geology* 37, 1131-1134.

Riley, J.P. and Tongudai, M. (1967) The major cation/chlorinity ratios in sea water. *Chemical Geology* 2, 263-269.

Risgaard-Petersen, N., Langezaal, A.M., Ingvardsen, S., Schmid, M.C., Jetten, M.S.M., Op den Camp, H.J.M., Derksen, J.W.M., Pina-Ochoa, E., Eriksson, S.P., Peter Nielsen, L., Peter Revsbech, N., Cedhagen, T. and van der Zwaan, G.J. (2006) Evidence for complete denitrification in a benthic foraminifer. *Nature* 443, 93-96.

Robbins, L.L. and Brew, K. (1990) Proteins from the organic matrix of core-top and fossil planktonic foraminifera. *Geochimica et Cosmochimica Acta* 54, 2285-2292.

Robert, S. and Murray, J.W. (1995) Characterization of cement mineralogy in agglutinated foraminifera (Protista) by Raman spectroscopy. *Journal of the Geological Society* 152, 7-9.

Rosenthal, Y., Boyle, E.A. and Slowey, N. (1997) Temperature control on the incorporation of magnesium, strontium, fluorine, and cadmium into benthic foraminiferal shells from Little Bahama Bank: Prospects for thermocline paleoceanography. *Geochimica et Cosmochimica Acta* 61, 3633-3643.

Russell, A.D., Hönisch, B., Spero, H.J. and Lea, D.W. (2004) Effects of seawater carbonate ion concentration and temperature on shell U, Mg, and Sr in cultured planktonic foraminifera. *Geochimica et Cosmochimica Acta* 68, 4347-4361.

Rutherford, S., D'Hondt, S. and Prell, W. (1999) Environmental controls on the geographic distribution of zooplankton diversity. *Nature* 400, 749-753.

Sadekov, A., Eggins, S.M., De Deckker, P. and Kroon, D. (2008) Uncertainties in seawater thermometry deriving from intratest and intertest Mg/Ca variability in *Globigerinoides ruber*. *Paleoceanography* 23, n/a-n/a.

Sadekov, A.Y., Eggins, S.M. and De Deckker, P. (2005) Characterization of Mg/Ca distributions in planktonic foraminifera species by electron microprobe mapping. *Geochemistry, Geophysics, Geosystems* 6, n/a-n/a.

Sandberg, P.A. (1983) An oscillating trend in Phanerozoic non-skeletal carbonate mineralogy. *Nature* 305, 19-22.

Sanyal, A., Hemming, N.G., Broecker, W.S., Lea, D.W., Spero, H.J. and Hanson, G.N. (1996) Oceanic pH control on the boron isotopic composition of foraminifera: Evidence from culture experiments. *Paleoceanography* 11, 513-517.

Sather, W.A. (2005) Selective Permeability of Voltage-Gated Calcium Channels, Voltage-Gated Calcium Channels. Springer US, Boston, MA, pp. 205-218.

Schiebel, R. (2002) Planktic foraminiferal sedimentation and the marine calcite budget. *Global Biogeochemical Cycles* 16, 3-1-3-21.

Schmidt, C., Kucera, M. and Uthicke, S. (2014) Combined effects of warming and ocean acidification on coral reef Foraminifera *Marginopora vertebralis* and *Heterostegina depressa*. *Coral Reefs* 33, 805-818.

Segev, E. and Erez, J. (2006) Effect of Mg/Ca ratio in seawater on shell composition in shallow benthic foraminifera. *Geochemistry, Geophysics, Geosystems* 7, n/a-n/a.

Sen Gupta, B.K. (1999) Modern Foraminifera. Kluwer Academic Publishers, Dordrecht.

Spero, H.J., Bijma, J., Lea, D.W. and Bemis, B.E. (1997) Effect of seawater carbonate concentration on foraminiferal carbon and oxygen isotopes. *Nature* 390, 497-500.

Stanley, S.M. (2006) Influence of seawater chemistry on biomineralization throughout phanerozoic time: Paleontological and experimental evidence. *Palaeogeography, Palaeoclimatology, Palaeoecology* 232, 214-236.

Stanley, S.M. (2008) Effects of global seawater chemistry on biomineralization: past, present, and future. *Chemical reviews* 108, 4483-4498.

Stanley, S.M. and Hardie, L.A. (1998) Secular oscillations in the carbonate mineralogy of reef-building and sediment-producing organisms driven by tectonically forced shifts in seawater chemistry. *Palaeogeography, Palaeoclimatology, Palaeoecology* 144, 3-19.

Stanley, S.M., Ries, J.B. and Hardie, L.A. (2002) Low-magnesium calcite produced by coralline algae in seawater of Late Cretaceous composition. *Proceedings of the National Academy of Sciences* 99, 15323-15326.

Staudt, W.J., Reeder, R.J. and Schoonen, M.A.A. (1994) Surface structural controls on compositional zoning of SO^{2-4} and SeO^{2-4} in synthetic calcite single crystals *Geochimica et Cosmochimica Acta* 58, 2087-2098.

Steuber, T. and Rauch, M. (2005) Evolution of the Mg/Ca ratio of Cretaceous seawater: implications from the composition of biological low-Mg calcite. *Marine Geology* 217, 199-213.

Steuber, T. and Veizer, J. (2002) Phanerozoic record of plate tectonic control of seawater chemistry and carbonate sedimentation. *Geology* 30, 1123.

Stoll, M.H.C., Bakker, K., Nobbe, G.H. and Haese, R.R. (2001) Continuous-Flow analysis of dissolved inorganic carbon content in seawater. *Analytical Chemistry* 73, 4111-4116.

Stramma, L., Brandt, P., Schafstall, J., Schott, F., Fischer, J. and Körtzinger, A. (2008a) Oxygen minimum zone in the North Atlantic south and east of the Cape Verde Islands. *Journal of Geophysical Research: Oceans* 113, n/a-n/a.

Stramma, L., Johnson, G.C., Sprintall, J. and Mohrholz, V. (2008b) Expanding Oxygen-Minimum Zones in the Tropical Oceans. *Science* 320, 655-658.

Stramma, L., Schmidtko, S., Levin, L.A. and Johnson, G.C. (2010) Ocean oxygen minima expansions and their biological impacts. *Deep Sea Research Part I: Oceanographic Research Papers* 57, 587-595.

Sun, W., Jayaraman, S., Chen, W., Persson, K.A. and Ceder, G. (2015) Nucleation of metastable aragonite $CaCO_3$ in seawater. *Proceedings of the National Academy of Sciences* 112, 3199-3204.

Ter Kuile, B. and Erez, J. (1987) Uptake of inorganic carbon and internal carbon cycling in symbiont-bearing benthonic foraminifera. *Marine Biology* 94, 499-509.

Toyofuku, T. and Kitazato, H. (2005) Micromapping of Mg/Ca values in cultured specimens of the high-magnesium benthic foraminifera. *Geochemistry, Geophysics, Geosystems* 6, n/a-n/a.

Toyofuku, T., Kitazato, H., Kawahata, H., Tsuchiya, M. and Nohara, M. (2000) Evaluation of Mg/Ca thermometry in foraminifera: Comparison of experimental results and measurements in nature. *Paleoceanography* 15, 456-464.

Toyofuku, T., Suzuki, M., Suga, H., Sakai, S., Suzuki, A., Ishikawa, T., De Nooijer, L.J., Schiebel, R., Kawahata, H. and Kitazato, H. (2011) Mg/Ca and $\delta^{18}O$ in the brackish shallow-water benthic foraminifer *Ammonia 'beccarii'*. *Marine Micropaleontology* 78, 113-120.

Tripati, A., Backman, J., Elderfield, H. and Ferretti, P. (2005) Eocene bipolar glaciation associated with global carbon cycle changes. *Nature* 436, 341-346.

Uchikawa, J., Penman, D.E., Zachos, J.C. and Zeebe, R.E. (2015) Experimental evidence for kinetic effects on B/Ca in synthetic calcite: Implications for potential $B(OH)_4^-$ and $B(OH)_3$ incorporation. *Geochimica et Cosmochimica Acta* 150, 171-191.

Uthicke, S., Momigliano, P. and Fabricius, K.E. (2013) High risk of extinction of benthic foraminifera in this century due to ocean acidification. *Scientific Reports* 3.

Van de Waal, D.B., John, U., Ziveri, P., Reichart, G.-J., Hoins, M., Sluijs, A. and Rost, B. (2013) Ocean acidification reduces growth and calcification in a marine dinoflagellate. *PloS one* 8, e65987.

Van der Zwaan, G., Jorissen, F. and De Stigter, H. (1990) The depth dependency of planktonic/benthic foraminiferal ratios: constraints and applications. *Marine Geology* 95, 1-16.

Van der Zwaan, G.J., Duijnstee, I.A.P., den Dulk, M., Ernst, S.R., Jannink, N.T. and Kouwenhoven, T.J. (1999) Benthic foraminifers: proxies or problems?: A review of paleocological concepts. *Earth-Science Reviews* 46, 213-236.

van Dijk, I., de Nooijer, L.J., Wolthers, M. and Reichart, G.-J. (2017) Impacts of pH and $[CO_3^{2-}]$ on the incorporation of Zn in foraminiferal calcite. *Geochimica et Cosmochimica Acta* 197, 263-277.

Veizer, J., Ala, D., Azmy, K., Bruckschen, P., Buhl, D., Bruhn, F., Carden, G.A., Diener, A., Ebneth, S. and Godderis, Y. (1999) $^{87}Sr/^{86}Sr$, $\delta^{13}C$ and $\delta^{18}O$ evolution of Phanerozoic seawater. *Chemical geology* 161, 59-88.

Walker, J.C. (1986) Global geochemical cycles of carbon, sulfur and oxygen. *Marine Geology* 70, 159-174.

Wall-Palmer, D., Hart, M., Smart, C., Sparks, R., Friant, A.L., Boudon, G., Deplus, C. and Komorowski, J. (2012) Pteropods from the Caribbean Sea: variations

in calcification as an indicator of past ocean carbonate saturation. *Biogeosciences* 9, 309-315.

Wallmann, K. (2001) Controls on the Cretaceous and Cenozoic evolution of seawater composition, atmospheric CO_2 and climate. *Geochimica et Cosmochimica Acta* 65, 3005-3025.

Wallmann, K. (2004) Impact of atmospheric CO_2 and galactic cosmic radiation on Phanerozoic climate change and the marine $\delta^{18}O$ record. *Geochemistry, Geophysics, Geosystems* 5.

Weiner, S. and Erez, J. (1984) Organic matrix of the shell of the foraminifer, *Heterostegina depressa*. *Journal of Foraminiferal Research* 14, 206-212.

Weinkauf, M.F.G., Moller, T., Koch, M.C. and Kučera, M. (2013) Calcification intensity in planktonic Foraminifera reflects ambient conditions irrespective of environmental stress. *Biogeosciences* 10, 6639-6655.

Wernli, R. (1988) Les protoglobigerines (foraminiferes) du Toarcien et de l'Aalenien du Domuz Dag (Taurus Occidental, Turquie). *Eclogae Geologicae Helvetiae* 81, 661-668.

Wernli, R. (1995) Les foraminiferes globigeriniformes (Oberhauserellidae) du Toarcien inferieur de Teysachaux (Prealpes medianes, Fribourg, Suisse). *Revue de Paléobiologie* 14, 257-269.

Wilkinson, B.H. and Algeo, T.J. (1989) Sedimentary carbonate record of calcium-magnesium cycling. *American Journal of Science* 289, 1158-1194.

Wit, J.C., Davis, M.M., Mccorkle, D.C. and Bernhard, J.M. (2016) A short-term survival experiment assesing impacts of ocean acidification and hypoxia on the benthic foraminifera *Globobulimina turgida*. *Journal of Foraminiferal Research* 46, 25-33.

Wit, J.C., De Nooijer, L.J., Barras, C., Jorissen, F.J. and Reichart, G.J. (2012) A reappraisal of the vital effect in cultured benthic foraminifer *Bulimina marginata* on Mg/Ca values: assessing temperature uncertainty relationships. *Biogeosciences* 9, 3693-3704.

Wit, J.C., De Nooijer, L.J., Wolthers, M. and Reichart, G.J. (2013) A novel salinity proxy based on Na incorporation into foraminiferal calcite. *Biogeosciences* 10, 6375-6387.

Wolthers, M., Charlet, L. and Van Cappellen, P. (2008) The surface chemistry of divalent metal carbonate minerals; a critical assessment of surface charge and potential data using the charge distribution multi-site ion complexation model. *American Journal of Science* 308, 905-941.

Wood, A. (1948) The structure of the wall of the test in the Foraminifera; its value in classification. *Quarterly Journal of the Geological Society* 104, 229-255.

Yu, J. and Elderfield, H. (2007) Benthic foraminiferal B/Ca ratios reflect deep water carbonate saturation state. *Earth and Planetary Science Letters* 258, 73-86.

Yu, J. and Elderfield, H. (2008) Mg/Ca in the benthic foraminifera *Cibicidoides wuellerstorfi* and *Cibicidoides mundulus*: Temperature versus carbonate ion saturation. *Earth and Planetary Science Letters* 276, 129-139.

Yu, J., Foster, G.L., Elderfield, H., Broecker, W.S. and Clark, E. (2010) An evaluation of benthic foraminiferal B/Ca and $\delta^{11}B$ for deep ocean carbonate ion and pH reconstructions. *Earth and Planetary Science Letters* 293, 114-120.

Zachara, J.M., Cowan, C.E. and Resch, C.T. (1991) Sorption of divalent metals on calcite. *Geochimica et Cosmochimica Acta* 55, 1549-1562.

Zeebe, R.E., Bijma, J., Honisch, B., Sanyal, A., Spero, H.J. and Wolf-Gladrow, D.A. (2008) Vital effects and beyond: a modelling perspective on developing palaeoceanographical proxy relationships in foraminifera. *Geological Society, London, Special Publications* 303, 45-58.

Zeebe, R.E. and Sanyal, A. (2002) Comparison of two potential strategies of planktonic foraminifera for house building: Mg^{2+} or H^{+} removal? *Geochimica et Cosmochimica Acta* 66, 1159-1169.

Zeebe, R.E. and Wolf-Gladrow, D.A. (2001) CO_2 in seawater: equilibrium, kinetics, isotopes. Gulf Professional Publishing.

Nederlandse samenvatting

De chemische samenstelling van schelpen van foraminiferen wordt vaak toegepast als proxy voor het reconstrueren van milieu omstandigheden in het verleden. Echter, foraminiferen zijn zelf ook onderhevig aan veranderingen in de chemie van zeewater, zoals bijvoorbeeld het verzuren van de oceaan. Het doel van dit proefschrift is om het effect van oceaan verzuring op de verkalking (calcificatie) van foraminiferen met verschillende calcificatie strategieën (i.e. perforaat versus imperforaat) te onderzoeken, om zo mogelijk nieuwe proxies te ontwikkelen en bestaande proxies te verbeteren. Hierdoor zullen foraminiferen als proxy-dragers waardevoller zijn voor het reconstrueren van chemische veranderingen in de oceaan.

In **hoofdstuk 2** ,'*The long-term impact of magnesium in seawater on foraminiferal mineralogy: mechanism and consequences*', wordt het voorkomen van fossiele foraminiferen met verschillende calcificatie strategieën (i.e. perforate versus imperforate soorten) gedurende het Phanerozoïcum geanalyseerd. Hoge Mg/Ca waarden van zeewater lijken te leiden tot meer aragoniet en hoog Mg carbonaat producerende foraminiferen, terwijl laag Mg foraminiferen dominanter zijn in perioden wanneer zeewater Mg/Ca laag is. Dit is in overeenstemming met de nucleatie velden van de polymorfen aragoniet en calciet bij anorganische carbonaat precipitatie. Deze observaties suggereren dat foraminiferen, ondanks de grote controle die zij uitoefenen op hun calcificatie vloeistof, toch gevoelig zijn voor veranderingen in de chemie van zeewater.

De invloed van zeewater Mg/Ca op calcificatie in foraminiferen is verder onderzocht in **hoofdstuk 3**, '*The impacts of seawater Mg/Ca and temperature on Mg incorporation in foraminiferal calcite*'. In dit hoofdstuk zijn de individuele en gecombineerde invloeden van zeewater Mg/Ca en temperatuur op de inbouw van magnesium in perforate (*Elphidium crispum*) en imperforate (*Quinqueloculina* sp.) foraminiferen geanalyseerd. Wij observeerden voor beide soorten, dat verandering in zeewater Mg/Ca de helling van de relatie tussen $Mg/Ca_{CALCIET}$ en temperatuur niet beïnvloedt; alleen absolute waarden van de gereconstrueerde temperatuur kunnen veranderen. Dit is een positieve uitkomst, want om zeewater Mg/Ca te reconstrueren d.m.v. $Mg/Ca_{CALCIET}$ van verschillende soorten foraminiferen (perforate en impeforate) is het cruciaal dat de gevoeligheid van deze relatie niet beïnvloed wordt door veranderingen in de zeewater Mg/Ca waarde.

Het analyseren en vergelijken van trends in element inbouw tussen perforate en imperforate foraminiferen kan nieuwe inzichten bieden in de verschillen tussen deze twee calcificatie strategieën. In **hoofdstuk 4**, '*Trends in trace element incorporation in larger benthic foraminifera*, presenteren we resultaten van acht grote benthische foraminiferen (perforaat en imperforate soorten) gekweekt onder verschillende pCO_2 condities. We observeerden dat de inbouw van magnesium (Mg), strontium (Sr) en natrium (Na) niet werd beïnvloed door veranderende carbonaat chemie. Daarentegen zagen we wel veranderingen in zink en barium t.o.v. calcium; Zn/Ca en Ba/Ca waarden namen toe bij hogere pCO_2 (en dus lagere $[CO_3^{2-}]$). Voor de perforate soorten observeerden wij een sterke afhankelijkheid tussen de inbouw van verschillende elementen. Foraminiferen die bijvoorbeeld meer Mg in hun schelp inbouwden, bouwden ook andere elementen meer in. Wij stellen voor dat foraminiferen ionen naar de plek van verkalking transporteren via calcium kanalen, eerder voorgesteld in een transmembraan transport (TMT) model, alhoewel de rol van TMT waarschijnlijk kleiner is in imperforate soorten, omdat deze soorten verkalken vanuit eerder ingesloten vacuolen met zeewater.

Agglutinerende foraminiferen zijn soorten die deeltjes verzamelen en fixeren met cement om een schelp te maken. Dit cement is meestal een organische matrix, maar in sommige gevallen gemaakt van calciumcarbonaat. In **hoofdstuk 5**, '*Combined impacts of ocean acidification and dysoxia on survival and growth of selected agglutinated foraminifera*', onderzoeken we de geïsoleerde en gecombineerde invloeden van zuurstofloosheid en oceaan verzuring op verschillende soorten agglutinerende foraminiferen. Wij vonden soort specifieke reacties op beide stressoren, maar de meeste soorten produceerde meer kamers en overleefde meer in het gecombineerde scenario (dysoxisch en oceaan verzuring). Verder produceerden alle bestudeerde soorten een organisch matrix, wat kan verklaren waarom ze geen negatieve reactie vertonen op de verlaagde verzadigingsgraad van het zeewater.

Het is een uitdaging om de invloeden van verschillende carbonaat systeem parameters op spoormetaal incorporatie in het carbonaat van foraminiferen te ontkoppelen, vooral in 'standaard' oceaan verzurings experimenten. In **hoofdstuk 6**, '*Impacts of pH and $[CO_3^{2-}]$ on the incorporation of Zn in foraminiferal calcite*', hebben we foraminiferen laten groeien in zeewater met twee verschillende behandelingen om de effecten van pH en carbonaat ion concentratie ($[CO_3^{2-}]$) op Zn inbouw te kunnen ontkoppelen. Wij vonden dat Zn inbouw voornamelijk beïnvloed wordt door $[CO_3^{2-}]$, vanwege de invloed op de speciatie van Zn en daardoor de hoeveelheid Zn die biologisch beschikbaar is. Deze resultaten laten zien dat Zn/Ca in foraminiferen mogelijk een

nuttige proxy is voor twee verschillende parameters. Als eerste kan deze relatie gebruikt worden voor het reconstrueren van [Zn] indien de zeewater [CO_3^{2-}] bekend is. In combinatie met de globale diepzee Zn:Si relatie, kan dit het reconstrueren van de zeewater samenstelling in het verleden en nutriënt profielen mogelijk maken. Ten tweede kan Zn/Ca van foraminiferen gebruikt worden om carbonaat ion concentraties van de oceaan te reconstrueren. In combinatie met een proxy voor een van de andere parameters van het carbonaat systeem, kan het complete carbonaat systeem gereconstrueerd worden, en dus ook atmosferisch CO_2 in het verleden.

In **hoofdstuk 7**, *'Sulfur in foraminiferal calcite as a potential proxy for sea water carbonate ion concentration',* onderzoeken we sulfaat inbouw in calciet van foraminiferen als een mogelijk proxy voor zeewater [CO_3^{2-}]. In theorie neemt de S/Ca in de schelpen van foraminiferen toe wanneer zeewater [CO_3^{2-}] afneemt. Wij laten zien dat $S/Ca_{CALCIET}$ van de perforate soort *Amphistegina gibbosa* en de imperforate *Marginopora vertebralis* inderdaad respectievelijk 21 en 19% toenemen bij een afname van 100 µm/kg [CO_3^{2-}]. Een ander groei experiment toont aan dat saliniteit geen invloed heeft op de S/Ca van *A. lessonii*. Doordat foraminiferen hun interne pH verhogen, is bijna al het anorganisch koolstof in de calcificatie ruimte aanwezig in de vorm van CO_3^{2-}. Omdat wij een verschil observeren in de hoeveelheid ingebouwd zwavel voor verschillende CO_3^{2-} condities, moet de carbonaat tot sulfaat ratio in de calcificatie ruimte ook veranderen. Dit suggereert dat de interne pH verhoogd wordt met een bepaalde factor ten op zichte van het omgevende zeewater

Acknowledgements

Although I wish it was narrated by Morgan Freeman, this is it.

Gert-Jan, thank you for all the time and effort you spent on my supervision. During second year fieldwork in Tremp, you were the one who sparked my interest in continuing in science. You are a great promotor: smart (sometimes too smart), funny (sometimes less or more than you think) and easily recognizable when coming down the hall towards my office (..the boots). Lennart, my co-promotor, I cannot thank you enough for all the hours you spent hovering over my manuscripts. My thesis would not have been here without your help. Thank you for reminding me that "doing a PhD is not romantic..", even though I slightly disagree. You are a creative, progressive scientist, with a great taste in the wine and dine area.

I'm honored to have such a great reading committee. Jack Middelburg, Lucas Lourens, Appy Sluijs, Howie Spero and Claire Rollion-Bard, thank you for the reconstructive comments and support.

I would like to thank my co-authors / scientists in crime, starting with Takashi Toyofuku, for the great experience at JAMSTEC. Joan Bernhard, thanks for having me as an observer at your department at WHOI, you taught me a lot about culturing (agglutinating) foraminifera. Thanks to Malcolm Hart, for his knowledge on (fossil) foraminifera, Mariëtte Wolthers for her help with chemical speciation modeling. Furthermore, I am very grateful to Jelle Bijma, Gernot Nehrke, Brett Metcalfe, Didier de Bakker, Lennart, Esmee and Alice for their support during the 2015 foraminiferal culture expedition on Statia.

I would like to thank the whole GEO/GCO/OCS department for all the nice coffee (and cake) breaks, lunches, dinners and department outings. A lot of you helped me (behind the scenes) and I'm very grateful that this is so easily possible at the NIOZ. Patrick and Karel, thanks for all the seawater measurements throughout my experiments. Bob (The Oracle), thanks for being handy in building and fixing stuff for us, ranging from a simple malfunctioning microscope, to a whole CO_2-controlled culture system. Steven, thanks for designing the aforementioned CO_2 system and making that crazy machine (VINDTA) work at the CNSI.

Even though there are so many people I would like to thank, inside and outside the NIOZ, on and off Texel, I can't name them all. So, here are some I singled out:

First, a shout-out to all new traditions: the Tuesday Craft club (started by Darci and Gabriella) the 'yearly' Appel Cider Festival (initiated by Yvo, Nicole and Rick) and Sinterkerst dinner by Team Statia.

Michelle and Laura, the dust girls! Thanks for the occasional distraction from my own PhD troubles, by sharing your own. I wish you two all the best in this last year of working your asses off. Make me proud ;-)

Maaike, I am so happy we met! What started out as simply hanging out during Switch gigs, ended up as a true friendship, in which I feel like I can share everything, without being judged. What wonderful Wednesday evenings!

Juliane, we not only shared an office, but also a lot of laughter, (IT) frustration, indie music and the occasional tears. I admire you for your passion (be it either in sports, candy, ice cream, Louis or science), your determination and scientific pigheadness. I wish you all the best.

Alice, my paraninja, you little French whirlwind. Thank you for showing me how to be awesome. I love your view on life, opinion about everything, your good (but also your bad) moods, energy, humor and French cooking. And for being one of the two best office mates I could wish for.

My paranimphs Marijke and Esmee, thank you for your help during the last phases of my PhD. Marijke, you stuck with me through it all, witnessed my whole PhD evolution. Thanks for all the long conversations and short chats, be it at the NIOZ or at home. Esmee, thank you for all your support during the last two years of my PhD. Even though I didn't notice you when you were working in our department as a master student (shame on me!), I certainly did afterward – and enjoyed it! You're a great listener, but also a great story teller. You were my perfect 'partner in crime' at the CNSI and on my couch watching Netflix. You are both, in short, wonderful people.

Besides my life on the island, I still had two groups of friends 'aan de overkant', of which I am grateful they forgave me for my occasional absence during the last four years: My friends from high school (Lisanne, Mariel, Willeke, Inger etc.) and Earth Science co-students 'Jaartje 007' (Nathalie, Jasper, Jedidja, Daniël, Mirke, Jantien, Sander etc.). Thanks for providing me with some distraction from the whole PhD experience with all the trips, game nights and dinners.

I would like to thank my family for being there for me and providing me with adorable nephews and a lovely little niece. I enjoy our family time, be it with dinners in Utrecht or trips to Texel. Mom and dad, thanks for all your support and belief in me. My creative mom, thanks for letting me do my own thing (although you probably hope that it was somewhere closer to Utrecht) and my practical dad, thanks for showing me how to be curious. I love you all.

And last, but definitely not least: Wim, thank you for your support and love, for everything.

Curriculum vitae

Inge van Dijk was born on the 18th of December 1987 in Utrecht, the Netherlands. She graduated from secondary school (VWO) at the 'O.R.S. Lek en Linge' in 2007. She enrolled in the Bachelor Earth Sciences at Utrecht University, with an emphasize on paleoclimate and the interaction between biology and geology. After which, she further specialized with a Master in Biogeology. For her MSc thesis, she studied the effect of combined temperature and seawater Mg/Ca on incorporation of Mg in different species of foraminifera, for which she spend 6 weeks in JAMSTEC, Japan, to learn how to culture foraminifera. In 2012, she started as a PhD candidate of the Darwin Centre for Biogeosciences at the department of Ocean Systems of the Royal Netherlands Institute for Sea Research. The PhD-thesis focusses on the impact of ocean acidification on foraminiferal calcification.

Bibliography

Van Dijk, I., De Nooijer, L.J., Hart, M.B., and Reichart, G-J., 2016. The long-term impact of magnesium in seawater on foraminiferal mineralogy: Mechanism and consequences, *Global Biogeochemical Cycles*, 30, 438–446, DOI:10.1002/2015GB005241.

Van Dijk, I., De Nooijer, L.J., Wolthers, M., and Reichart, G-J., 2017. Impacts of pH and [CO_3^{2-}] on the incorporation of Zn in foraminiferal calcite, *Geochimica et Cosmochimica Acta*, 197, 263-277, DOI: 10.1016/j.gca.2016.10.031.

Van Dijk, I., De Nooijer, L.J., Boer, W. and Reichart, G-J., In review. Sulfur in foraminiferal calcite as a potential proxy for seawater carbonate ion concentration, *Earth and Planetary Science Letters*.

Van Dijk, I., De Nooijer, L.J., and Reichart, G-J., In review. Contrasting trends in element incorporation in hyaline and miliolid foraminifera, *Biogeosciences Discussions*, DOI:10.5194/bg-2016-402.

De Nooijer, L.J., **Van Dijk, I.,** Toyofuku, T., and Reichart, G-J., In review. The impacts of seawater Mg/Ca and temperature on element incorporation in foraminiferal calcite, *Geochimica et Cosmochimica Acta*.

Van Dijk, I., Bernhard, J.M., de Nooijer, L.J., and Reichart, G-J., In review. Combined impacts of ocean acidification and dysoxia on survival and growth of four agglutinating foraminifera, *Journal of Foraminiferal Research*.

Geerken, E., De Nooijer, L.J., **van Dijk., I**., Reichart, G-J., In review. Biomineralization controls on incorporation of sodium in the foraminifer Amphistegina lessonii, *Geochimica et Cosmochimica Acta*.

Van Bree, L., Cremer, H., Donders, T., Schuren, F., **Van Dijk**, I., Hopmans, E., Reichart, G-J., In preparation. Reconstruction of past cyanobacterial nitrogen fixation in a Dutch artificial lake.